Berichte
zur Polar-
und Meeresforschung

613
2010

Reports
on Polar and Marine Research

The Expedition of the Research Vessel "Polarstern" to the Antarctic in 2009 (ANT-XXV/3 - LOHAFEX)

Edited by
Victor Smetacek and Syed Wajih A. Naqvi
with contributions of the participants

HELMHOLTZ GEMEINSCHAFT

ALFRED-WEGENER-INSTITUT FÜR
POLAR- UND MEERESFORSCHUNG
In der Helmholtz-Gemeinschaft
D-27570 BREMERHAVEN
Bundesrepublik Deutschland

ISSN 1866-3192

Hinweis

Die Berichte zur Polar- und Meeresforschung werden vom Alfred-Wegener-Institut für Polar-und Meeresforschung in Bremerhaven* in unregelmäßiger Abfolge herausgegeben.

Sie enthalten Beschreibungen und Ergebnisse der vom Institut (AWI) oder mit seiner Unterstützung durchgeführten Forschungsarbeiten in den Polargebieten und in den Meeren.

Es werden veröffentlicht:

- Expeditionsberichte (inkl. Stationslisten und Routenkarten)
- Expeditionsergebnisse (inkl. Dissertationen)
- wissenschaftliche Ergebnisse der Antarktis-Stationen und anderer Forschungs-Stationen des AWI
- Berichte wissenschaftlicher Tagungen

Die Beiträge geben nicht notwendigerweise die Auffassung des Instituts wieder.

Notice

The Reports on Polar and Marine Research are issued by the Alfred Wegener Institute for Polar and Marine Research in Bremerhaven*, Federal Republic of Germany. They appear in irregular intervals.

They contain descriptions and results of investigations in polar regions and in the seas either conducted by the Institute (AWI) or with its support.

The following items are published:

- expedition reports (incl. station lists and route maps)
- expedition results (incl. Ph.D. theses)
- scientific results of the Antarctic stations and of other AWI research stations
- reports on scientific meetings

The papers contained in the Reports do not necessarily reflect the opinion of the Institute.

The „Berichte zur Polar- und Meeresforschung” continue the former „Berichte zur Polarforschung”

* Anschrift / Address
Alfred-Wegener-Institut
für Polar- und Meeresforschung
D-27570 Bremerhaven
Germany
www.awi.de

Editor in charge:
Dr. Horst Bornemann

Assistant editor:
Birgit Chiaventone

Die "Berichte zur Polar- und Meeresforschung" (ISSN 1866-3192) werden ab 2008 ausschließlich als Open-Access-Publikation herausgegeben (URL: http://epic.awi.de).

Since 2008 the "Reports on Polar and Marine Research" (ISSN 1866-3192) are only available as web based open-access-publications (URL: http://epic.awi.de)

The Expedition of the Research Vessel "Polarstern" to the Antarctic in 2009 (ANT-XXV/3 - LOHAFEX)

Edited by
Victor Smetacek and Syed Wajih A. Naqvi
with contributions of the participants

Please cite or link this item using the identifier
hdl: 10013/epic.35169 or http://hdl.handle.net/10013/epic.35169

ISSN 1866-3192

ANT-XXV/3 - LOHAFEX

7 January 2009 - 17 March 2009

Cape Town - Punta Arenas

Chief Scientists
Victor Smetacek
Syed Wajih A. Naqvi

Coordinator
Eberhard Fahrbach

CONTENTS

1. ZUSAMMENFASSUNG UND FAHRTVERLAUF

V. Smetacek[1], S.W.A. Naqvi[2]

[1)]AWI
[2)]NIO

Wissenschaftliche Fragestellung

Fahrtabschnitt ANT-XXV/3 war ein gemeinsames indisch-deutsches Eisendüngungs-Experiment, dessen Kosten von beiden Seiten zu etwa gleichen Teilen getragen wurden. LOHAFEX (Loha ist das Hindi-Wort für Eisen) war das dritte derartige Experiment, das von der *Polarstern* durchgeführt wurde und den Aufbau und Niedergang einer Phytoplankton-Blüte untersuchte. Die Blüte wurde durch Eisensulphat-Düngung im Kern eines mesoskaligen Wirbels entlang der Polarfront hervorgerufen. Im Gegensatz zu vorherigen Experimenten wurde LOHAFEX im produktiven südwestlichen Atlantik-Sektor des Antarktischen Zirkumpolarstroms (ACC) durchgeführt. Dieses Gebiet liegt näher an Landmassen als andere Teile des ACC und wird deshalb von Eisen aus natürlichen Quellen gedüngt. Diese natürlichen Quellen stammen in erster Linie aus dem Kontakt mit der Antarktischen Halbinsel und ihren angrenzenden Inseln, insbesondere Südgeorgien, aber auch von Staub aus Patagonien und schmelzenden Eisbergen aus dem Weddellmeer. Das Phyto-plankton dieser Region umfasst mehr schnell wachsende Küstenarten, von denen erwartet wird, dass sie stärker auf die Eisenzufuhr reagieren als die langsamer wachsenden, dickwandigeren ozeanischen Diatomeenarten, die in vorherigen Düngungsexperimenten untersucht wurden. Untersuchungen der Sedimente aus dieser Region haben gezeigt, dass Diatomeenarten, die typisch für diese produktiven Küstenregionen sind – Sporen bildende *Chaetoceros* Arten – bis Südgeorgien vorherrschen. Weiter östlich werden sie von Diatomeenschlamm ersetzt, in dem die stark verkieselten Arten *Fragilariopsis kerguelensis* und *Thalassiothrix antarctica* – beide charakteristisch für den Antarktischen Zirkumpolarstrom – dominieren.

Während des letzten eiszeitlichen Maximums breiteten sich hingegen Sedimente, die von *Chaetoceros* Sporen beherrscht wurden, über den gesamten südatlantischen Sektor des ACC aus. Dies deutet darauf hin, dass sich die gegenwärtige hoch-produktive Zone unter dem Einfluss von Küstenplankton-Arten ostwärts bis südlich von Afrika ausgebreitet hat. Dies war durch die höhere Eisenzufuhr während der kalten, trockenen Eiszeiten bedingt, als viel mehr eisenreicher Staub in den Südlichen Ozean transportiert wurde, im Vergleich zu den warmen, nassen Warm-zeiten. Die Schwankungen in der Eisenzufuhr spiegeln sich in ozeanischen Sedimentkernen, aber auch in den kontinentalen Eiskernen wider. Daher ist anzunehmen, dass diese Region damals viel mehr atmosphärisches CO_2 gespeichert hat als heute und damit eine der großen Senken von eiszeitlichem CO_2 war, nach denen noch immer gesucht wird.

Eisendüngungs-Experimente sind das Äquivalent zu Störungs-Experimenten, die von allen wissenschaftlichen Disziplinen durchgeführt werden, um Struktur und Funktion

von Systemen zu untersuchen, die zu komplex sind, um sie durch die bloße Beobachtung zu entschlüsseln. Das übergeordnete Ziel dieser interdisziplinären Fahrt war also, unser Verständnis darüber zu fördern, wie Ökosysteme im offenen Ozean funktionieren und wie sich die Organismen des Planktons untereinander und ihre Umgebung beeinflussen und dadurch biogeochemische Kreisläufe und das Absinken von partikulärem Material in die Tiefsee antreiben. Künstliche Eisendüngung simuliert natürliche Prozesse, durch die Eisen in eisenlimitierte, landferne Meeresgebiete eingebracht wird. Das Phytoplankton reagiert darauf mit einer Erhöhung der Wachstumsraten. Die Anhäufung von Biomasse ist jedoch von einer Reihe physikalischer, chemischer und biologischer Faktoren abhängig, die zusammen die Eigenschaften der Wachstumsumgebung bestimmen. Die Akkumulationsrate der Biomasse ist die Differenz zwischen Wachstums- und Verlustraten. Letztere sind durch die Mortalität der Algenzellen und schließlich den Abbau von organischer Materie durch pelagische Konsumenten bedingt: Bakterien, Protozoo- und Metazooplankton auf der einen Seite, und dem Absinken der Partikel in die Tiefsee auf der anderen Seite. Wir beabsichtigten, das Verhältnis zwischen dem Wachstum des Phytoplanktons und den Effekten durch Wegfraß und Absinken auf die Bestände der biogenen Elemente zu untersuchen. Gleichzeitig wird der Vertikalfluss durch das Aussetzen von freischwimmenden Sedimentfallen und mit einem Unterwasser-Videogerät – einem optischen Instrument, das Partikel bis in 3.000 m Tiefe fotografiert - verfolgt.

Ein Hauptziel der Fahrt war es, das Schicksal der Eisen gedüngten Blüten-Biomasse in einem produktiven Gebiet des ACC zu untersuchen: wird deren Biomasse in der Oberflächenschicht von Bakterien und Zooplankton in CO_2 zurückverwandelt, oder sinkt zumindest ein Teil davon ab, und entfernt damit CO_2 aus der Atmosphäre und lagert es in die Tiefsee ein. Die Antwort auf diese Frage ist für das Verständnis der vergangenen Klimakreisläufe von Bedeutung, aber auch für die Umsetzbarkeit der Anwendung von künstlicher Eisendüngung des ACC als Technik die globale Erwärmung abzuschwächen.

Reiseverlauf

Die *Polarstern* verließ Kapstadt pünktlich um 20:00 Uhr am 7. Januar 2009 mit allen 49 Teilnehmern und Ausrüstung an Bord – dank der exzellenten Logistik des AWI. Das interdisziplinäre internationale Wissenschaftler-Team der physikalischen, chemischen und biologischen Ozeanographen umfasste 29 Teilnehmer aus Indien, 10 aus Deutschland, 3 aus Italien, je 2 aus Spanien und Großbritannien und jeweils einen Teilnehmer aus Chile und Frankreich.

Die Erfahrung aus der Vergangenheit hat gezeigt, dass ein geschlossener Kern eines mesoskaligen Wirbels entlang einer ozeanischen Front, die besten Bedingungen bietet, um ein solches Experiment durchzuführen, weil der gedüngte Fleck innerhalb der Lebenszeit des Wirbels – im allgemeinen mehrere Monate - bewahrt wird. Folglich kann die Entscheidung, welcher Wirbel ausgesucht wird, erst kurz vor dem Experiment getroffen werden. Wir hatten das Wirbelfeld nördlich von Südgeorgien angepeilt, da in vorherigen Jahren dort mesoskalige, beständige Wirbel auf den Altimeter-Aufnahmen der Meeresoberfläche beobachtet wurden und weil die Region in der Mitte der hochproduktiven Zone liegt. Kurz nachdem wir Kapstadt verlassen hatten, wurde das Experiment von einer nichtstaatlichen Organisation

(ETC Group) angefochten. Das Bundesministerium für Bildung und Forschung legte die Fahrt auf Eis, um zu klären, ob das Experiment die Bedingungen für legitime wissenschaftliche Forschung, die von der UN Konvention für Biologische Vielfalt und der London Convention über Meeresverschmutzung im Mai bzw. Nov. 2008 unterzeichnet wurden, erfüllt.

Die Zeit während der ersten 3 Wochen der Fahrt wurde mit der Untersuchung mehrerer Wirbel verbracht, die während der vergangenen Monate auf ihre Tauglichkeit für das Experiment überwacht wurden. Der erste war ein vielversprechender, sich im Uhrzeigersinn drehender Wirbel mit kaltem Kern auf 48°S, 15°W an der Flanke des Mittelatlantischen Rückens. Derselbe frontale Strom formte einen benachbarten Wirbel mit warmem Kern. Der Schiffskurs wurde nur leicht verändert, um den Kern des kalten Wirbels zu überqueren, wo am 16. Januar eine Versuchsstation durchgeführt wurde. Wie von den Satellitenbildern angedeutet, waren die Chlorophyll-Konzentrationen innerhalb des Wirbels mäßig erhöht (0,7 mg Chl m^{-3}) und deutlich höher als Werte weiter im Osten und Norden. Das Schiff fuhr dann weiter nach Westen und Süden, um einen von mehreren großen in den Satellitenbildern sichtbaren Eisbergen, zu besuchen. Es stellte sich heraus, dass er aus einem ausgedehnten Feld aus Eisgeröll bestand, das mehrere mittelgroße Eisberge umgab, die offensichtlich aus dem Zusammenbruch eines einzigen großen Eisbergs von mehreren Kilometern Länge entstanden waren. Im Verlaufe eines Tages (19. Januar) wurden mehrere Stationen innerhalb und außerhalb des Eisfeldes genommen, um die vertikale Ausdehnung des Schmelzwassers und seinen Einfluss auf das Plankton zu berechnen. Grund für die Eisbergbegutachtung war es, herauszufinden, ob die Durchführung einer Prozess-Studie an einem solchen Ort möglich war - falls die Erlaubnis zur Fortführung des Experiments nicht erteilt würde. Die genommenen Profile deuteten auf kleinskalige Heterogenität hin, die die Bewertung der Prozesse schwierig gemacht hätte. Außerdem war der Einfluss auf die Chlorophyll-Konzentrationen, die nur wenig höher als in der Umgebung waren, unzureichend für die Zwecke eines Störungs-Experiments. So wurde dieser „Plan B“ nicht als geeignete Alternative zum Düngungs-Experiment in Betracht gezogen.

Nach der Untersuchung eines Wirbels weiter südlich, der jedoch als zu nah an der Ausschließlichen Wirtschaftszone des Süd-Sandwichinselbogens lag, steuerte *Polarstern* die Wirbel nördlich von Süd-Georgien an. Modellstudien, die auf Altimeter-Bildern basierten, deuteten an, dass diese Wirbel nicht stabil waren, was ADCP-Profile von zwei dieser Wirbel bestätigten. Es zeigte sich, dass ein geschlossener Kern fehlte und der Fleck deshalb „ausgelaufen“ wäre, wenn wir das Experiment in einem dieser Wirbel durchgeführt hätten. Daher entschlossen wir uns, zurück zum ersten Wirbel auf 48°S 15°W zu fahren, der eindeutig der geeignetste Wirbel in der gesamten Region war, und zwar aus folgenden Gründen: 1) er hatte einen geschlossenen Kern, 2) die darunterliegenden Sedimente enthielten *Chaetoceros* Sporen, die anzeigten, dass er noch unter dem Einfluss von Küstenplankton stand und damit innerhalb der produktiven Zone lag, jedoch an deren östlicher Grenze, 3) das pelagische System im Wirbel war repräsentativ für die gesamte Gebiet im südwestlichen Atlantik-Sektor, das wir durchquert hatten. Die Merkmale dieser Region umfassten: a) sehr niedrige Kieselsäure-Konzentrationen, b) mäßige Chlorophyll-Konzentrationen, c) Phytoplankton, das von kleineren Formen - nicht Diatomeen - beherrscht wurde, d) Zooplankton, repräsentiert von einer großen

Copepoden-Population, die hauptsächlich aus späten Larven-Stadien einer einzigen Art (*Calanus simillimus*) bestand, e) der Amphipoden-Art *Themisto gaudichaudii* als Haupt-Räuber, f) Salpen und andere große Zooplankton-Arten waren kaum vorhanden.

Wir erreichten den Wirbel am 25. Januar, setzten eine Driftboje, die in 30 m Tiefe im Zentrum des Kerns verankert wurde, aus und nahmen die erste lange Station, um die Ausgangsbedingungen in Wirbelnähe zu bestimmen. Am 26. Januar, als wir noch mit der Station beschäftigt waren, erhielten wir vom Ministerium grünes Licht, mit dem Experiment fortzufahren. Nachdem wir die Tanks mit Eisensulphat und Seewasser gefüllt hatten, wurde eine zweite Boje näher am Zentrum ausgesetzt (festgelegt nach der Umlaufbahn der ersten Boje, aber nur 2 km von ihr entfernt). Um sie herum wurde ein 300 km^2 großer kreisförmiger Fleck mit 2 Tonnen gelöstem Eisen (10 Tonnen granuliertes $FeSO_4$) gedüngt. Der Fleck kreiste während der ersten 3 Wochen zweimal innerhalb des Wirbels und bewegte sich dann südwärts, als er während der letzten 2 Wochen des Experiments aus dem zusammenbrechenden Wirbel herausgedrückt wurde. Leider drifteten die Bojen aus dem Fleck, so dass neue Bojen ausgesetzt werden mussten, um das Fleckzentrum zu markieren. Nach 18 Tagen wurde der Fleck erneut mit zusätzlichen 2 Tonnen gelöstem Eisen gedüngt.

Die Prozesse, die im Fleck abliefen, wurden mit Messungen der physikalischen, chemischen und biologischen Parameter in regelmäßigen Abständen (die Innen-Stationen) verfolgt und mit der Situation des Wassers außerhalb des Flecks verglichen (Außen-Stationen). Frei schwimmende Sedimentfallen, die zu vorprogrammierten Zeiten an der Oberfläche auftauchen und geborgen werden, wurden in regelmäßigen Abständen ausgesetzt, um die absinkenden Partikel in 200 m und 400 m Tiefe innerhalb und außerhalb des Flecks einzufangen. Die meisten der 39 Tage des Experiments wurden in der Nähe des Flecks verbracht, entweder um Innen- und Außen-Stationen zu nehmen oder Profile durch den Fleck zu fahren. Das Schiff musste den Wirbel zweimal verlassen, um Stürmen auszuweichen und ein Profil wurde über den benachbarten warmkernigen Wirbel gefahren, um ihn mit dem LOHAFEX-Wirbel zu vergleichen. Das Schiff verließ den Fleck nach der letzten Innen-Station am 6. März und kam pünktlich am 17. März in Punta Arenas an.

Zusammenfassung der Ergebnisse

Innerhalb der ersten 2 Wochen verdoppelte sich die Chlorophyll-Konzentration auf 1,5 mg m^{-3}, aber im Gegensatz zu früheren Experimenten war Kieselsäure in limitierenden Konzentrationen vorhanden und hinderte so die Diatomeen daran, Biomasse aufzubauen. Kleine Flagellaten (< 10 µm) trugen am meisten zur Phytoplankton-Biomasse bei, die während des 39-Tage-Experimentes ungefähr auf gleichem Niveau blieb. Die zweite Düngung hatte keinen erkennbaren Einfluss auf Wachstumsraten oder Biomasse des Phyto- oder Bakterioplanktons. Offensichtlich war der Hauptgrund, dass keine Biomasse in größerem Umfang aufgebaut wurde, der starke Fraßdruck der großen Copepoden-Population. Inkubations-Experimente deuteten an, dass die Copepoden ihre Fraß- und Kotballenproduktionsraten innerhalb des Flecks erhöhten. Die Kotballen wurden innerhalb der Oberflächenschicht wiederverwertet und trugen nicht maßgeblich zum Vertikalfluss bei, wie die Fallenfänge andeuteten. Nichtsdestotrotz waren die täglichen Sink-

Verluste, die aus Thorium-Messungen abgeschätzt wurden, innerhalb des Wirbels relativ hoch, aber im Wesentlichen innerhalb und außerhalb des Flecks gleich. Folglich hatte die Düngung dieser Planktongesellschaft wenig Einfluss auf den Vertikalfluss. Eine unerwartete Erkenntnis, die durch das horizontale Schleppen des RMT-Netzes (Rectangular Midwater Trawls) geliefert wurde, waren die viel höheren Dichten der räuberischen Amphipoden-Art *Themisto gaudichaudii*, die sich von Salpen und Copepoden ernährt, innerhalb des Flecks. Da wenig über die Ökologie dieser Art bekannt ist, die die Hauptnahrung der Kalmare im nördlichen ACC ist und deshalb „Krill des Nordens“ genannt wird, ist dieser Fund von besonderem Interesse. Es wurden keine negativen Auswirkungen der Eisendüngung auf die Umwelt in Form von Spurengasen oder toxischen Algen beobachtet.

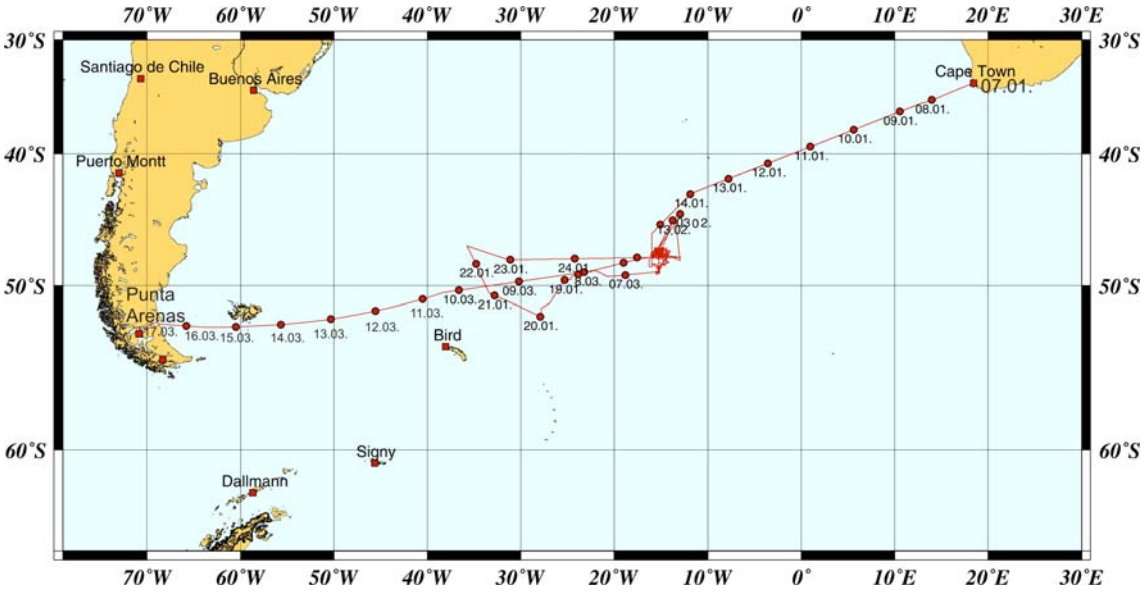

Abb. 1.1: Fahrtverlauf von Polarstern zwischen Kapstadt und Punta Arenas
Fig 1.1: Cruise track of Polarstern between Cape Town and Punta Arenas

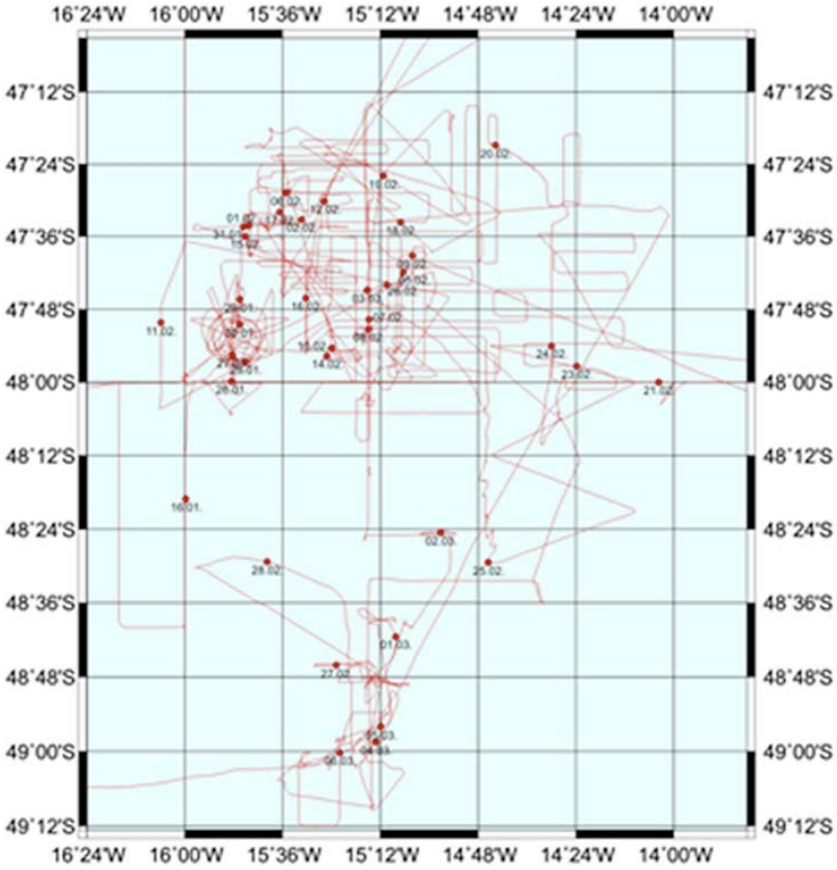

Abb. 1.2: Fahrtverlauf von Polarstern innerhalb des Wirbels
Fig. 1.2: Cruise track of Polarstern within the eddy

SUMMARY AND ITINERARY

Rationale

Cruise ANT-XXV/3 was a joint Indo-German iron fertilisation experiment the costs of which were equally shared by both countries. LOHAFEX (*loha* is the Hindi word for iron) was the third such experiment carried out from *Polarstern* that studied the growth and demise of a phytoplankton bloom induced by fertilising an area in the core of a mesoscale eddy along the Polar Front with iron sulphate. In contrast to previous experiments LOHAFEX was carried out in the productive south-western Atlantic of the Antarctic Circumpolar Current (ACC). This region is closer to land masses than other parts of the ACC hence fertilised by iron from natural sources supplied by contact with the Antarctic Peninsula and its various islands, in particular South Georgia, as well as dust from Patagonia and melting icebergs emanating from the Weddell Sea. Phytoplankton of this region comprise more fast-growing coastal species that are expected to respond more vigorously to iron input than the slower-growing, thicker-shelled oceanic diatom species studied in previous fertilization experiments. Studies of the sediments underlying this region have shown that diatoms typical of productive coastal regions – spore-forming *Chaetoceros* species – dominate the microfossil assemblage and extend downstream well to the East of South Georgia where they are eventually replaced by diatom ooze dominated by the heavily silicified species *Fragilariopsis kerguelensis* and *Thalassiothrix antarctica* that are both characteristic of the ACC.

During the last glacial maximum, however, sediments dominated by *Chaetoceros* spores extended across the entire South Atlantic Sector of the ACC indicating that the current high-productive zone under the influence of coastal plankton species extended eastward to South of Africa. This was due to the greater iron supply during the cold, dry glacials when much more iron-rich dust was transported to the Southern Ocean than during the warm, wet interglacials, reflected both in the cores of ocean sediments but also in continental ice cores. Hence this region will have sequestered much more atmospheric CO_2 than today and could well be one of the major sinks of glacial CO_2 that are still being looked.

Iron fertilization experiments are the equivalent of perturbation experiments carried out by all disciplines of science to study the structure and functioning of systems too complex to be analysed by observation alone. Hence the overarching goal of this interdisciplinary cruise was to further our understanding of how open ocean ecosystems function and how the organisms of the plankton interact with one another and with the environment to drive biogeochemical cycles and sinking of particulate matter to the deep sea. Artificial iron fertilisation simulates natural processes that introduce iron to iron-limited, land-remote ocean waters. The phytoplankton respond by increasing growth rates but accumulation of biomass is dependent on a range of

physical, chemical and biological factors that together determine the characteristics of the growth environment. However, accumulation rate of biomass is the balance between growth and loss rates due to mortality of algal cells and eventual breakdown of organic matter by pelagic heterotrophs: bacteria, protozoo- and metazooplankton on the one hand, and sinking out of particles to the deep sea on the other. We intended studying the relationship between growth of the phytoplankton and the concomitant effects of grazing and breakdown on the inventories of biogenic elements and monitoring vertical flux by deploying neutrally buoyant sediment traps and an Underwater Video Profiler (UVP), an optical instrument that photographs particles *in-situ* down to 3,000 m depth.

A major aim of the cruise was to investigate the fate of iron fertilised bloom biomass in a productive region of the ACC: is their biomass retained in the surface layer and converted back into CO_2 by bacteria and zooplankton or does at least a part of it sink out, thereby removing significant amounts of CO_2 from the atmosphere and storing it in the deep ocean. The answer to this question is of relevance to understanding past climate cycles but also to the feasibility of using artificial iron fertilisation of the ACC as a technique to mitigate global warming caused by anthropogenic accumulation of atmospheric CO_2.

Itinerary

Polarstern left Cape Town punctually at 20.00 on 7 January 2009 with all 49 participants and equipment on board, thanks to the excellent logistics of the AWI. The interdisciplinary, international scientific crew of physical, chemical and biological oceanographers comprised 29 participants from India, 10 from Germany, 3 from Italy, 2 each from Spain and the UK and 1 each from Chile and France.

Past experience has shown that the closed core of a mesoscale eddy formed by a frontal jet provides the best conditions to carry out such an experiment because the fertilized patch is retained within it for the lifetime of the eddy which is generally several months. Hence the decision on which eddy to select can only be taken shortly before the experiment. We had targeted the eddy field north of South Georgia, where meso-scale, persistent eddies had appeared in altimeter images of sea surface height in previous years and because the region is well inside the high productive zone. Shortly after leaving Cape Town the experiment was challenged by an organisation known as the ETC Group and put on hold by the German Ministry for Education and Research in order to clarify whether it met the conditions for legitimate scientific research outlined by the UN Convention on Biological Diversity and the London Convention on Ocean Dumping drawn up in May and November of 2008, respectively.

The time during the first 3 weeks of the cruise was spent in inspecting several eddies that had been under surveillance over the past months for their suitability for the experiment. The first was a promising clock-wise, hence cold-core eddy located at 48°S 15°W on the flank of the Mid-Atlantic Ridge. The same frontal jet formed an adjacent warm-core eddy. The ship's track was deviated only slightly to cross the

core of the cold-core eddy where the trial station was carried out on 16 January. As indicated by satellite images, chlorophyll concentrations were moderately high within the eddy (0.7 mg Chl m^{-3}) and distinctly higher than values further to the East and North. The ship then proceeded westward and southward to visit one of several large icebergs visible in satellite images. It was found to consist of an extensive field of ice rubble surrounding several medium-sized icebergs that were evidently formed by the collapse of a single, large iceberg of a few km length. Several stations were taken within and around the ice field over the course of a day (19 January) in order to assess the vertical extent of melt-water and its effect on the plankton. The reason for the iceberg survey was to ascertain the feasibility of carrying out a process study in such a site in case permission was not granted to go ahead with the experiment. The profiles taken indicated small-scale heterogeneity which would have rendered quantification of the processes difficult; besides, the impact on chlorophyll concentrations, which were only slightly higher than in the surroundings, was insufficient for the purposes of a perturbation experiment. So this “Plan B” was not considered a good option to the fertilization experiment.

After inspecting an eddy further to the South, which was found to be too close to the EEZ of the South Sandwich Island arc, *Polarstern* headed for the eddies north of South Georgia. Modelling studies based on the altimeter images indicated that these eddies were not stable, which was confirmed by ADCP transects across 2 of them that showed that they lacked closed cores and would have “leaked” the patch out in the form of a streak had we conducted the experiment in one of them. We therefore decided to go back to the first eddy at 48°S 15°W which was clearly the most suitable eddy in the entire region for the following reasons: 1) it had a closed core, 2) the underlying sediments contained *Chaetoceros* spores indicating that it was still under the influence of coastal plankton and within the productive zone, albeit at its eastern border, 3) the pelagic system in it was representative of the entire region we had traversed. The plankton characteristics of the region included a) very low silicic acid concentrations, b) moderate chlorophyll concentrations c) phytoplankton dominated by non-diatomaceous, small forms, d) zooplankton represented by a large population of copepods consisting mainly of late larval stages of a single species (*Calanus simillimus*), e) the amphipod *Themisto gaudichaudii* as the main predator with salps and other large zooplankton conspicuous by their relative absence.

We reached the eddy on 25 January and deployed a drifting buoy tethered at 30 m depth in the centre of its core and took the first long station to determine the initial conditions close to it. On 26 January the green light to proceed with the experiment was received from the Ministry while we were still occupied with the station. After filling the tanks with iron sulphate and sea water, another buoy was deployed closer to the centre (determined from the trajectory of the first buoy but only 2 km from it) around which a 300 km^2 circular patch was fertilized with 2 tonnes of dissolved iron (10 tonnes of granular $FeSO_4$) the next day. The patch circled within the eddy twice during the first 3 weeks and then moved southward as it was squeezed out of the collapsing eddy during the last 2 1/2 weeks of the experiment. Unfortunately the buoys did not keep track of the patch so new buoys had to be deployed to mark its

centre. After 18 days the patch was re-fertilized with an additional 2 tonnes of dissolved iron.

The processes occurring in the patch were followed with measurements of physical, chemical and biological parameters at regular intervals (the in-stations) and compared with the situation in outside waters (out-stations). Neutrally buoyant sediment traps that surface and can be retrieved at pre-programmed times, were deployed at regular intervals to intercept sinking particles at 200 and 400 m depths inside and outside the patch. Most of the 39 days of the experiment were spent in the proximity of the patch either taking in- or out-stations or transects through the patch. The ship had to leave the eddy twice to avoid storms and one transect was taken across the neighbouring warm-core eddy for comparison with the LOHAFEX eddy. The ship left the patch after the last in-station on 6 March and arrived punctually on the 17 March in Punta Arenas.

Summary of the results

Within the first 2 weeks, chlorophyll concentrations doubled to 1.5 mg m^{-3}, but, unlike previous experiments, silicic acid was present at limiting concentrations hence prevented diatoms from accumulating biomass. Small flagellates (<10 μm) contributed most of the phytoplankton biomass, which was maintained at about the same level throughout the 39-day experiment. The second fertilization had no noticeable effect on growth rates or biomass of phyto- or bacterioplankton. Apparently, the main reason why biomass did not build up to higher levels was due to heavy grazing of the large copepod population. Incubation experiments indicated that the copepods increased their feeding and faecal production rates inside the patch. Faecal pellets were recycled within the surface layer and did not contribute significantly to vertical flux as indicated by trap catches. However, daily sinking losses estimated from Thorium isotope measurements were quite high within the eddy but essentially the same inside and outside the patch. Thus, fertilization of this type of community had little effect on vertical flux. An unexpected finding, revealed by horizontal tows of the Rectangular Midwater Trawl, were the much higher densities inside the patch of the predatory amphipod *Themisto gaudichaudii*, which preys on salps and copepods. As little is known of the ecology of this amphipod, which is the main food of squid in the northern ACC and has been called the “krill of the north”, this finding is of particular interest. No adverse environmental effects in terms of trace gases and toxic algae were observed due to iron fertilization.

2. WEATHER CONDITIONS

R. Hartig Deutscher Wetterdienst

Polarstern left Cape Town on January 7, 2009 sailing southwest bound for the southern Atlantic Ocean. During the first days weather was dominated by a low pressure system giving westerly's of 6 to 7 Bft and up to 4 m sea swell. Two days later conditions improved. Cold fronts alternating with high pressure ridges produced winds about force 5 from west and 3 - 4 m swell for some days. On 15 January scientific work started with the survey of a first eddy (vertical column of rotating water) at 47°S 16°E. High pressure influence caused moderate easterly winds and light to moderate swell.

After survey was finished in this area *Polarstern* headed for 57°S 25°W. This region was covered by lots of growlers, bergy bits as well as some big icebergs. On January 18 and 19 dense fog dominated the weather down here, due to northerly winds of about 4 Bft generating a flow of warm air (+7°C) over cold water (+4°C).

On January 20 *Polarstern* sailed towards a position north of South Georgia in order to survey another eddy in the southern ocean. Wind from northwest to southwest of force 7 to 8, occasional rain combined with poor visibility and rough sea caused uncomfortable weather conditions. As this eddy did not suit the scientific needs *Polarstern* returned' to the previous one on January 22. Westerly's between 5 and 8 Bft, occasional rainfall with poor visibility and swell between 3 and 5 m were observed enroute.

From January 26 to March 06 *Polarstern* worked in the LOHAFEX area between 47°-49°S 14°-16°W. Highly unstable weather conditions characterize these weeks. Depressions and high pressure ridges changed periodically. Westerly winds outnumbered other wind directions and wind force varied from force 5 to 7 Bft. Swell of 2.5 to 5 m was observed in this period. Winds veering to northwest produced poor visibility (advection of warm air over colder water). Vice versa visibility improved when winds were backing to southwest.

On February 2/3 and February 12/13 *Polarstern* sailed some 200 nm northeast to avoid any kind of damage due to upcoming severe storms. Even in the less stormy region we registered north-westerly winds force 9 and a swell up to 6 m.

The atmosphere became more turbulent by the end of February when a number of severe storms hit the LOHAFEX area. Winds of force 10 Bft (10 min mean) as well as short periods of hurricane-force 11 Bft with gusts of 12 Bft were registered (Fig. 2.1).

Wind speed registered and significant sea state observed during the LOHAFEX experiment is shown in Fig. 2.2 and Fig. 2.3. A second graph shows the observation data of the EIFEX experiment in 2004. It clearly can be seen that the wind speed was higher during the LOHAFEX period than during EIFEX while sea state appeared to be higher during the EIFEX experiment. A possible reason for this could be the fact that the sea state combines the locally produced waves and the swell running in from afar.

Scientific work ended in the afternoon of March 06. *Polarstern* then headed for Punta Arenas, Chile. Within in the first hours of our way back gale from west to northwest and rough sea were observed. However, wind and swell were already decreasing during the night from March, 7 to 8 the vessel still had to encounter rogue waves which caused remarkable heeling. As soon as the next day the wind abated and sea decreased to 2 m. From March 10 on the strong west drift dominated again with varying weather conditions and moderate to rough sea.

On March 17 *Polarstern* arrived in Punta Arenas where this expedition ended.

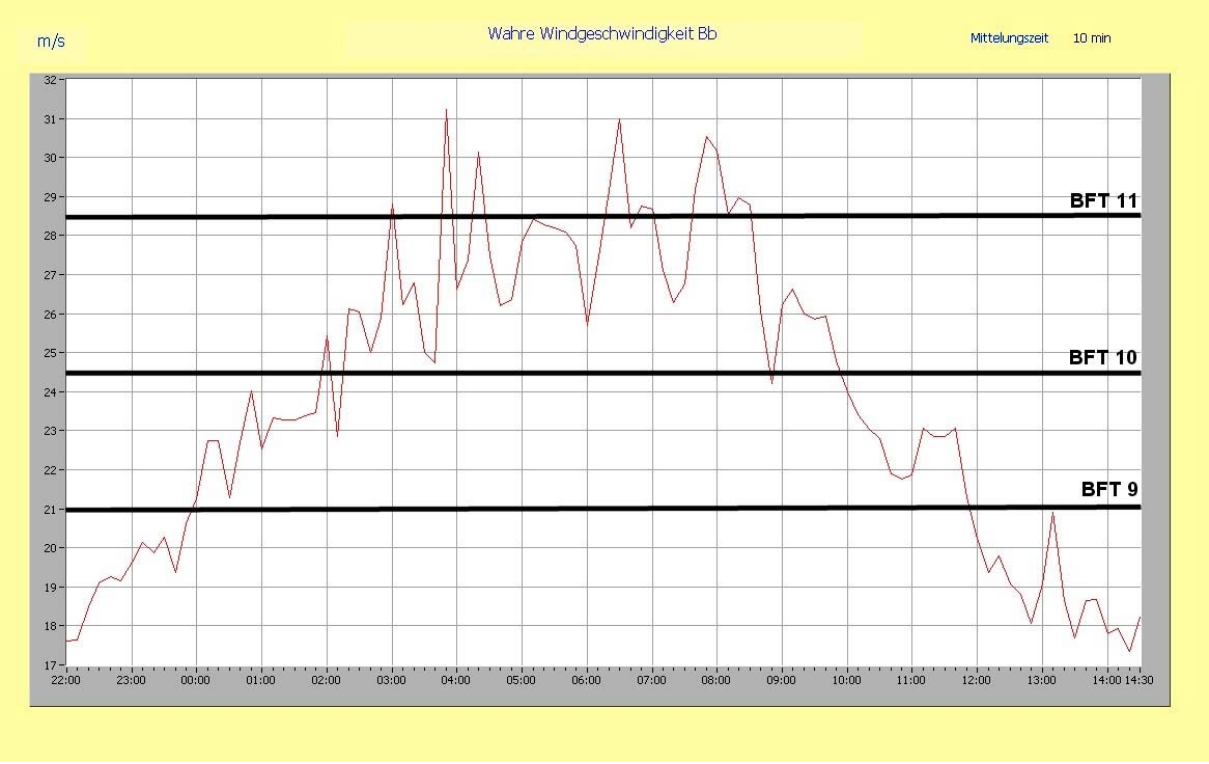

Fig. 2.1: Registration of wind speed during severe storm from February 27 to 28, 2009

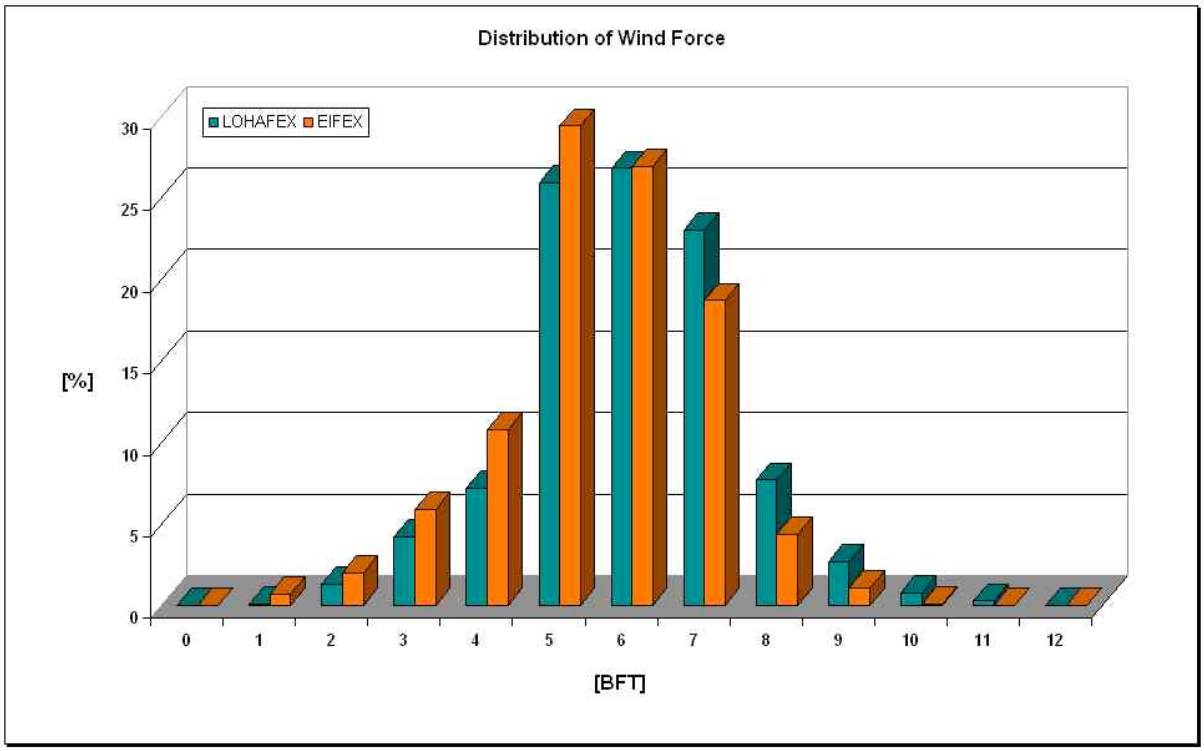

Fig. 2.2: Distribution of wind force during Lohafex and EIFEX experiment

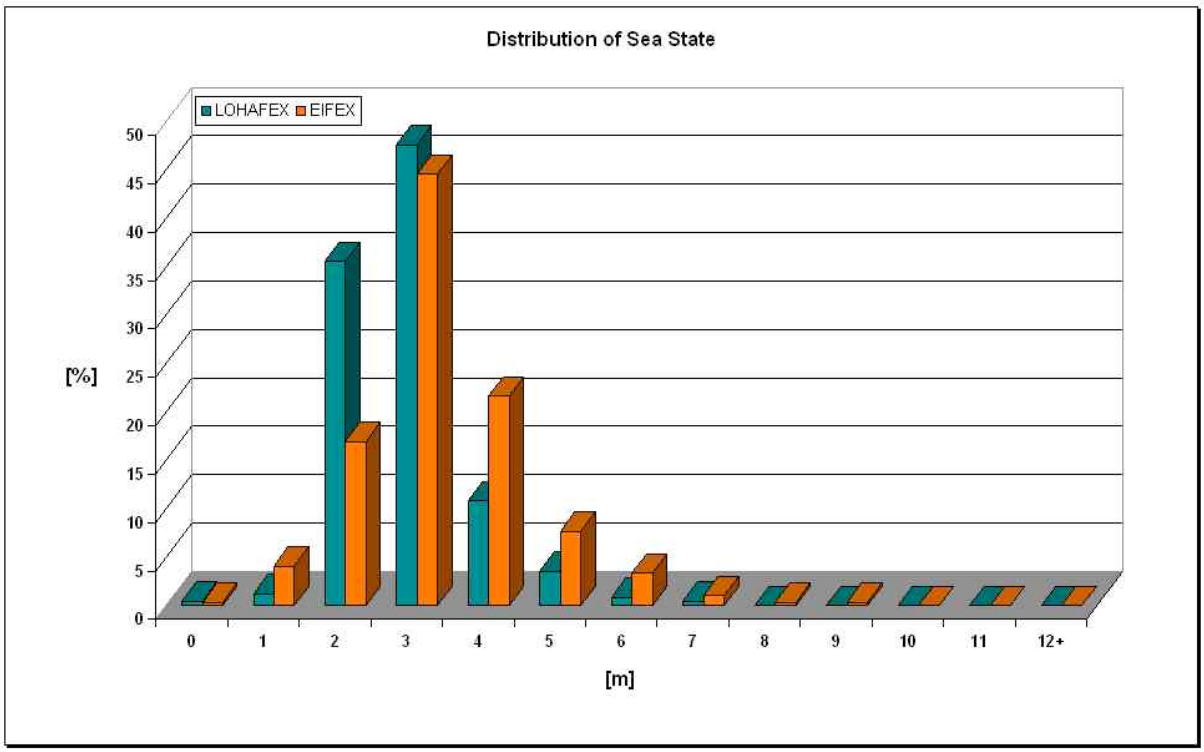

Fig. 2.3: Distribution of sea state during Lohafex and EIFEX experiment

3. PHYSICAL OCEANOGRAPHY

V.S.N. Murty[1], A. Almeida[1], P. Narvekar[1], A. Methar[1], A. Kankonkar[1], I. Borrione[2], P. Vandrommes[3], F. d'Ovidio[4], M. Ribera d'Alcalà[5], D. Wolf-Gladrow[2]

[1)] NIO
[2)] AWI
[3)] UPCM-CNRS
[4)] ISC-Paris
[5)] SZN

Introduction and objectives

The iron fertilization experiment LOHAFEX was planned to carry out in a meso-scale cold core eddy in the western Atlantic sector of the Southern Ocean. The selection of the suitable eddy was one of the main objectives of the Physics group (*Objective 1*). First of all it had to be stable for at least 2 months. Further selection criteria included its chemical (nutrients) and biological (plankton assemblage) nature and location (north of 50°S). The stability of eddy candidates was investigated before and during the cruise by Francesco d'Ovidio (ISC, Paris) who applied a numerical model using data from satellite altimeter observations. He exploited methods from the chaos theory toolbox including Lyapunov exponents for application to the study of eddies appearing and dispersing in altimeter images.

After selecting a suitable eddy, its centre had to be located (*Objective 2*). The main methods were satellite images of sea surface height (SSH), ADCP (Acoustic Doppler Current Profiler) sections, and underway temperature and salinity measurements. The fertilized patch had to be followed during the course of the experiment (*Objective 3*). For this objective a whole suite of methods and instruments were used, including drifter buoys, ADCP, CTD, SCANFISH. In order to understand the time development of the fertilized patch the eddy and its environment had to be examined (*Objective 4*). This could be done with larger scale CTD and ADCP sections and deployments of several buoys.

Work at sea

3.1 Satellite altimeter derived sea surface height anomaly

The prior requirement was examining the satellite derived altimeter Sea Surface Height Anomaly (SSHA) images for a longer period. Accordingly, the SSHA maps generated at Colorado Center for Astrodynamics Research (CCAR) website (http://argo.colorado.edu/~realtime/gsfc_global-real-time_ssh/) were downloaded onboard and examined in detail; SSHA maps were composites over a period of 2 days. The SSHA images were examined in detail starting from November 2008 to understand the history and evolution of eddies found in the region of interest. For various scientific reasons, the suitable cold core eddy (with an adjacent warm core eddy) was selected at 16°W and 48°S in the central South Atlantic. An examination of the SSHA maps from November 2008 onwards revealed that this cold core eddy was persistent and consistent in its location (together with its nearby counterpart, the

warm core eddy). Fig. 3.1 shows the snap shot of SSHA on 7 January 2009 from the western Atlantic to the central Atlantic; the red rectangle box highlights the area in which the chosen cold core eddy is located for the Iron Fertilization.

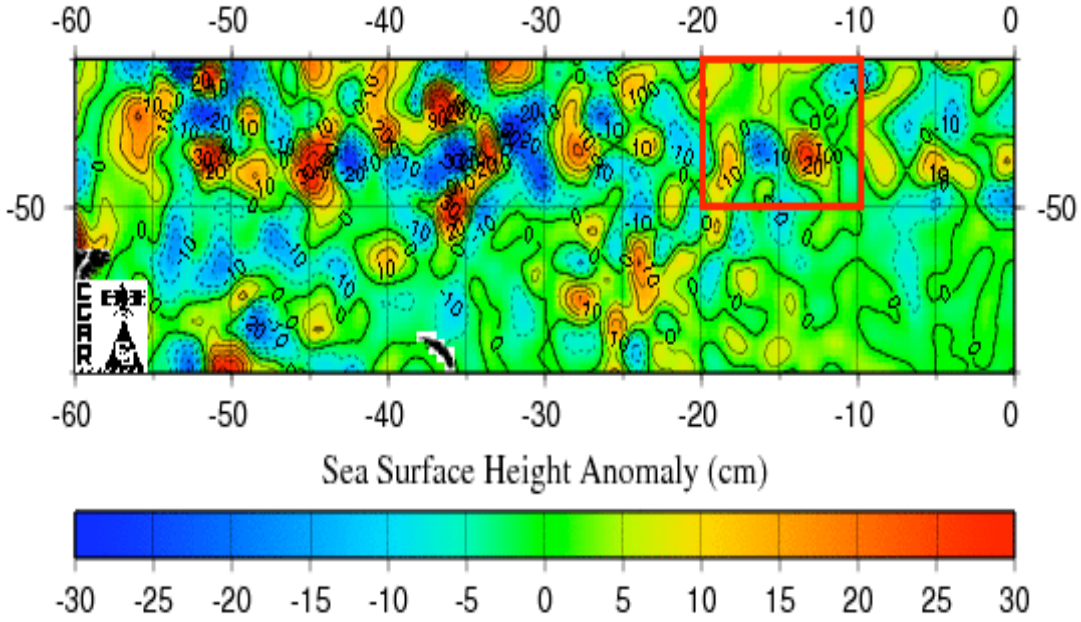

Fig. 3.1: Real-Time Meso-scale Altimetry image as on 7 January 2009. The red rectangle highlights the area where the selected cyclonic eddy was located.

The SSHA maps were downloaded on day-to-day basis to look into the variability in the eddy characteristics and the possible shift in its centre. The SSHA maps were monitored and the ADCP currents were superimposed to see whether the observed currents agreed with the expected geostrophic flow pattern. Similarly, the drifter trajectories were superimposed on the eddy structure. Drifters showed inertial oscillations (of period $T=2\pi/f$, where f is the Coriolis parameter = 16.1 h at 48°S) which are generated by the prevailing stronger winds over the LOHAFEX area. On the other hand, the SSHA maps represent the water characteristics of the entire water column and particularly reflect the thermocline variability. Composite SSHA images/drifter tracks were regularly observed till the end of experiment, showing a clear waning of the cold core eddy with weaker gradients in the sea surface heights around its center (for example, Fig. 3.2 a-c)

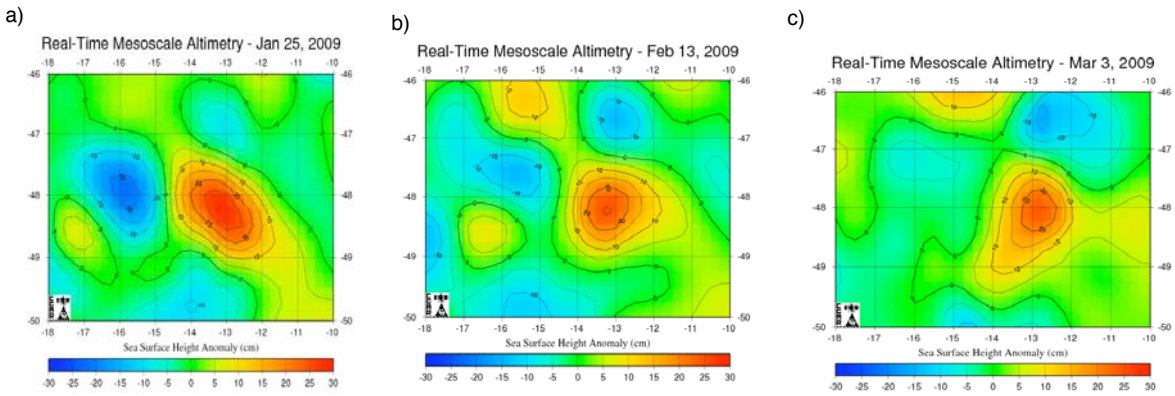

Fig. 3.2: SSHA images of the selected area on (a) 25 January 2009, (b) 13 February 2009 and (c) 3 March 2009. The comparison of the three images indicates a clear weakening of the cyclonic eddy (blue colour) centered approximately at 16°W 48°S.

3.2 Hydrographic station work with conductivity-temperature-depth (CTD) measurements and water bottle sampling

During LOHAFEX, the SBE 911 plus CTD (SeaBird Electronics, USA) was used extensively to measure temperature and conductivity (salinity) profiles of the water column at depths ranging between 100 m and 4000 m. The CTD system was mounted onto a SBE32 bottle carousel with 24 *12 litre* bottles. A UVP (Underwater Video Profiler, compare Section 16) to obtain the images of living organisms was also fitted to the CTD rosette thus reducing by one number of total bottles. The CTD sensor system was fitted with two sets of temperature (Sr. No. 1373 & 2929) and conductivity (Sr. No. 3290 & 2490) sensors. A SBE 43 Dissolved Oxygen (Sr. No. 0743) sensor, a Wetlabs C-star light transmissometer and Dr. Haardt's fluorometer (Sr. No. 8060) along with a bottom altimeter with a range of 100 m were also attached. The temperature and conductivity sensors were pre-calibrated at the Seabird, USA with an arrangement to have these re-calibrated after the cruise for any possible drift during the LOHAFEX observational period. During the cruise, the sets of temperature and salinity sensors showed only small deviations and these deviations were consistent for the entire cruise period in the observed depth range. The water sampling was done for core chemical parameters and various other biological and bacterial studies and other experimental purposes. A sampling protocol was followed for all the sampling stations. Water samples from deeper depths (below 800 m) were also collected at several stations for salinity analysis using onboard AUTOSAL (Model No. 8400B, Guildline, Canada). A total of 153 CTD casts were carried out. Water sampling was done at 128 casts. There were 26 deep CTD casts below 1,000 m depth. CTD casts were made along shorter transects within the cold core eddy and also in the warm core eddy.

3.3 Underway measurements of currents with the vessel-mounted Acoustic Doppler Current Profiler (ADCP)

The vessel-mounted ADCP (153.7 kHz, RD Instruments, USA) was operated continuously throughout the cruise to collect underway current profiles. The bin size was selected at 4 m and the first bin value started from 18.96 m. The data acquisition was done using RDI VMDAS software with continuous pinging and the ensemble interval was fixed at 1 minute for Short-Time Average (*.STA file) and at 5 minutes for Long-Time Average (*.LTA). The data acquisition was done in Navigational Mode and data quality appeared to be good. The data has been stored on the PC's hard disk and from time to time, the acquired data were copied to another PC for preliminary processing and analysis. The WINADCP software programme was used to store the data during acquisition and also to export the data from the *.LTA files. The VM-ADCP had been calibrated during the ANT-XXV/2 cruise, just prior to LOHAFEX (ANT-XXV/3) and hence no special calibration survey was done during LOHAFEX. A glance of the acquired currents data during LOHAFEX across the shorter transects showed consistency in the currents pattern. The ship's navigational data was fed to the ADCP PC so that the data transformation from beam coordinates into Earth coordinates (East, North, Up directions) was done internally through the VMDAS software. The size of the data file was fixed at 1.0 MB for each STA and LTA file. The VM-ADCP was operated since the vessel left Cape Town on 7 January 2009. Longer ADCP transects were obtained from Cape Town to the LOHAFEX cold core eddy, and also from the cold core eddy to the far western longitudes in the Western Atlantic. Longer ADCP transects were also obtained during the return sailing of the vessel towards Punta Arenas. The ADCP currents data were used to identify the flow pattern of the cold core eddy along 16°W longitude and its centre. The eddy centre was identified with the zone of weaker currents over a stretch of 10 km. Occasionally, larger currents were noticed whenever the vessel took sharp turns and when the sea was rough with large swells and the vessel was tossing up and down. Also, whenever the GPS string was not available, the measured currents showed larger magnitudes equivalent to ship's speed. The *.LTA files were used to carry out preliminary processing and to present quick results. MATLAB routines were written onboard and current vector plots were prepared. The current vector plots at different depths (eg., 20 m, 40 m, … 100 m etc.) and also the vector plots for mean layers (eg. 20 - 40 m layer, 40 - 60 m layer, 40 - 100 m layer) were prepared. Consistency in the flow pattern was seen at each depth and in each layer. For example, Fig. 3.3 shows the ADCP current vectors at 100 m depth along the longitudinal cross-section of cold core eddy and along a section to the west of the cold core eddy.

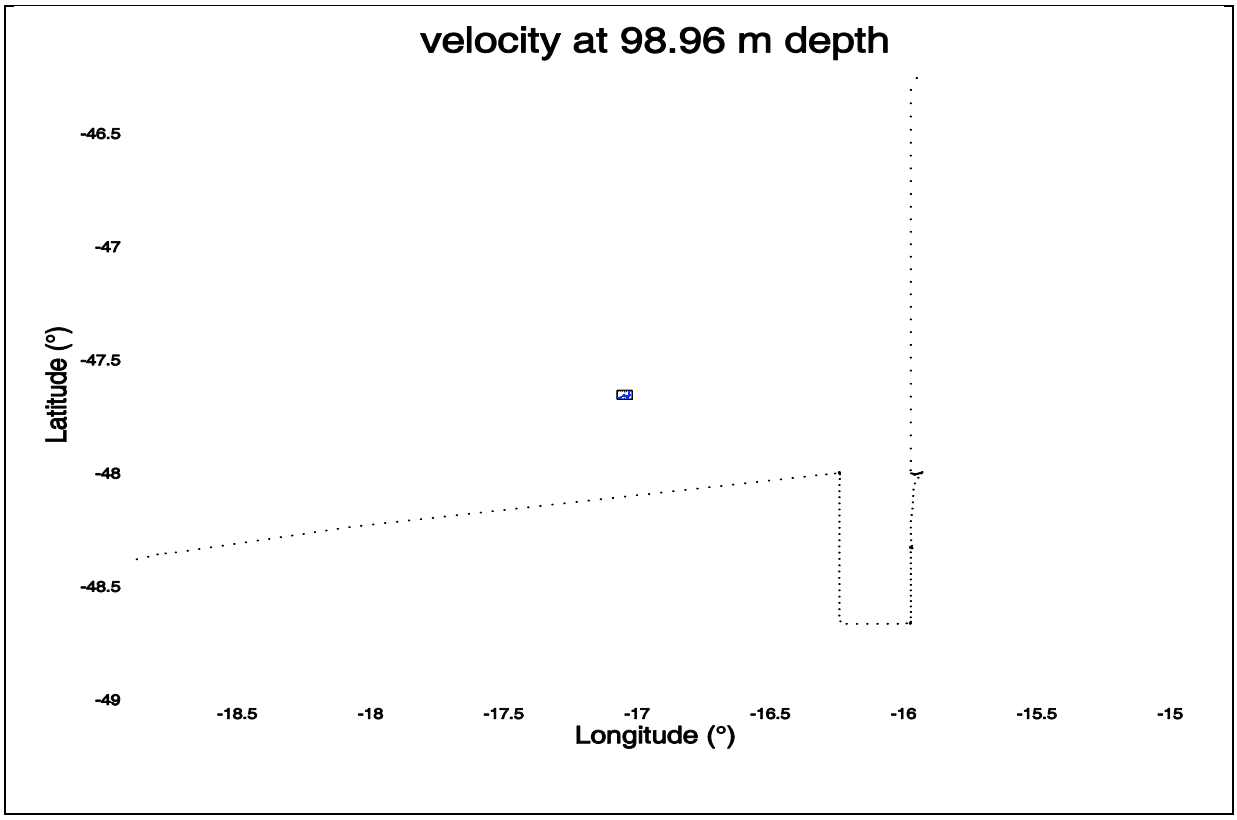

Fig. 3.3: ADCP current vectors at 100 m depth along the longitudinal cross-section of the cold core eddy and along a section on the southwestern side of the cold core eddy.

3.4 Drifter buoys

The drifters employed were of the WOCE SVP type with 16 inch surface floats with sensors for SST, battery voltage and submergence. The drogue consisted of a 7 meter by 36 inch Holey sock made of cordura material and centered at 30 m below surface. The buoy had a GPS receiver for its position tracking. It transmitted its position to the server in the USA every 10 minutes using the IRIDIUM telemetry. This signal was also received by the base station mounted onboard *Polarstern*. The base station in turn had a GPS receiver and received its position update ever 10 seconds along with the position from the drifter every 10 minutes. The base station had a problem in that every day it had to be power cycled to re-initialize its data reception from the server. Further, in rough weather it was noticed that the GPS position of the drifters were degraded and sometimes it was not possible to obtain the drifters' positions for a couple of hours at a stretch. The drifter position was also downloaded from the company's web site using internet onboard.

Initially only one drifter (#1) was deployed and later another drifter (#2) was deployed next to it at the cold core eddy centre. Both drifters traced each other very well through most of the time, which gave confidence that both the drifters were being subject to the same forcing. During the LOHAFEX cruise, iron fertilization was done twice. In order to track the movement of the fertilized patch, surface drifters were

deployed. 4 drifters were deployed in the LOHAFEX cold core eddy and one drifter was deployed in the warm core eddy to understand the nature of flow pattern in it. The drifters exhibited inertial oscillations within the centre of the cold core eddy and moved with the flow to the periphery of the eddy. After a couple of weeks as it was felt that drifter #1 had detached itself from the patch, it was recovered and redeployed in the patch (from then on called #1A).

The deployment details of the drifters are provided in Table 3.1. Drifter #3 provided excellent structure of inertial oscillation around the centre of the warm-core eddy (Fig. 3.4) but stopped communication after 6 days of its deployment. Near the end of LOHAFEX, two drifters left the cold core eddy and were lost to the large-scale flow pattern of the ACC beyond the warm-core eddy. These drifters (#1a and #4) gave interesting trajectories, which are being analyzed further to understand the dynamics of the warm core eddy, together with the dynamics of the LOHAFEX cold core eddy. One drifter (#5) was making perfect inertial oscillations on the southernmost boundary of the warm core eddy and was drifting to southern latitudes. Later this was also recovered and redeployed closer to the patch. At the end of the experiment, the drifters were not recovered and left for drifting further.

Tab. 3.1: Details of deployment drifter buoys during LOHAFEX

Drifter	**Date deployed**	**Time UTC**	**Lat**	**Long**
NIO #1	25.01.09	19:08	47° 59.70' S	15° 48.21' W
NIO #2	27.01.09	11:20	47° 56.01' S	15° 48.83' W
NIO #3	04.02.09	16:48	48° 13.78' S	12° 58.70' W
NIO #4	09.02.09	20:57	47° 54.26' S	15° 07.84' W
NIO #1A	20.02.09	10:55	47° 20.53' S	14° 44.57' W
NIO #5	27.02.09	16:44	48° 48.12' S	15° 14.04' W
NIO #5A	04.03.09	19:08	48° 58.61' S	15° 12.67' W

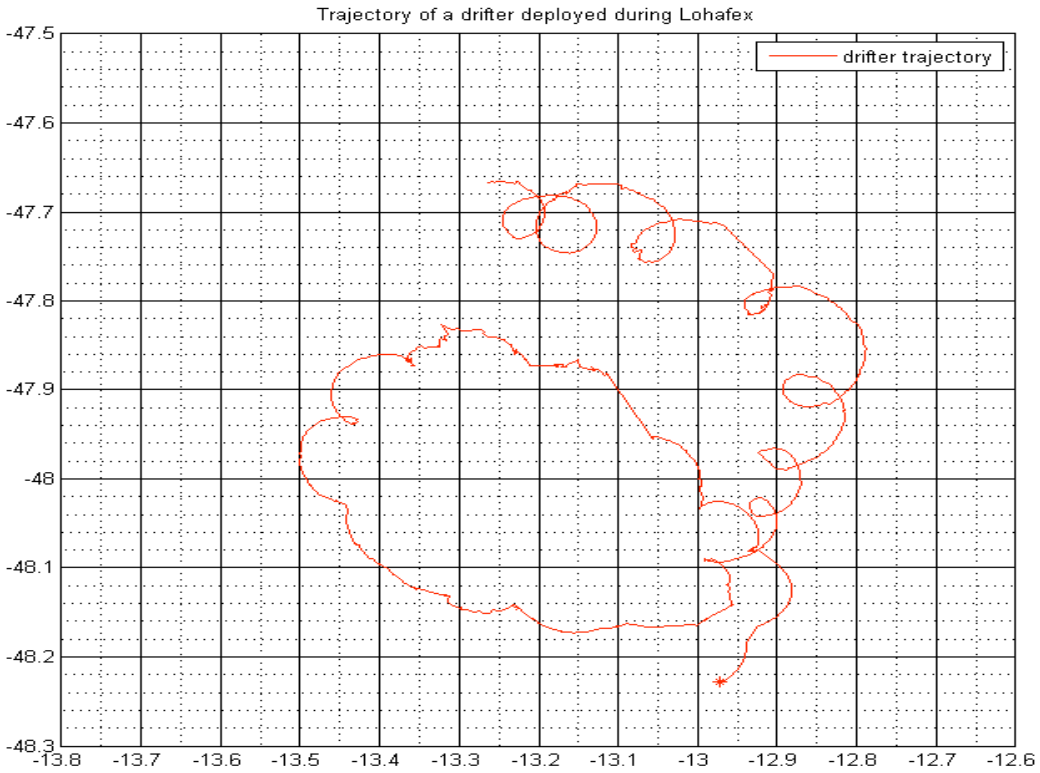

Fig. 3.4: Trajectory of drifter #3 deployed in the warm eddy

3.5 Measurements with the towed undulating vehicle 'SCANFISH'

The SCANFISH (MK II, EIVA, Denmark) was purchased for the LOHAFEX cruise in order to track the water properties in the upper water column within the fertilized patch. It is a wing-shaped body weighing around 120 kg (with instrumentation) and attached by means to a double armored conductive cable (approx. 10.5 mm) to a winch and towed behind the steaming ship. It has 2 electrically adjustable flaps at its rear. With the help of an active winch (KC, Denmark) it is made to undulate vertically through the upper water column. With a vessel speed of 4 knots it can undulate from 250 m to the surface with the undulation depths increasing or decreasing inversely to the vessel's speed. The SCANFISH was deployed with a dive rate of 1 m s^{-1} and was towed at ship speeds of 5 knots to give an undulation depth of 200 m. The SCANFISH has its own sensors for pressure, attitude and altimeter to provide feedback on its movement through the water column. The movement of the SCANFISH is controlled using the EIVA Flight software by feeding the relevant parameters into the software. The ship heading, GPS position and echo sounder data were fed from the ship's LAN to the Flight software through an Ethernet to Serial Port converter. Along with the data from the winch, the SCANFISH is able to calculate its position with respect to the vessel.

The SCANFISH is fitted with the following instrumentation

1. A SBE49 FastCat CTD with temperature, conductivity and pressure sensor.
2. SBE43 DO sensor for oxygen
3. C-star transmissometer sensor for light attenuation
4. Wetlabs FLNTU fluorometer and turbidity sensor for chlorophyll *a*
5. and the Fast Repetition Rate Fluorometer FRRF II from Chelsea

The data obtained from these sensors were logged in the NaviPac software from EIVA. This module was installed only after the ship left Cape Town.

The SCANFISH was deployed on three occasions and two surveys were conducted. On the first occasion when the SCANFISH was deployed, it was noticed that it was frequently getting towed upside down. Several attempts were made to correct its attitude, but after an hour of operation it was decided to bring it up to the deck to inspect it for its erratic behaviour. It was noticed that the cable was twisted and entangled. It was thought that this twist in the cable could have come about when the cable was removed from the winch drum by the manufacturers at the Cape Town warehouse for repairing the drum after the ANT-XXV/1 cruise. When the SCANFISH was brought on deck, several checks were done and finally it was found that one of the pins securing the flaps to the motor had fallen out. This was replaced and the cable cut and re-terminated once again by the ships technician on board. The SCANFISH was then tested and it responded well. Later during the cruise the SCANFISH was deployed twice successfully and it collected data for more that 30 hours each time. In the first attempt the Fv/Fm values from the FRRF were not logged as the driver for this was not ready by EIVA, however, all other sensors were logged. (The Fv/Fm ratio provides an estimate of the maximum efficiency of photo-system II (also termed photosynthetic efficiency) within dark-adapted phytoplankton cells, where Fv is the variable fluorescence and Fm the maximum fluorescence signal of dark-adapted cells). In the second deployment of SCANFISH, the new driver was installed and the complete data set for all the above sensors were logged. However as the number of parameters being logged in this SCANFISH configuration is very large, the software needs further modification to accommodate all the parameters being logged.

Initial comparison of the SCANFISH data logged along with other underway instruments showed a good relationship with other underway instrumentation. In the laboratory, the value of Fv/Fm was consistently lower (0.32) than another FRRF instrument (0.42) drawing seawater from the ship's moon pool. However this could be attributed to the source of water drawn; as one was fresh from the moon pool, whereas the other was from the ships pumped seawater supply. Once the SCANFISH was deployed, it was found that the Fv/Fm values ranged from 0.5 to 0.1 for surface to deeper depths. It was also noticed that the Chlorophyll-*a* data from the fluorometer showed consistently higher values (1.2 mg Chl-*a* m^{-3}) than the values obtained by extraction (0.5 mg Chl-*a* m^{-3}). However it was assumed that the relative values were consistent and the values did not change from one undulation profile to another. The temperature, conductivity, pressure, and oxygen data quality was assumed to be good as the respective sensors were calibrated prior to the cruise.

Preliminary results

Preliminary processing of the CTD data was done onboard. The analysis showed that the waters of the cold core eddy in which LOHAFEX was conducted, are characterized with three distinct water masses. The top 200 m layer showed variability in both temperature and salinity during the cruise period. The intermediate layer between 200 m and 1500 m (and at some stations up to 1850 m to 2000 m) has relatively constant low temperature (< 2°C) and slightly increasing salinity with depth. The deep layer (> 1500 m) is cold and less saline, with decreasing values of temperature and salinity with depth nearer to seabed. The mixed layer depth (MLD) is varied between 50 m to 75 m. The watermass structure of the cold core eddy was persistent through the cruise period. At the southern edge of the cold core eddy, the MLD was deep up to 100 m on the last days of the observations. Fig. 3.5 shows the typical vertical profiles of temperature, salinity, density and chlorophyll *a* at a station (#114) in the vicinity cold core eddy. The water characteristics of the nearby warm core eddy has distinct water mass structure with deeper MLD up to 100 m and warm and low saline waters at the eddy centre.

The access to on-line available satellite information (SSHA and ocean colour) turned out to be extremely useful and led, for example, to a very fast identification of the eddy centre.

Another new feature compared to former iron fertilization experiments as, for example, EIFEX (2004) is the near real-time numerical simulation of flows using satellite information. The prediction of the stability of various eddies was crucial for the choice of a suitable eddy for the fertilization experiment.

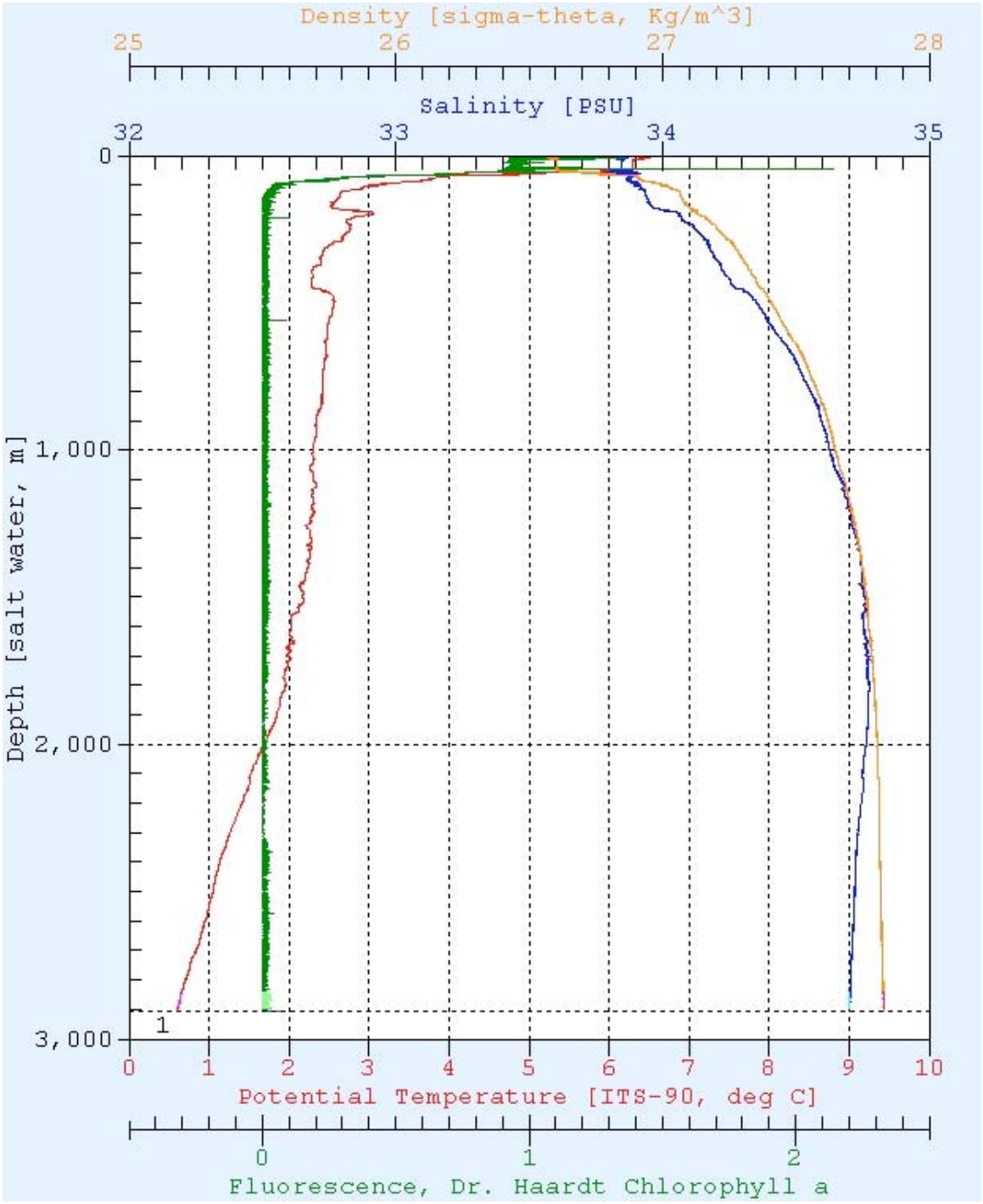

Fig. 3.5: Vertical profiles of CTD temperature, salinity, density (Sigma-theta) and chlorophyll a at a station in the vicinity of cold core eddy.

The deployment and re-deployment of several drifter buoys has been extremely useful to elucidate the time development of the fertilized patch and the eddy as a whole. Although the deep-rooted eddy was a relatively stable feature during LOHAFEX, the surface flow was quite complicated due to strong and variable wind forcing causing inertial oscillations, Ekman transport, vertical shear, and loss of 'eddy

water' to the strong currents of the adjacent Polar Front. In order to better characterize the vertical shear in the upper 100 m it might be useful to apply buoys with different drogue depths.

Acknowledgements

Thanks to Captain Stefan Schwarze for giving advice for when to deploy instruments and when not and to his crew. Special thanks to Helmut Muhle for taking care of the CTD from time to time. Thanks to Uwe the Chief Mate and Reiner, the bosun and his team for deploying and recovering the SCANFISH flawlessly. Special thanks to Frank Himmel, onboard technician for carrying out the re-termination of SCANFISH cable and to Nasis Ilias for installing the software required for taking screen shots of the Simrad Fish Finding echsounder display. Thanks to Astrid Bracher for sending satellite images.

4. SULPHUR HEXAFLUORIDE

V. Desai, R. Roy, S.W.A. Naqvi NIO

Objective

To map the iron-fertilized patch and to determine the degree of dilution of fertilized water through horizontal and vertical mixing.

Work at sea

We used a SF_6 saturation system fabricated and kindly made available to us by Dr. Phil Nightingale of Plymouth Marine Lab. This system consists of a stainless steel equilibrium chamber in which a shower of seawater comes in contact with a headspace of pure SF_6. The SF_6-saturated water was then mixed with seawater spiked with $FeSO_4$ and released to the propeller wash of the vessel. The pumping/mixing rate was adjusted to release about 500 g of SF_6 over 300 km^2 area. SF_6 saturation was monitored in the outflowing water using a gas chromatograph equipped with a thermal conductivity detector (TCD). A Porapak-Q column was used for separation of gas mixtures. The variability of SF_6 concentration in the outflowing water was generally within <20 % of the saturation value. Because of the equipment malfunction, SF_6 could not be added during the second half of the refertilization carried out after about three weeks of the first one.

Mapping of the fertilized patch: Discrete samples were collected both from the ship's underway water supply (300 samples) as well as at several stations located inside the patch (200 samples from casts to 100 m depth). Glass-stopped flasks with an outlet at the bottom were used for sub-sampling, and the samples were introduced into a stripping chamber avoiding any contact with air. SF_6 was purged using a stream of nitrogen and trapped for 10 minutes in a stainless steel column dipped in liquid nitrogen. The trap-column was then inserted in hot water and the desorbed SF_6 was separated over a MS 5A column and analyzed using a gas chromatograph equipped with an electron capture detector (ECD). Measurements were calibrated against SF_6 gas standards diluted in oxygen-free nitrogen.

Preliminary results

Due to the variability of SF_6, in saturated water the data could only be used in a semi-quantitative way. Nevertheless, these measurements along with other data (surface chlorophyll and photosynthetic efficiency (f_v/f_m)) were very useful for marking the fertilized patch. As expected, SF_6 concentrations within the fertilized patch decreased with time, but remained above background at the last in-patch station (Fig. 4.1). The decrease in SF_6 toward the surface is presumably due to air-sea gas exchange. Out-patch station values were close to background.

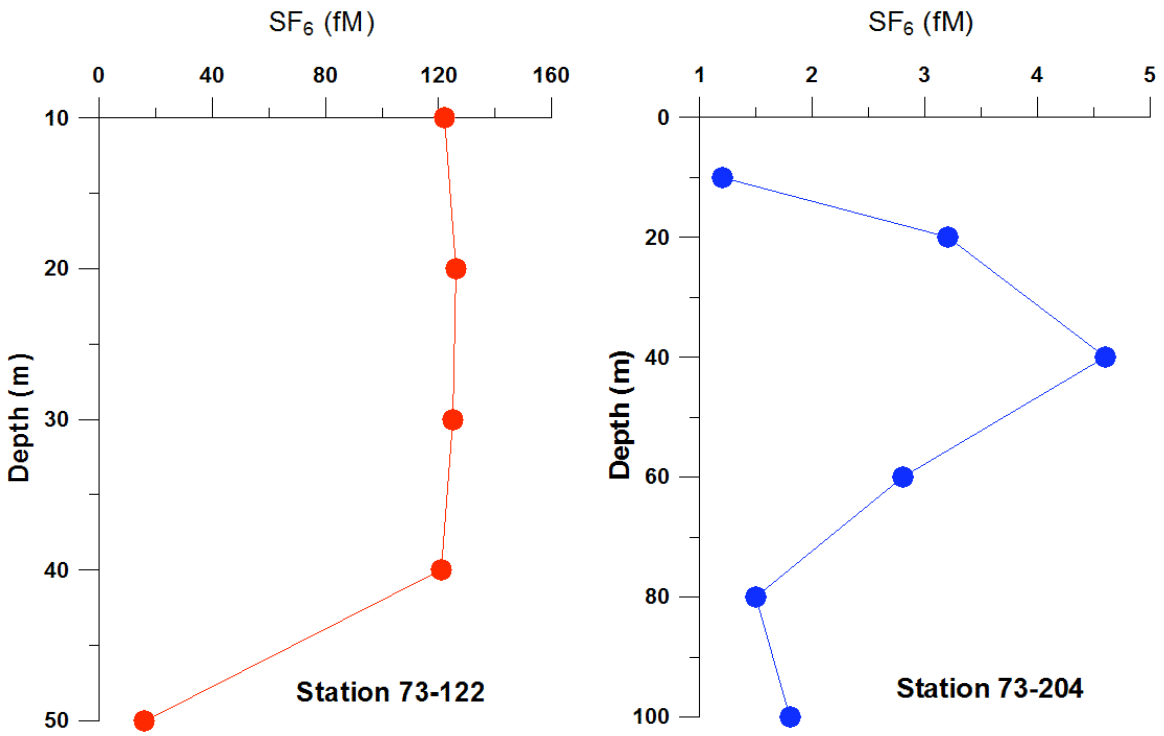

Fig. 4.1: Vertical profiles of SF_6 just after the first fertilization (station 73 - 122) and toward the end of the experiment (station 73 - 204).

5. MACRO NUTRIENTS

A.K. Pratihary, D. Baraniya, S.W.A. Naqvi NIO

Objective

To investigate variations in macronutrients in the water column as a result of iron fertilization.

Work at sea

Nutrient samples were collected from standard depths to 3000 m at all major stations located inside as well as outside the fertilized patch. In addition, sampling was also performed to 200 m depth at the stations forming an east-west and another north-south sections across/along the fertilized patch. The samples were stored in plastic bottles for no more than 2 hours before analysis using a SKALAR segmented flow autoanalyzer using standard procedures. The precision of measurement was ±0.05 μM for NO_3^-, ±0.004 μM for NO_2^-, ±0.005 μM for NH_4^+, ±0.003 μM for PO_4^{3-} and ±0.5 μM for SiO_4^{4-}. In addition to these depth profiles, a number of nutrient measurements were also made on discrete samples collected from the ship's underway system that drew water from 10 m depth. Samples were also collected and frozen for the analyses of Total N and Total P in the shore laboratory (at NIO).

Preliminary results

The eddy selected for fertilization had low SiO_4^{4-} concentrations (0.5 - 2 μM) in surface waters; by contrast, concentrations of NO_3^- (19 - 20 μM) and PO_4^{3-} (1.2 - 1.3 μM) were quite high. We assume that observed SiO_4^{4-} depletion was due to production (by diatoms) in spring/early summer (i.e. during the period preceding our experiment). The most important consequence of low SiO_4^{4-} concentration was that diatoms did not grow to the extent observed in previous OIF experiments (including the SOFEX north patch that was located within the Subantarctic zone). Nitrate concentrations within the fertilized patch decrease substantially (by about 2.5 μM) after the first fertilization; such was also the case with PO_4^{3-} (Fig. 5.1). Chlorophyll concentrations increased at the same time indicating algal uptake of nutrients stimulated by iron enrichment. Similar decreases in NO_3^- and PO_4^{3-} were not observed after the second fertilization carried out three weeks after the first one. The overall decrease in NO_3^- is comparable to that observed during EIFEX even though the EIFEX bloom was dominated by diatoms. A striking aspect of nutrient distributions was the frequent appearance of maxima in NO_2^- and NH_4^+ profiles between 80 and 100 m depths. The ammonium maximum was presumably due to its excretion by zooplankton (largely copepods and amphipods) which were abundantly present around these depths. The NO_2^- maximum could arise due to oxidation of this NH_4^+ (nitrification) as well as incomplete assimilatory reduction of NO_3^- in the algal

cells. Nitrite concentration at 80 - 100 m increased after fertilisation, peaked around 9 - 12 days, and decreased thereafter perhaps due to both Fe saturation in surface waters and also oxidation to NO_2^- by the nitrifiers. Ammonium concentration at 80 - 100 m increased after the first fertilisation as the grazers proliferated with time. It reached a maximum of 3.5 μM at the end of the experiment. These results demonstrate that much of the nutrients taken up by the phytoplankton were recycled in the upper water column.

The integrated NO_3^-+ NO_2^- inventory to 200 m decreased from 4.61 mol m^{-2} at PS73-114 to 4.03 mol m^{-2} at PS73 - 192 (Fig. 5.2), corresponding to the production of 1.4 gC m^{-2} d^{-1}. Assuming that wintertime NO_3^- concentration at the surface was ~25 µM (corresponding to the concentrations observed at ~150 m at the two stations), comparable production should have occurred before our observations.

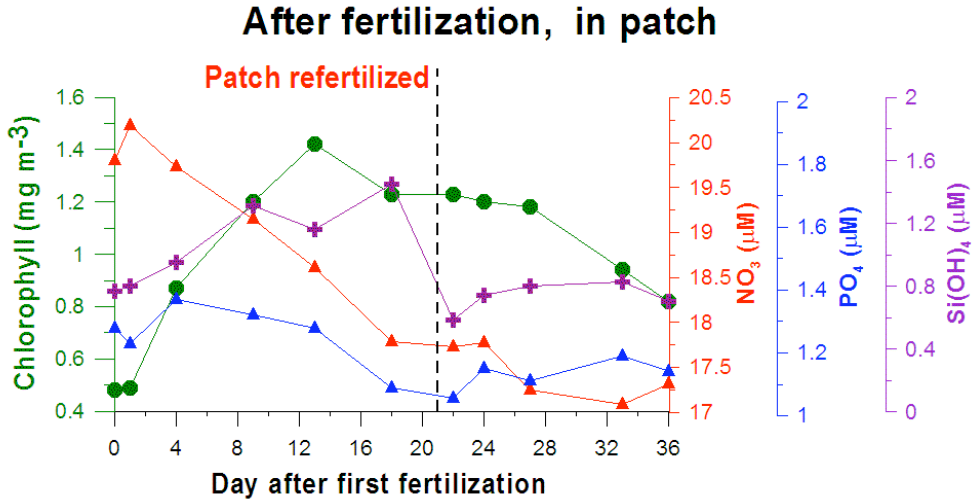

Fig. 5.1: Changes in surface nutrient concentrations with time inside the patch

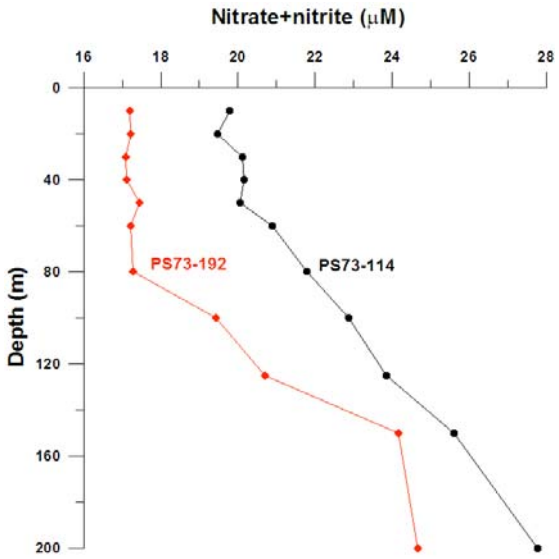

Fig. 5.2: Vertical profiles of nitrate+nitrite at two stations showing depletion in the upper layer due to phytoplankton uptake

6. CARBON DIOXIDE

G. Narvenkar NIO

Introduction and objectives

Ocean iron fertilization (OIF) experiments are essentially designed to test their potential for sequestration of atmospheric carbon dioxide and to determine the fate of photosynthesized organic matter associated with enhanced phytoplankton growth. All previous OIF experiments conduced in the Southern Ocean have demonstrated substantial drawdown of pCO_2 in surface waters. However, whether the organic carbon produced is largely recycled in near-surface waters or is exported to the deep sea is still being debated. Measurements made on LOHAFEX expedition included three observables to constrain the inorganic carbon system: total alkalinity (TA), total carbon dioxide (TCO_2), and partial pressure of carbon dioxide (pCO_2) in the surface layer.

Work at sea and methodology

Total alkalinity was measured in discrete samples collected from standard depths at major stations located within as well as outside the fertilized patch. An automated potentiometric titration system (VINDTA 3S) was used for TA measurements; 80 mL of the sample was titrated with 0.1 M hydrochloric acid following the procedure outlined in the operating manual. Calibrations were achieved with SIO's CRMs Batch 90 with a TA value of 2216.00 ± 0.52 μeqt/kg.

TCO_2 in discrete samples was determined using an automated coulometric titration system (VINDTA 3D); 20 mL of sea water sample was used for each titration. The system was calibrated with CRMs Batch 90 with a TCO_2 of 1985.61 ± 0.89 μmol/kg. Two automated systems (General Oceanics, USA) were used for underway pCO_2 measurements during the expedition. One of them is permanently installed on the vessel and belongs to the Royal Netherlands Institute for Sea Research (NIOZ); the other was installed by NIO especially for the expedition. Seawater was drawn continuously from a depth of 11 m while the air was pumped from the crow's nest. The two enter an equilibrator and the mole fraction of CO_2 in the equilibrated air is measured by a LiCor to compute pCO_2 (Dickson et. al., 2007). The system was regularly (3 hr) calibrated using calibration gases (CO_2-in-air mixtures of 310 ppm from MED Gas Agency India and 352.9 and 451.6 ppm CO_2 from Air Liquide).

The two underway pCO_2 systems used different calibration gas mixtures. Accordingly, there was a constant offset in the pCO_2 data with the values from the NIO analyzer being lower by about 7 μatm than those from the NIOZ unit.

Preliminary results

Surface TCO_2 concentrations in the fertilized patch were lower than in surrounding waters - the difference in concentrations was generally small but significant (<10 μmol/kg).

Similarly pCO_2 was also consistently lower (by 7 - 15 μatm) inside the patch than in surrounding waters. The underway data are shown in Fig. 6.1 for a 19 day long period during which the fertilized patch was repeatedly criss-crossed. The lowest values corresponded to the centre of the fertilized patch. The pCO_2 showed a good correlation with chlorophyll as exemplified in Fig. 6.2 based on sampling in and around the fertilized patch on 17 February. These observations clearly show a significant drawdown of pCO_2 in the surface layer. However, the magnitude of the decrease was relatively modest with the refertilization not leading to much further depression of the pCO_2 and the values rising with time after about a month.

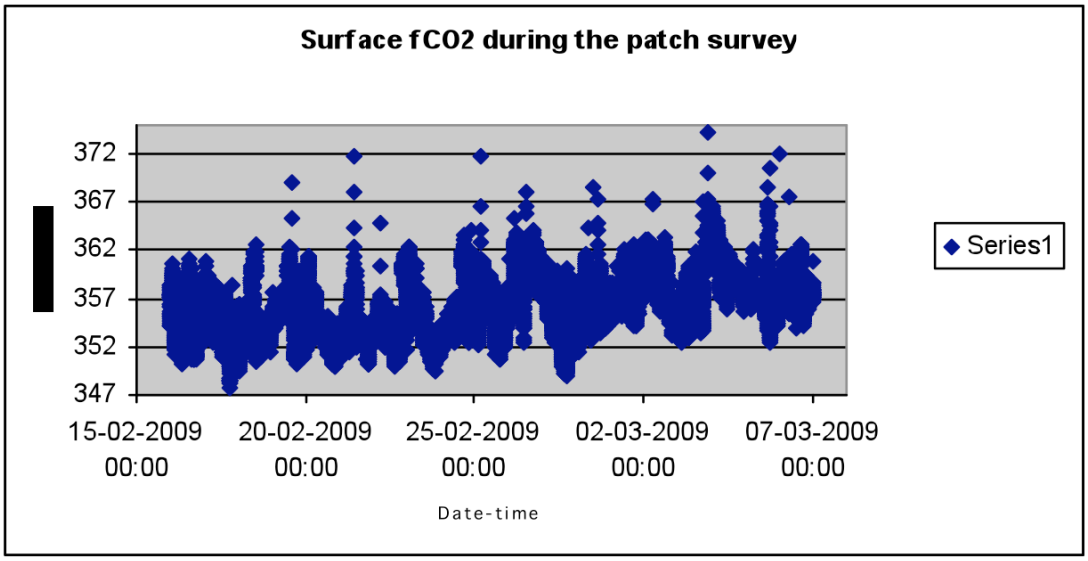

Fig. 6.1: Underway pCO_2 record from 16 February 2009 (about 3 weeks after the first fertilization and just before the refertilization till the end of the observations).

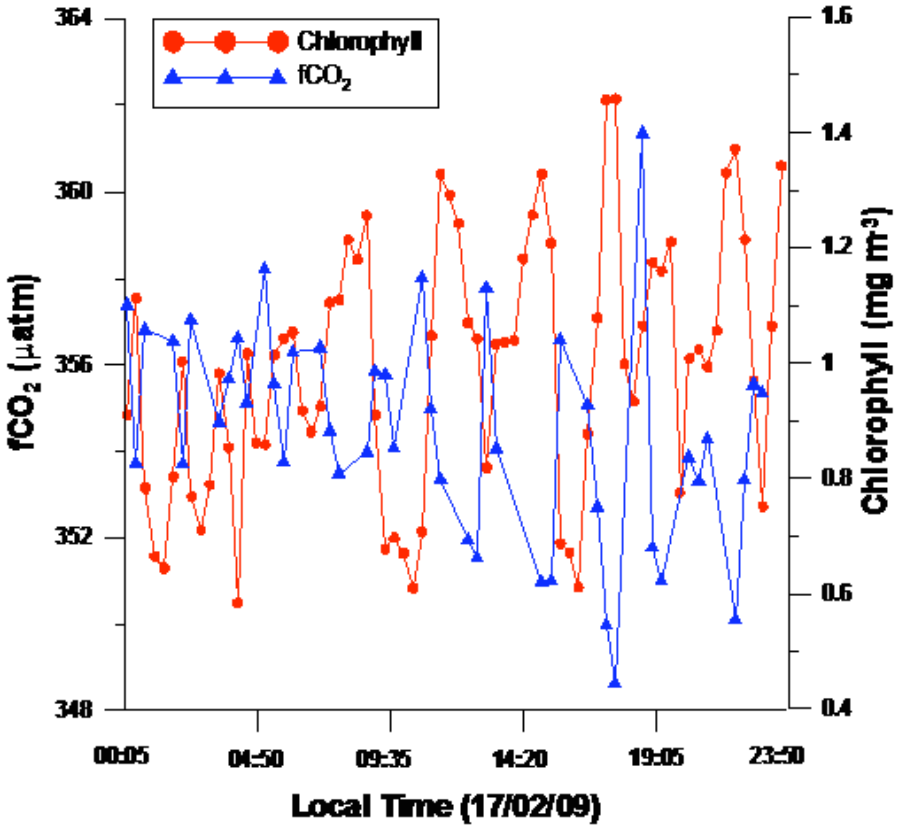

Fig.6.2: High resolution pCO_2 and chlorophyll variability in the surface layer (ship's underway water sampling at 11 m depth) on 17 February 2009 corresponding to early part of the pCO_2 record shown in Fig.6.1.

References

Dickson AG, Sabine CL, Christian JR eds. (2007) *Guide to Best Practices for Ocean CO_2 Measurements* PICES Special Publication 3, North Pacific Marine Science Organization.

VINDTA 3 Versatile INstrument for the Determination of Titration Alkalinity (2008) Manual for version 3S and 3D.

7. DISSOLVED GASES OTHER THAN CO_2

P.V. Narvekar, R. Roy, K.B. Sujith, B.R. Thorat, S.W.A. Naqvi — NIO

Introduction

There is a possibility that ocean iron fertilization (OIF) may affect production of certain biogenic gases that contribute to the maintenance of earth's radiation balance and/or destruction of ozone in the stratosphere. The most important of such gases are nitrous oxide, methane, dimethyl sulphide and halocarbons. Therefore, one of the main objectives of LOHAFEX was to investigate changes in concentrations of these gases before and after fertilization. Except for methane, analyses for all gases were performed on board ship, and the salient results are presented below. For methane, samples were preserved for measurements in the shore laboratory.

7.1 Dissolved oxygen

Objective

To investigate changes in oxygen production/consumption triggered by iron fertilization.

Work at sea

Dissolved oxygen (DO) samples were routinely collected from all CTD casts taken for other chemical measurements. These samples came from standard depths (maximum 3000 m) from 29 stations within the fertilized patch and 16 stations outside the patch. DO distribution within the patch was also studied in the upper 200 m water column along two short (30 - 40 km) sections oriented in the north-south and east-west directions.

DO in water samples was fixed immediately and analyzed within a few hours of collection at a high precision (±0.003 μM) using the SIO (Scripps Institution of Oceanography) automated titration system.

Preliminary results

The DO concentration decreased from ~325 μM (7.3 ml/l) in the surface layer to ~175 μM (3.9 ml/l) at 800 m depth. Below this depth, a steady increase in the DO concentration occurred with depth to values exceeding 220 μM (4.9 ml/l). Variations in DO at the same density level from one location to another were quite small, except in the surface layer (Fig. 7.1.1).

In the two sections (N-S and E-W) across the fertilized patch, significantly higher DO levels were observed in the surface waters relative to waters just outside the patch

(Fig. 7.1.2). The concentrations were above saturation with reference to atmospheric oxygen resulting in negative values for apparent oxygen utilisation (AOU). This provides evidence of enhanced photosynthesis and net oxygen production oxygen production in the fertilised patch.

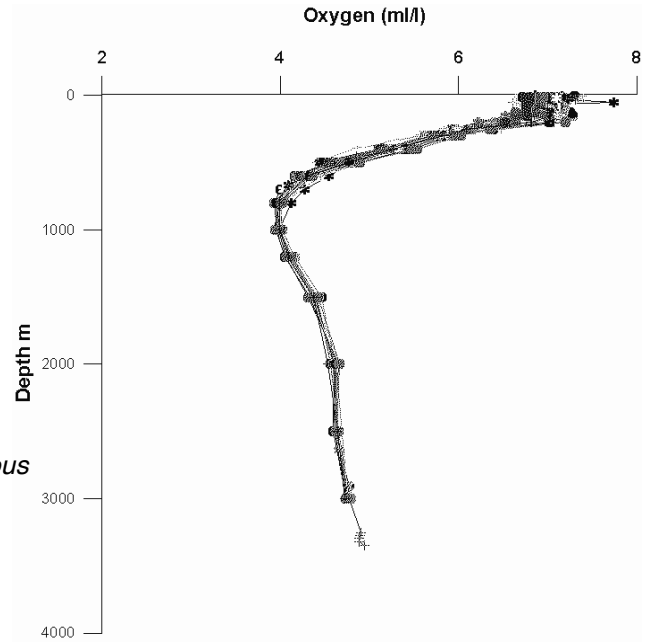

Fig. 7.1.1: Dissolved Oxygen profiles at various stations during the Lohafex cruise

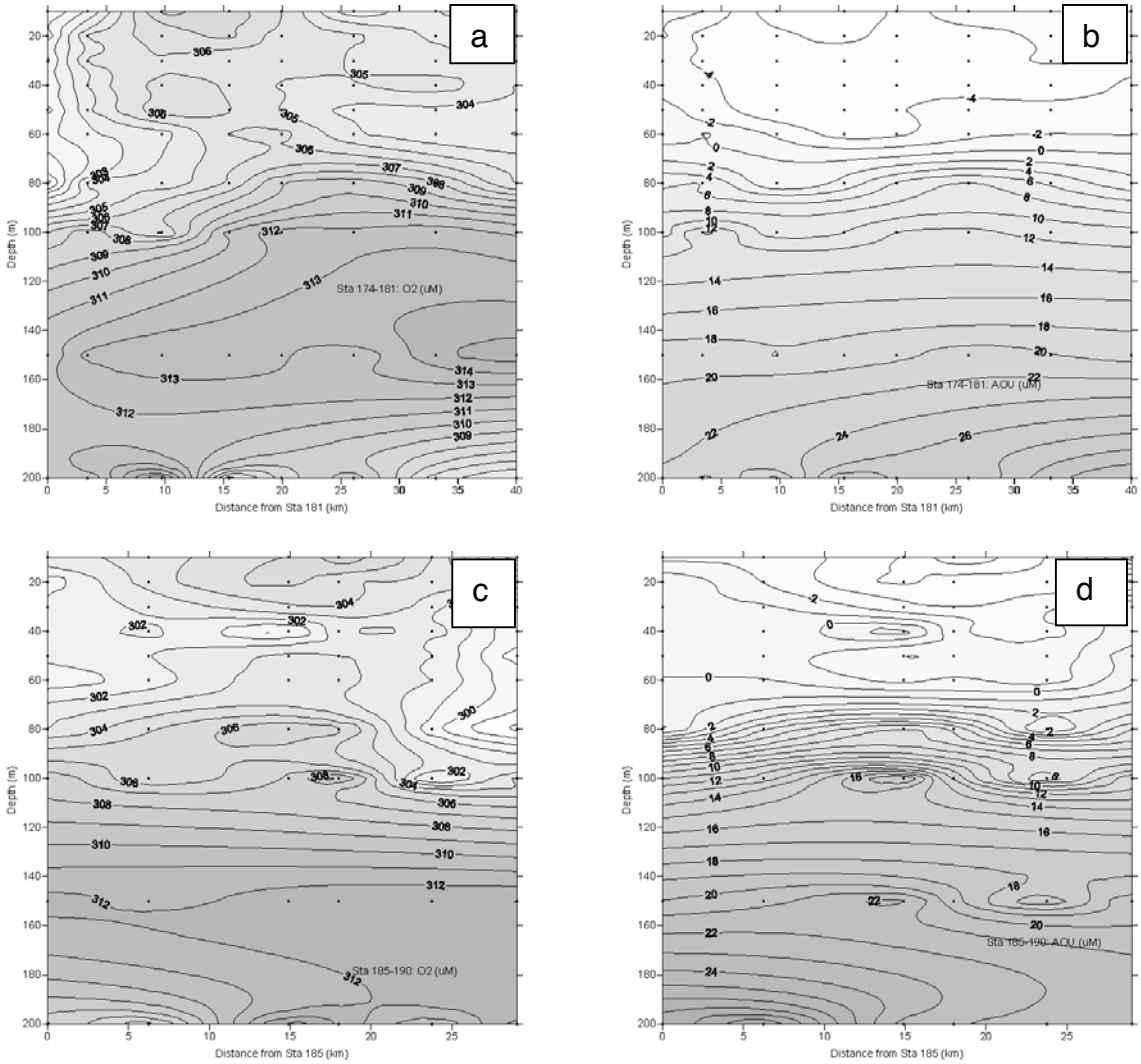

Fig. 7.1.2: Dissolved Oxygen (a, c) and AOU (b, d) in two sections across the fertilised patch

7.2 Halocarbons

Introduction and objectives

The study of volatile halogenated organics has been of interest due to their potential to create halogen loading in the atmosphere, thus producing significant changes in climate. They are now known to play an important role in chemistry of marine boundary layer (Pechtl et al., 2006). Among these gases, methyl iodide (CH_3I), dibromomethane (CH_2Br_2) and bromoform ($CHBr_3$) are produced by both macrophytes and microplankton giving rise to typical open ocean depth profiles – high concentrations in surface waters especially in coastal areas. Some investigators have suggested that photochemical production could also be important in surface waters (Jones and Carpenter, 2005). Some of these gases have been studied during the previous OIFs in the Southern Ocean (Liss et al., 2005). Here we provide a brief account of their distribution in the fertilized patch and just outside it during LOHAFEX.

Work at sea and methodology

Water samples in duplicate were collected in 25-ml Hamilton gas-tight syringes and kept in running seawater until they were analyzed (within a few hours of collection) following the method of Moore and Tokarczyk (1993). Briefly, 5 ml of water the sample was injected into a glass vessel of Tekmar purge-and-trap system and purged with helium at a flow rate of 40 ml/min for 5 minutes at 40˚C. Halocarbons were trapped in Vocarb 3000 trap under ambient conditions. The trap was then heated to 180˚C and the desorbed gases were injected into a Varian GC-ECD system (carrier flow 5 ml/min). Separation was achieved over a 60 m long DB624 column and the detector temperature was 290˚C. The GC column oven was programmed to get optimum separation with an initial temperature of 40˚C for 1 min that was raised to 140˚C @ 4˚C/min and maintained thereafter for 10 min. Linear 5 point external standard calibration was made by using synthetic standards procured from Sigma Aldrich. Working standards were made by serial dilution of these standards in nitrogen-purged distilled water to remove any background contamination. Working standards were used daily to perform calibration checks and average calibration factor was used to calculate the concentration in the sample. Under these analytical conditions, the detection limits were around 0.01 ng/L for most of the compounds studied. Suitable blank run was performed after each analysis to check for any carryover in between each run.

Preliminary results

Typical vertical profiles of these gases at an in-patch station are shown in Fig. 7.2.1. CH_3I concentrations ranged from 0.1 to 1.47 ng/L and showed a subsurface maximum at ~40 m with a mean value of 1.07 ng/L. CH_2Br_2 occurred in low concentrations that varied from 0.03 to 0.08 ng/L, averaging 0.05 ng/L. $CHBr_3$ showed a maximum just below 40 m and its mean concentration was 3.96 ng/L with a range of 0.63 - 11.8 ng/L. The observed concentrations are very similar to those previously measured in the Southern Ocean with the CH_3I levels observed by us being marginally higher by 0.2 - 0.4 ng/L. Concentrations below the mixed layer are also comparable to those observed during the EisenEx (Liss et al., 2005). Temporal trends at both the in-patch and out-patch

stations (not shown) were generally similar with the in patch values being generally higher .

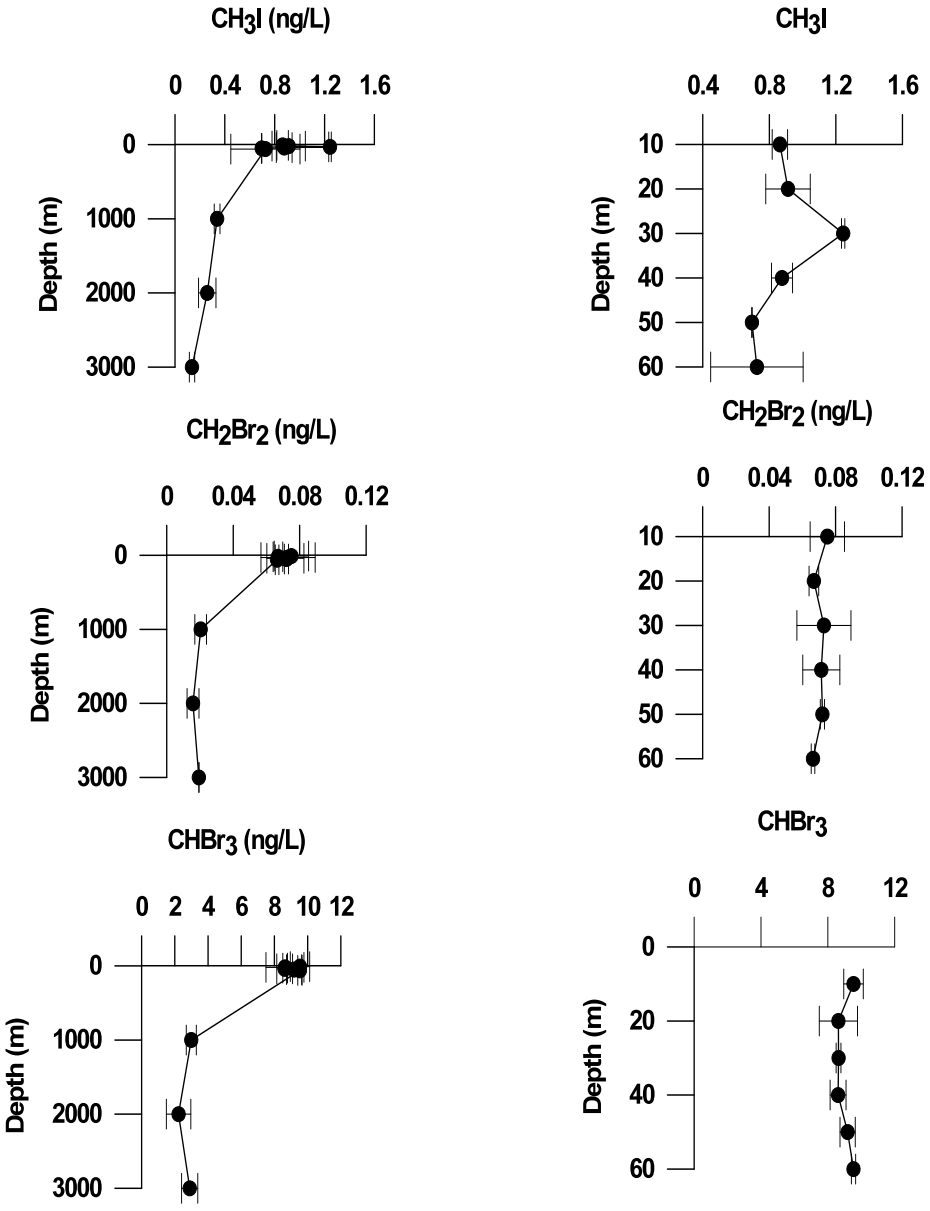

Fig. 7.2.1: Depth profiles of the halogenated trace gases measured in an in patch station (PS73-192)

References

Jones CE et al., (2005) Solar photolysis of CH_2I_2, CH_2ICI and CH_2IBr in water, saltwater and seawater. Environ.Sci.Technol: 39, 6130-6137, doi 10.1021/eso580226.

Liss et al., (2005) Ocean fertilization with iron: effects on climate and air quality. Tellus: 57 B, 269-271.

Moore RM, Tokarczyk R (1993) Volatile biogenic halocarbons in the Northwest Atlantic. Global Biogeochem. Cycles, 7, 195-210.

Pechtl S et al., (2006), Modeling the possible role of iodine oxides in atmosphere new particle formation. Atmos. Chem. Phys: 6, 505-503.

7.3 Dimethyl sulphide

Introduction and objectives

Dimethylsulphide (DMS) is one of the most important natural sources of atmospheric sulphur. It plays an important role in the global sulphur cycle and in climate regulation (Lovelock et al. 1972). DMS production is dependent on the activity of DMSPlyase, which has been found in bacteria and algae. Dimethylsulphoniopropionate (DMSP) is a metabolite found in marine phytoplankton, seaweeds and some terrestrial and aquatic vascular plants. DMSP serves as a principal osmolyte in many marine algal species. DMSP and its breakdown products also appear to have several other metabolic functions including active grazing defence. DMS is oxidized into dimethylsulphoxide (DMSO) in the upper ocean, the size of sink is still not well known. Inter-cellular production of DMSO also occurs in phytoplankton in addition to DMSP. Once produced, DMS is lost from seawater by three major pathways - sea-air exchange, biological consumption and photochemical transformation, with the latter two processes leading to formation of DMSO**.**

Earlier studies of OIF in the Pacific and Southern oceans have shown an approximately three fold increase in DMSP over a few days. This was because of the quick response of DMSP-producing phytoplankton to the new iron. We carried out a similar study during LOHAFEX with the twin objectives of (a) to evaluate the variations of climatically important organic sulphur species, and (b) to understand the role of bacteria in the production of DMSO, and the role of DMSO in the global sulphur budget.

Work at sea and methodology

Subsamples taken from Niskin bottles in 60 ml amber coloured glass bottles were kept in 4°C until analysis that was performed within a few hours of collection. A Shimadzu-2010A series gas chromatograph equipped with a flame photometric detector (FPD) was used for the analysis of organic sulphur compounds after pre-concentration by the purge and trap method as described in detail by Shenoy et al. (2002). In brief, 20 ml of sample was purged with nitrogen. After removing moisture the sulphur gases were cryogenically trapped in a teflon column using liquid nitrogen. The teflon column was then heated in a water bath maintained at >80°C and the trapped gases were injected into the GC-FPD. Separation was achieved over a teflon Chromosil 330 column. Carrier gas flow was 35 ml per minute, and the hydrogen and air flows were adjusted to 80 and 120 ml/min, respectively. The oven and detector temperatures were 40 and 200°C, respectively. DMS retention time was 1.86 minute under these conditions. For measuring DMSPt (total DMSP), 1 ml of cold 10 M NaOH was added to the sample, after the analysis of DMS. Alkali hydrolysis resulted in the

cleavage of DMSP into DMS and acrylic acid. DMSO was measured by treating the sample with 2 ml of 50 % HCl, and 0.4 g sodium borohydrate and purged for 20 minutes. Both DMSP and DMSO were quantified using DMS calibration. DMSO calibration was carried out onboard and the calibration curve was compared with DMS calibration curve to determine the conversion rate and to ensure the efficiency of the method.

Preliminary results

Typical inpatch and outpatch profiles for DMS, DMSPt and DMSO are shown in Fig. 7.3.1. The values were generally higher inside the patch than outside it. There were two significant peaks in DMS values inside the patch, the first on the 12 day after the first fertilization, and the second a few days after second fertilization. DMSPt in both in patch and out patch, showed covariance with the Chl *a* concentration. The highest value of DMSPt was observed on the day when the phaeocystis colony counts were at maximum. DMSO showed some elevated values (up to 11 nM) at the inpatch stations, whereas the out patch maximum was about 5 nM.

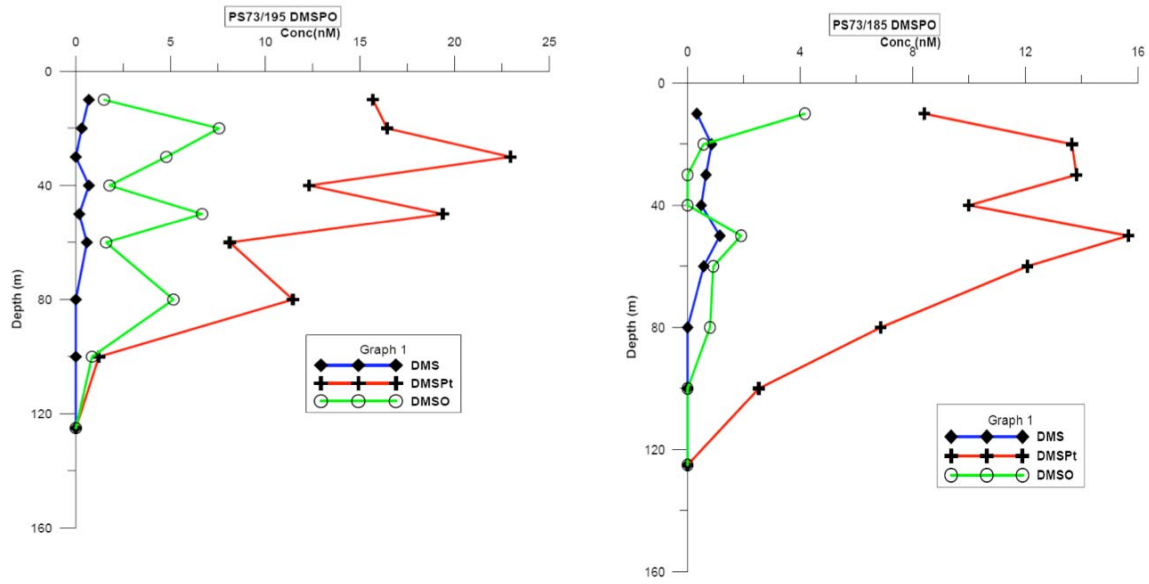

Fig. 7.3.1: Vertical profiles of DMS, DMSPt and DMSO at an in-patch station (PS73-195, left panel) and an out-patch station (PS73-185, right panel)

Reference

Lovelock JE, Maggs R, Rasmussen RA (1972) Atmospheric dimethyl sulphide and the natural sulfur cycle. *Nature* 237, 452–453.

Shenoy, DM, S Joseph, M Dileep Kumar, and MD George (2002) Control and interannual variability of dimethyl sulfide in the Indian Ocean. Journal of Geophysical Research, Vol. 107, No. D19, doi:10.1029/2001JD000371

7.4 Nitrous oxide

Introduction and objectives

Nitrous oxide (N_2O) is not only an important greenhouse gas, over 300 times more potent than CO_2 on a per molecule basis, but it also contributes to the stratospheric ozone destruction. Attention has been focussed on this gas because of widespread concerns that degradation of organic matter produced as a result of large-scale OIF could result in a substantial decrease in subsurface oxygen levels, thereby promoting its production that might in part offset the gains due to CO_2 sequestration (Jin and Gruber, 2003). Of the OIFs conducted in the Southern Ocean, N_2O was measured on SOIREE (Law and Ling, 2001) and EIFEX (Walter et al., 2005). A significant decrease in N_2O was recorded in the thermocline during SOIREE, but not during EIFEX in spite of its longer duration. Additional measurements are therefore needed to reconcile these differences.

Work at sea and methodology

Samples for N_2O were routinely collected from all CTD casts taken for other chemical measurements. These samples were taken from standard depths to a maximum of 3,000 m at stations located both within and outside the fertilized patch. N_2O distribution within the patch was also studied in the upper 200 m water column along two short (30 - 40 km) sections oriented in the north-south and east-west directions.

Estimation of N_2O was carried out by multiple phase analysis (McAuliff, 1971). Briefly, after equilibriating the sample (25 mL) with an equal volume of He, the latter was dried by passing over a moisture trap and introduced into a HP 5890 Series II Gas Chromatograph (via a 6-port valve). After separation over a stainless steel column packed with Chromosorb 102 (80/100 mesh) and maintained at 80ºC, N_2O was detected using an electron capture detector (ECD; 10 mCi ^{63}Ni foil conditioned at 300ºC). Calibration was achieved with a gas standard (510 ppb N_2O in nitrogen procured from Alltech Assoc. Inc, IL., USA). Air samples were run frequently to check the drift.

Preliminary results

Nitrous oxide profiles were similar to those reported previously from the Southern Ocean (e. g. Walter et al., 2004). Surface values were close to saturation, and the N_2O and O_2 profiles were mirror images of each other (Fig. 7.4.1). Iron fertilization had no consistent and significant effect on N_2O distribution as revealed by a comparison of vertical profiles taken a day before fertilization (Sta. PS73-114) and toward the end of the experiment (Sta. PS73-204). Concentrations in the upper 500 m at these stations were virtually indistinguishable (Fig. 7.4.1). Although there was substantial divergence below this depth to about 1,500 m, the change was in the opposite sense (a decrease) of what one would expect from the degradation of organic matter sinking from the surface. This was most likely related to a change in water mass as the patch had moved out of the eddy and the intermediate water characteristics had obviously changed.

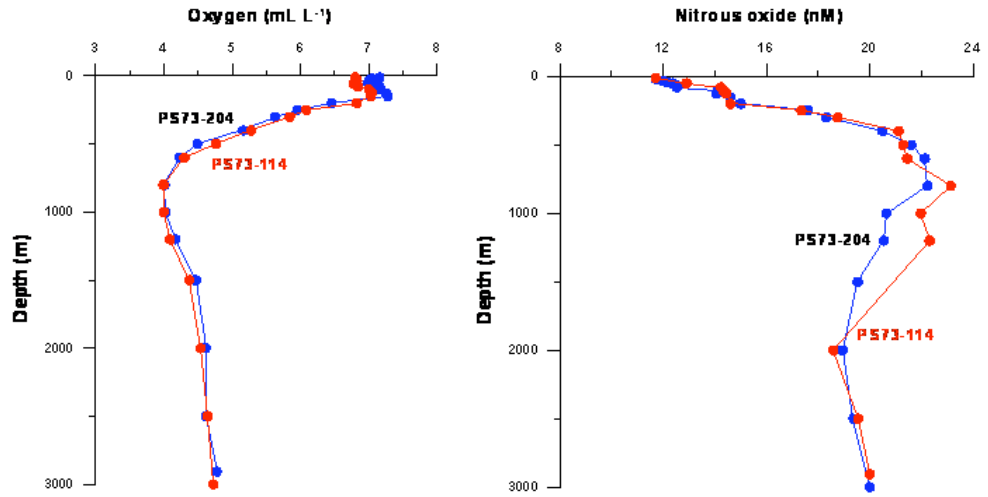

Fig. 7.4.1: Vertical profiles of nitrous oxide just before fertilization (red symbols) and toward the end of the experiment (blue symbols)

References

Jin X, Gruber N. (2003) Offsetting the radiative benefit of ocean iron fertilisation by enhancing N_2O emissions. *Geophys. Res. Lett.*, 30, doi:10.1029/2003GL018458.

Law CS, Ling R. D. (2001) Nitrous oxide flux and response to increased iron availability in the Antarctic Circumpolar Current. *Deep-Sea Res. II,* 48, 2509–2527.

McAuliff, C. (1971) Gas chromoatographic determination of dissolved hydrocarbons in various aqueous media by repeated equilibration of sample with gas. Abstracts of papers of the American Chemical Society, pp. 5-10 Publisher: American chemical Soc., 1155 16th ST, NW, Washington, DC 20036.

Walter S., Peeken I, Lochte K, Webb A, Bange HW (2005) Nitrous oxide measurements during EIFEX, the European Iron Fertilisation Experiment in the subpolar South Atlantic Ocean. *Geophys. Res. Lett.*, 32, doi:10.1029/2005GL024619.

8. IRON CYCLING

L. Laglera[1], R. Martinez [1], H. Naik [2],
A. Bansiwal [3]

[1)]CSIC-IMEDEA
[2)]NIO
[3)]NEERI

Objectives

It is a well know fact that iron is a limiting factor in controlling primary production in the nutrient-rich surface waters of the Southern Ocean and this has been proved by several experiments previously carried out in these waters.

Fertilization experiments are based on the dumping of high concentrations of acidified ferrous salts. Iron(II) is a thermodynamically unstable species that oxidizes to Fe(III) in the time frame of minutes to hours depending on other factors such as temperature, the concentration of electron receptors (oxygen, superoxide, hydrogen superoxide, etc), light intensity and so on. It is also well studied that iron is bound to precipitate eventually due to the low solubility of Fe(III) at natural seawater conditions and the rapid formation of colloidal iron (Boye et al., 2005). However, the slow development of phytoplankton blooms after fertilization in the frame of days implies that some poorly understood mechanism must be present to hold this extra iron in surface waters in a form readily available for the phytoplankton. During LOHAFEX cruise we made an attempt to address the above issue via the assessment of the dissolved and particulate iron concentration in the water column. The study of the particulate fraction is a hard task usually not conducted in oceanographic studies and no data are available from previous fertilizations. This is because of the risk of poor reproducibility and to the assumption that this fraction is either already assimilated by cells or strongly refractory in the case of big oxyhydroxide particles.

Work at sea

Sampling

Water samples were collected by using 5L Niskin samplers mounted on epoxy paint coated Aluminium rosette that was held at the end of a kevlar line. Once on deck after collection these were immediately covered by plastic bags and brought to a clean air plastic "bubble". The "bubble" had two laminar flow systems running continuously that maintained positive pressure ultimately leading to ultraclean air of class100. A pressure line carrying high purity nitrogen was plugged to the sampling bottles to allow filtration by overpressure. Samples were stored in acid clean teflon [for Fe(II)] or LDPE (for total iron) containers.

Iron partition

The initial design included the determination of the iron partition from the ultrafiltered (or truly solved) fraction (< 0.05 μm) to particulate. However, the filtration unit brought

onboard presented persistent contamination problems probably due to a wrong selection of the material used for the o-ring that seals the filter holder. Therefore, the study was more focused at estimating the particulate fraction. The determination of the absolute concentration should lead to a better description of the overall iron budget.

Samples from key stations, both raw and filtered (online by passing through a 0.22 μm polycarbonate filter), were analyzed onboard after 24 hours acidification by cathodic stripping voltammetry (CSV) (Obata and van den Berg, 2001). This treatment has revealed to be enough for total recovery of dissolved species (Johnson et al., 2007). The estimation of the absolute iron concentration (dissolved plus particulate) is essential, despite of the analytical difficulties, to estimate the whole iron budget remaining in the surface waters during the experimental development. In order to verify onboard measurements, raw and filtered samples from several stations were preserved frozen for lab-based ICP-MS analyses.

Fe(II)
The reduced form of iron is highly soluble and it is known to be the most rapidly bioavailable form. Fe(II) measurements were carried out by using the flow injection system FeLume (Waterville Analytical). The chemiluminescence (CL) is obtained by the quick oxidation of Fe(II) at high pH in the presence of luminol. In previous iron fertilization experiments, Fe(II) concentrations reported were much higher than expected (Croot et al., 2005). In this cruise we measured Fe(II) concentrations in unfiltered samples in addition to those in the dissolved fraction of the water column. We have also monitored the continous flow measurements from the underway system while moving though the fertilized patch.

Iron Speciation
In seawater the speciation of iron is dominated by the presence of binding ligands at concentrations higher than the dissolved iron concentrations (Boye et al., 2005; Rue and Bruland, 1995). The analytical method consists on the titration of the sample with iron and the determination of the labile fraction by CSV. The concentration of these ligands changed dramatically during the EISENEX experiment (Boye et al., 2005). During LOHAFEX, samples were taken to determine the concentration of iron ligands but due to the long time these analysis require, samples were forzen for their analysis back in lab.

Iron in excretion products
One of the important roles of zooplankton in ocean biogeochemistry is that they are found to take part in trace metal cycling in the Southern Ocean waters (Tovar-Sanchez et al., 2007). During LOHAFEX we tried to understand how much of the iron is excreted by zooplankton in the non-fertilized and fertilized areas. This included the development of clean protocols for handling of those samples.

Growth induced by slow iron release matrices (NEERI)
The impact of slow iron release in opposition to massive single event fertilizations was assessed by onboard incubations in the presence of several iron-enriched

matrixes: chitin, chitosan, bentonite and zeolite-A. Phytoplankton growth was monitored through the measurements of Chlorophyll *a* and nutrients consumption over time. Bacteria growth was monitored by bacterial secondary production and cytommetry.

Effect of zooplankton metabolites on phytoplankton performance
As complementary experiments the effect of zooplankton excretion products on algae growth and primary production was monitored in ondeck incubations. Both amphipodes and copepods were collected and their excretion products collected, filtered and inoculated in water samples.

Preliminary results

Sampling during the first few days of the experiment was scarce due to problems with the software that control the bottle closure mechanism of the clean rosette. Once those problems were solved, 85 stations were sampled down to 150 m depth from in- and outside the fertilized patch.

The analyses of raw samples required method development because raw sample are not barely analyzed in oceanographic studies and for not being clear that the whole iron budget is labile after acidification. The microscopic observation of intact cells after 24 hours of incubation at pH 2 suggests that the acidification of raw samples do not include intracellular iron. This was supported by the analysis of unicellular culture suspension, where leachable iron concentrations barely varied in samples from different species and cell concentrations. So herein after we will denominate the concentration obtained as leachable iron. This preliminary observation will be confirmed by ICP-MS analysis after digestion of raw ocean and culture samples where absolute concentration will be obtained.

Preliminary onboard results showed leachable iron concentrations consistently higher than total dissolved. The data scattering of replicates from the same unfiltered sample was low for deep waters and higher in surface waters. However, the high similarity of results when different casts are compared suggests the validity of the approach. The increase in concentration in the leachable fraction was about two fold with respect to the dissolved fraction but with a slight different pattern. The decrease of dissolved iron concentrations is constant with depth from surface (as found in EISENEX) while leachable iron profiles show a perfect mixing in the first 40 meters. This can be important in order to describe export mechanisms and rates.

The analyses of Fe(II) concentrations in underway and depth profile samples showed a very interesting feature. The CL signal was consistently higher in the unfiltered fraction. Fe(II) is usually understood to be present as a transient species in its free ionic form due to its high solubility and the preference of natural ligands for the Fe(III) species. Just recently, the possible presence of natural Fe(II) ligands was suggested due to the lower than expected oxidation rates found in natural waters after Fe(II) additions but not concentrations in the particulate fraction were reported before. Moreover, the CL technique is prone to suffer from chemical interferences. The

puzzling higher CL signal found due to the presence of particulate matter required experimental testing due to the high risk of interfering species other than Fe(II) leading to the unexpected CL signal. For this purpose, high Fe(II) concentrations were added to filtered and unfiltered surface waters and while the response falls to a significant and constant value in the first case, filtered waters loose completely the response after 2 - 3 hours. The experiment also brings light into the mechanism that prevents the rapid export of the added iron from surface waters after the fertilization. The response in cell cultures thoroughly washed with clean filtered water to remove adsrobed species was also tested and the results showed agreement with the presence of adsorbed Fe(II). The CL signal of aged seawater (free of Fe(II)) did not increase after cells addition and the signal held nicely to a significant value after the addition of Fe(II). Additional work will be conducted in lab to definetely confirm or discard the presence of significant concentrations of adsorbed Fe(II) onto particulate matter.

With respect to the excretion products of zooplankton, we could not study the effect of krill according to the pre-cruise plan due to its poor presence in the LOHAFEX study area. Preliminary experiments with amphipods and copepods showed no significant iron changes in the dissolved fraction after accumulation and incubation for hours. Therefore all the attention subsequently was diverted on the iron contained by faecal pellets. Samples from the WP2 nets were concentrated and their faecal pellets were accumulated using clean techniques in collaboration with the zooplankton group. Equilibrium for 24 hours at pH 2 showed that copepod pellets leach out important amounts of iron. The concentrations of intra pellet leachable iron were in the order of units to tens of millimolar. Depending on the comparison with the local production rates of faecal pellets, our finding points in the direction that pellets can be a major reservoir of iron in the ocean and their sinking and degradation rates are essential to understand the cycling of iron in oceanic waters.

In the slow release incubations conducting by NEERI, the phytoplankton growth was strongly incremented by the presence of the slow released matrices with respect to the incubations in the presence of $FeSO_4$ and the control.

Incubations of surface seawater in the presence of zooplankton metabolites showed clear differences with respect to the control suggesting the importance of zooplankton on the recycling of nutrients.

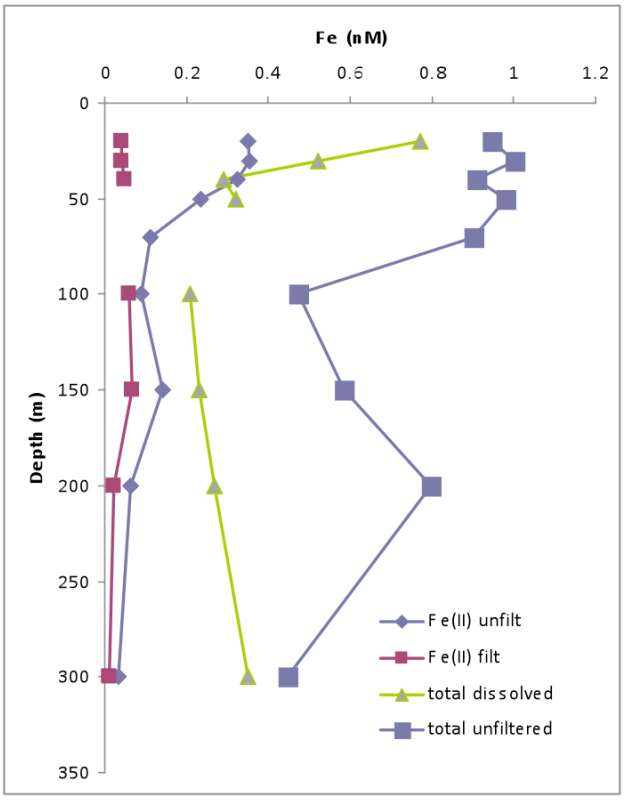

Fig. 8.1: Profiles of leachable and dissolved total iron and of unfiltered and filtered Fe(II) at station 139. The profile shows all the common features found after fertilization: different dissolved and leachable patterns, subsurface maximum unfiltered Fe(II). Preliminary results as the sensitivity of the Fe(II) measurements has to be corrected.

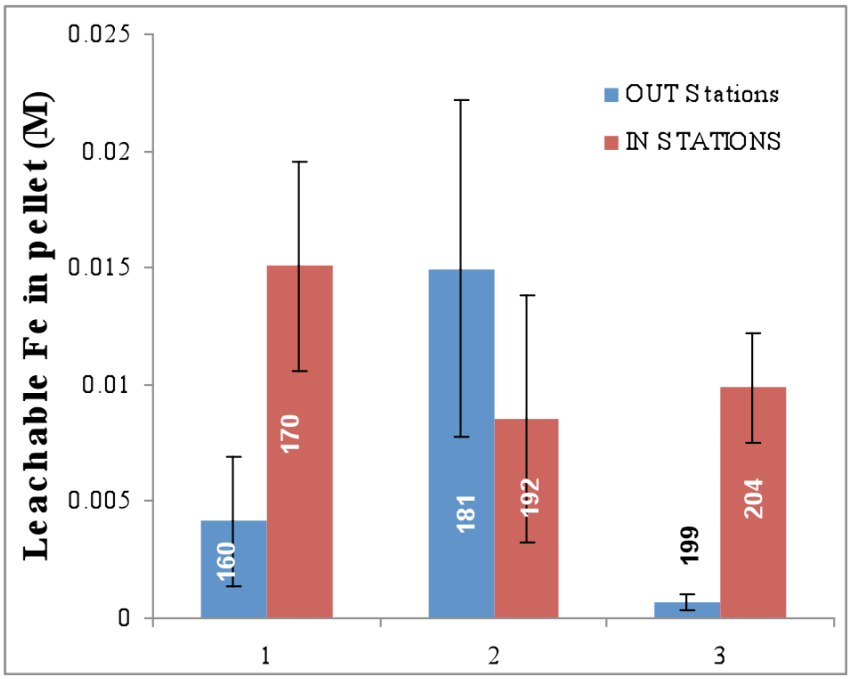

Fig. 8.2: Concentration of leachable iron found in copepod faecal pellets extracted from 6 different stations. Station are plotted in temporal order and divided in in and out stations. Concentration are in the millimolar range.

References

Boye, M. et al., (2005) Major deviations of iron complexation during 22 days of a mesoscale iron enrichment in the open Southern Ocean. Marine Chemistry, 96(3-4): 257-271.

Croot PL et al., (2005) Spatial and temporal distribution of Fe(II) and H_2O_2 during EisenEx, an open ocean mescoscale iron enrichment. Marine Chemistry, 95(1-2): 65-88.

Johnson KS et al., (2007) Developing standards for dissolved iron in seawater. Eos, 88(11): 131-132.

Obata H, van den Berg CMG (2001) Determination of picomolar levels of iron in seawater using catalytic cathodic stripping voltammetry. Analytical Chemistry, 73(11): 2522-2528.

Rue EL, Bruland KW (1995) Complexation of iron(III) by natural organic ligands in the Central North Pacific as determined by a new competitive ligand equilibration / adsorptive cathodic stripping voltammetric method. Marine Chemistry, 50: 117-138.

Tovar-Sanchez A, Duarte CM, Hernandez-Leon S, Sanudo-Wilhelmy SA (2007) Krill as a central node for iron cycling in the Southern Ocean. Geophysical Research Letters, 34(11).

9. NATURAL RADIONUCLIDES AND RADIUM ISOTOPES

R. Rengarajan[1], M. Soares[2], M. Rutgers van der Loeff[3]

[1)] PRL
[2)] NIO
[3)] AWI

9.1 ^{234}Th as tracer of export production of POC

Objectives

An essential parameter of the progress of the induced plankton bloom is the rate at which particulate matter, and especially POC is exported from the surface mixed layer to greater depths. Apart from the measurements by carbon budgets and sediment traps, we planned to quantify this flux by the measurement of the depletion of ^{234}Th in the surface waters. Repeated measurements of the integrated ^{234}Th depletion allow quantifying the downward flux of particulate ^{234}Th out of the surface water. In order to convert this flux to a carbon flux we have determined the POC/^{234}Th ratio of large suspended and of sinking particles.

Work at sea

^{234}Th profiles

Profiles of total ^{234}Th were measured according to the method of Cai et al. (2006) at 21 stations: 2 in the eddy before iron fertilization, 10 in-stations, 5 out-stations and 4 stations outside the eddy.

An aliquot of 4 - L of seawater was collected at depths of 7 m (ship's seawater intake), 25, 50, 75, 100, 150, 200 and 300 m. Thorium was collected by coprecipitation with MnO_2 and counted for beta activity to determine the ^{234}Th content. Chemical yield was monitored with a ^{230}Th spike.

POC/^{234}Th ratios

In order to determine the POC flux from the surface water to greater depth, we collected particulate material on precombusted quartz fiber (QMA, nominal pore size 1μm) filters for analysis of the POC/^{234}Th ratio. In determining the depth of export production we considered that (1) the ^{234}Th depletion was largely confined to the upper 100 m, (2) the mixed layer was between 65 m and 100 m deep, (3) the chlorophyll and light distribution showed that phytoplankton activity was limited to the upper approx. 200 m and (4) the neutrally buoyant traps could be deployed from about 150 m. We selected 200 m as the depth of export but included some additional analyses at 100 m depth as alternative export depth.

Total suspended particulate was obtained at 200 m at 19 stations by filtering 8 L of seawater. Size-fractionated suspended particulate matter was obtained at 100 m and 200 m with *in-situ* pumps. These pumps, deployed at 12 stations, filtered 150 - 680 L of seawater consecutively through 50 μm and 10 μm nylon screens and QMA (142 mm diameter). The material collected on the screens was ultrasonically removed and filtered over QMA. At three stations (137, 139, 146) no 50 μm fraction was collected at 200 m.

Sinking material was obtained from splits of the neutrally buoyant sediment traps.

^{234}Th in surface water

In parallel to the profiles at stations, ^{234}Th was measured every 4 hours in the surface water from the ship's seawater intake at 7 m depth with an automated system operated over the entire experimental period.

Preliminary results

1. Scenario at the Start of the Experiment

At the start of the experiment ^{234}Th was depleted in the surface 50 - 75 m by 25 - 30 % with respect to its parent ^{238}U. The automatic analyses yielded a depletion of about 20 % in the surface water, indistinguishable from the value observed during our first visit to this eddy, 10 days earlier. This implies that within the past approx. 2 months (just over 2 half lives of ^{234}Th) an export of particles from the surface water had occurred. This means that, as we had expected from the low nutrient data, our experiment took place in a region where an algal bloom had already taken place and resulted in a downward particle flux. In this respect our experiment was similar to EIFEX but different from EISENEX which started earlier in the season. At the start of EISENEX, ^{234}Th was in near equilibrium with its parent ^{238}U, i.e. the ^{234}Th/^{238}U ratio was close to equilibrium value of 1 at all depths.

2. Development of the ^{234}Th distribution

As a highly particle-reactive element, thorium binds to all available particles. The increase of particulate ^{234}Th over the course of the experiment by a factor of 2 is a clear indication of an increase in particle load (Fig. 9.1). Remarkably, there is no difference between in and out patch stations: the increase was observed throughout the eddy, irrespective to our location with respect to the fertilised patch. The increase in particulate ^{234}Th is more than compensated by a decrease in dissolved activity. The resulting small decrease of total ^{234}Th that we see in the results of the semi-automated analysis would suggest a small increase in export, but again without any difference between in and out patch.

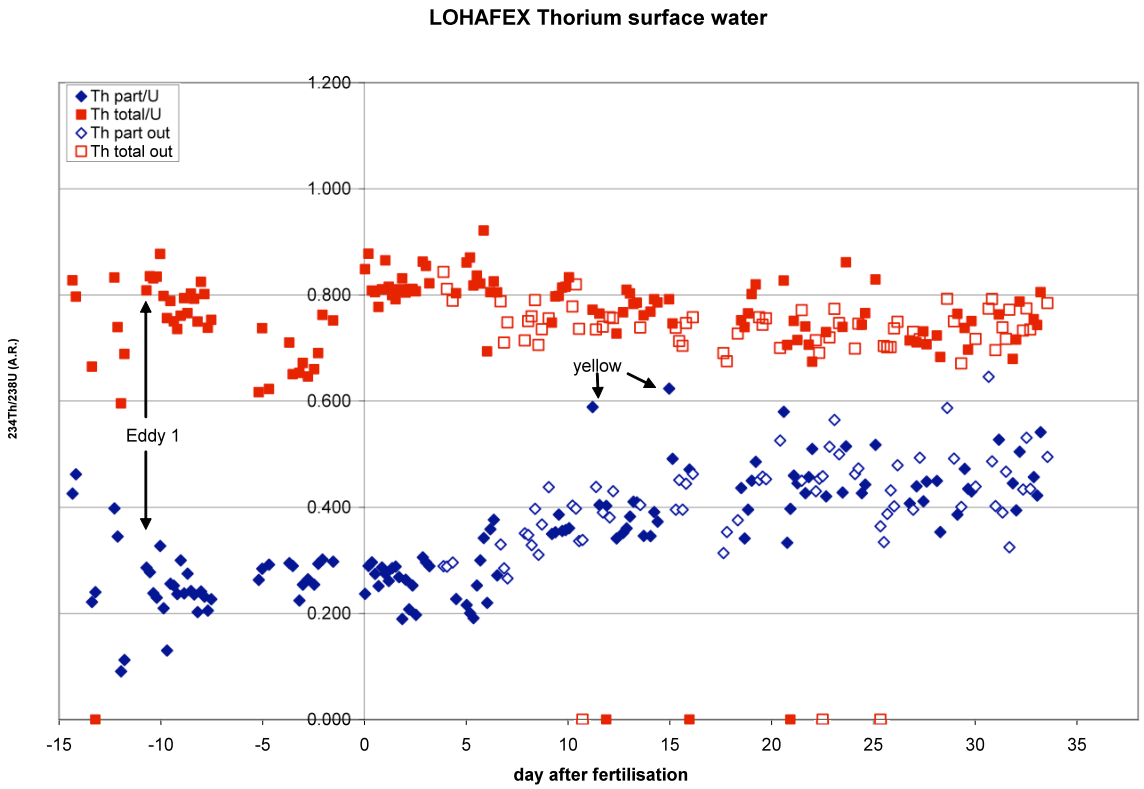

Fig. 9.1: Distribution of particulate (blue) and total (red) ^{234}Th in surface water over time before and after iron fertilisation. In-patch (closed symbols) and out-patch samples (open symbols) were distinguished based on the distance (within and above 10 nm, respectively) to the active buoy. Two samples with distinctly different yellow-brown colour presumably due to Phaeocystis had abnormally high percentage of ^{234}Th in the particulate phase.

3. Development of the export flux

A more precise result for the ^{234}Th export will be obtained from the profiles, especially after the correction for chemical yield, which can only be performed after the analysis of the ^{230}Th spike in the home laboratory. The preliminary, uncorrected, on-board results do not show any net change in the ^{234}Th depletion over time and no difference between in and outstations (Fig. 9.2). The depletion in the upper 100 m remains at about 5.7 dpm.cm^{-2} (Fig. 9.3) corresponding to a steady state (SS) ^{234}Th export flux of 1,600 dpm m^{-2} d^{-1}. With a POC/^{234}Th ratio of order 5 μmol dpm^{-1} (results obtained by Cai during ANT-XXIV/3) this amounts to carbon export of 100 mg m^{-2} d^{-1}. The time series observations also allow the calculation of a non-steady state export flux. The result is merely a wide range of fluxes around the SS value, which we interpret to be due to the variability in the fertilised patch rather than to real temporal differences in the flux. This contrasts with the results of EIFEX, where a clear change in export was found in the last phase of the experiment.

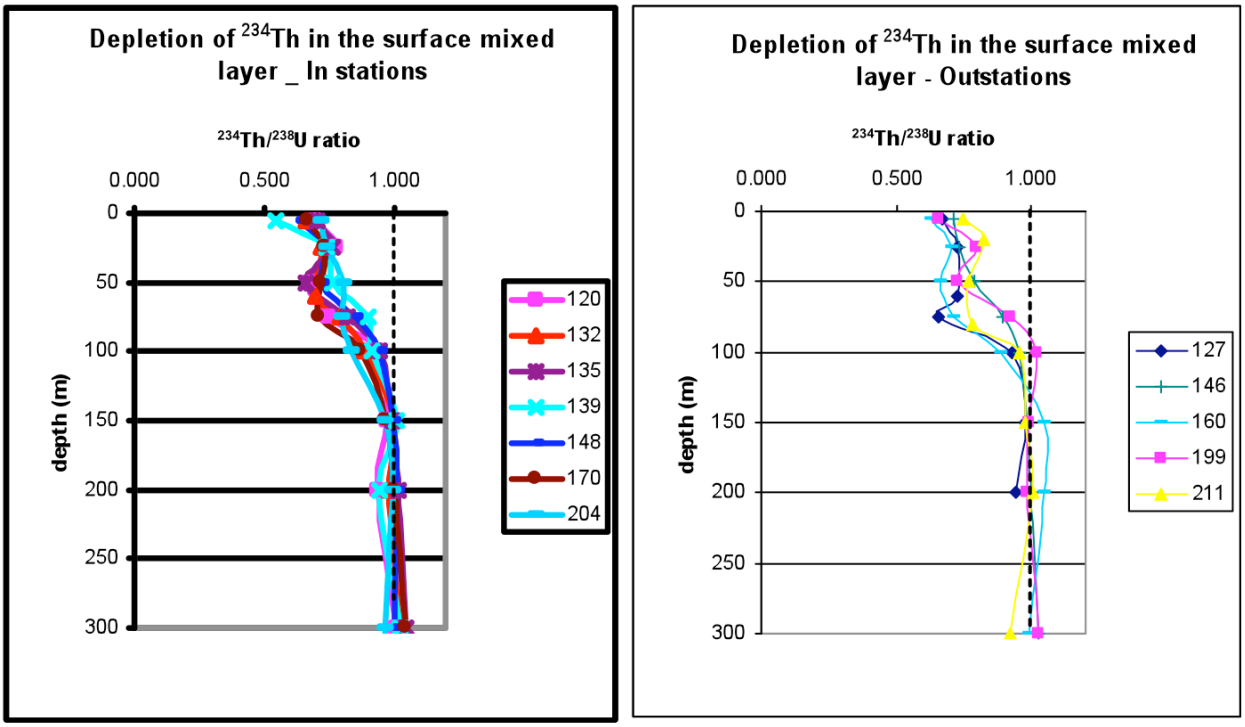

Fig. 9.2: Seawater total ^{234}Th (dissolved + particulate) profiles from the In and Out stations from the patch location after iron fertilisation. The vertical dashed line represents ^{234}Th:^{238}U radioactive equilibrium. In-stations 137, 162 and 192 are not included as they have outliers suspected to be due to low chemical yield.

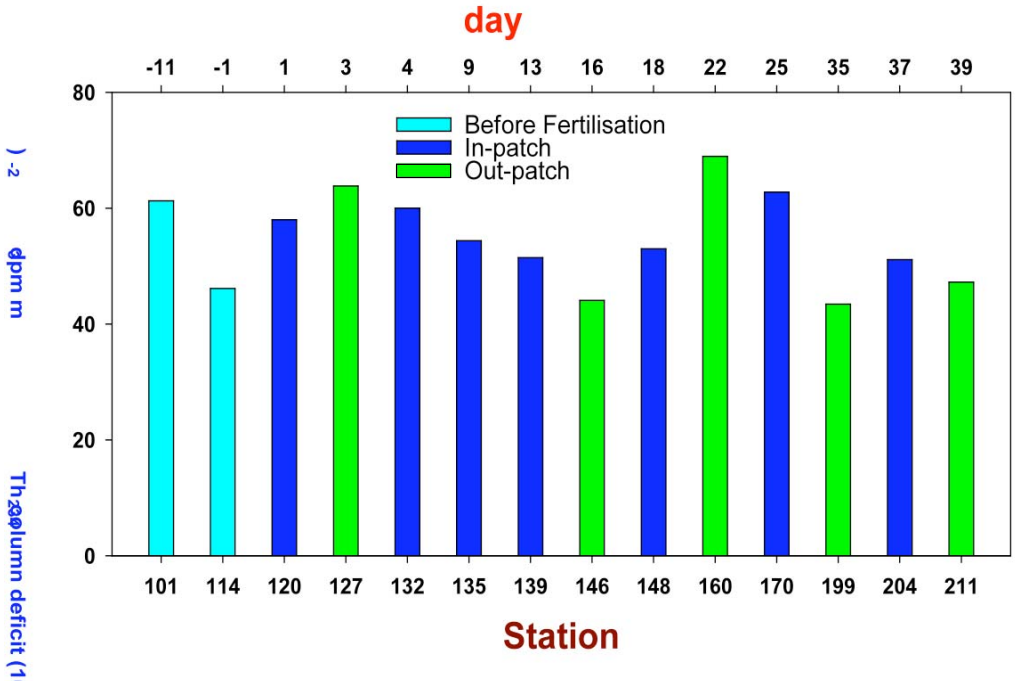

Fig. 9.3: Measured ^{234}Th deficit in the water column (0 - 100 m) from the stations in and out of the fertilized patch in the South Atlantic Ocean. The days indicated above are the elapsed days from the first iron fertilisation. Values from station numbers 137, 162 and 192 are not included in this plot as they have unusually low values at one of the depths suspected to be due to a low chemical yield.

4. Distribution of ^{234}Th over Size Fractions

The larger part of particulate ^{234}Th is in the fraction 1 - 10 µm, but the contribution of the larger size fractions is more at 200 m than at 100 m (Fig. 9.4). The increase in particle load over time, which was observed in the surface water (Fig. 9.1) is seen at 100 m, but is no longer perceptible at 200 m.

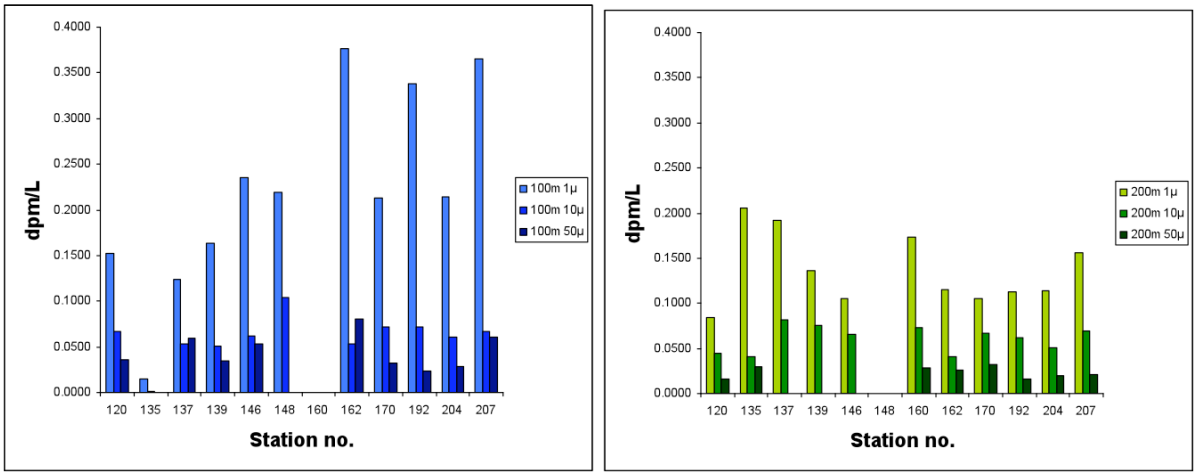

Fig. 9.4: Particulate ^{234}Th in the fractions 1 - 10 µm, 10 - 50 µm, and >50 µm at 100 m (left) and 200 m (right). At 200 m, the 10 - 50 µm and >50 µm fractions have been combined at stations 137, 139 and 146.

9.2 Radium isotopes

Objectives

Four radium isotopes are supplied to the ocean by contact with the continent or (deep-sea)-sediments: ^{223}Ra (half-life 11.4 d); ^{224}Ra (3.7 d), ^{226}Ra (1620 y) and ^{228}Ra (5.8 y). The distribution of these isotopes in seawater has been shown to be most helpful to evaluate shelf-basin exchange and water residence times. They can therefore help us to determine whether the water masses have been influenced by natural iron enrichments by contact with shelf sediments in preceding months (^{228}Ra), weeks (^{223}Ra) or days (^{224}Ra).

Work at sea

The original plan was to use radium isotopes as tracers of terrestrial sources on the shelf of South Georgia. As we did not visit that island, this part of the study could not be executed. Radium isotopes can also trace terrestrial inputs from icebergs (Smith et al., 2008). We have measured ^{224}Ra in the vicinity of iceberg at station 102. ^{224}Ra activities were very low and we could not detect an excess, which would have implied a terrestrial source. During these measurements, it turned out that the ship's seawater supply could not be used for ^{224}Ra measurements. The activities in water collected through the ship's seawater system in the fish lab was 10 times as high as in water obtained with a membrane pump aspiring seawater through a snorkel mounted in the moon pool. Apparently, the seawater tubing has been coated with

^{228}Th (1.9 y half-life parent of ^{224}Ra) during the long expeditions to the central Arctic in the past two years (see cruise report ARK-XXII/2, Schauer, 2008).

References

Cai P, Dai M, Lv D, Chen W (2006) An improvement in the small-volume technique for determining thorium-234 in seawater. *Mar. Chem.* 100(3-4), 282-288.

Schauer U (2008) The expedition ARKTIS-XXII/2 of the research vessel "Polarstern" in 2007 / ed. by Ursula Schauer with contributions of the participants. *Reports on polar and marine research* 579, 271 pp.

Smith KLJ, Robison BH, Helly JJ, Kaufmann RS, Ruhl HA, Shaw TJ, Twining BS, Vernet M (2008) Free-Drifting Icebergs: Hot Spots of Chemical and Biological Enrichment in the Weddell Sea. *Science* 317, 478, DOI: 10.1126/science.1142834.

10. Primary production, new and regenerated production, size-fractionated production

M. Gauns[1], C. Klaas[2], S. Mochemadkar[1], G. Mahadik[1], S. Patil[1], R. Roy[1], S.W.A. Naqvi [1]

[1)] NIO
[2)] AWI

Photosynthesis by phytoplankton, the unicellular algae responsible for the primary production in world's ocean, are about half of the total net photosynthesis on earth. The Southern Ocean, one of the High-Nutrient, Low-Chlorophyll (HNLC) areas, is known to have the necessary amounts of macronutrients (nitrate and phosphate) for production at the surface. However, the region remains relatively unproductive due to the lack of iron. During this study, a small area of the Southern ACC was manipulated by adding iron to assess the effect of iron addition on carbon uptake by the phytoplankton, the transfer of carbon to the food chain and to the deep sea. Our objectives were to i) follow the increase and spatial distribution of total and size-fractionated (>20 μm and <20 μm) phytoplankton biomass based on chlorophyll *a* measurements and to estimate ii) rates of primary production in and out of the fertilized patch, iii) variations in photosynthetic efficiency of cell, and iv) the stable isotope content in mesozooplanktons of in- and outpatch stations.

10.1 Primary productivity (PP) ^{14}C-based

Objectives

One of the objective of primary productivity measurements was to provide ^{14}C uptake rates for normalizing other nutrient uptake and/or growth rates measured during the experiment. And, secondly to understand the response of different phytoplankton size fractions (>20 and <20 μm) during the fertilization experiment.

Work at sea

All samples were collected and processed based on JGOFS protocol (UNESCO, 1994). CTD rosette sampler fitted with Niskin bottles (12L capacity) were used to collect samples from different depths basically covering the euphotic zone. Samples from both in-patch and out-patch stations were collected during early morning hours well before sunrise. Clean technique was used to transfer known volume of samples into polycarbonate bottles (3 light and 1 dark at each depth) to minimize trace metal contamination. Care was taken to avoid exposure of deeper samples to surface light intensity. All samples were inoculated with ^{14}C tracer and incubated for 13 - 14 h (capturing whole daylight period) in on-deck incubators shaded with blue sheet filters and neutral density screening to simulate 7 *in-situ* light levels in upper 100 m. Flowing surface seawater was used to maintain sea-surface temperature during incubation. Samples were filtered onto GF/F filters (nominal pore size ~0.7 µm) to give "total" primary productivity. At few stations sample were fractionated (>20 µm

and < 20 µm) to give size-fractioned primary productivity. Total and size fractionated production was carried out at 14 stations (10 in- and 4 out-patch stations). Due to the lack of time, size fractionated primary productivity data could not be processed onboard.

Preliminary results

Roughly, thirteen-fourteen days after the Fe-release significant increases in algal photosynthetic competence was observed, followed by elevated algal biomass (Fig. 10.1). Integrated primary production ranged between 600 & 900 mg C m^{-2} d^{-1} (in upper 100 m) outside the fertilized patch. Inside the fertilized patch productivity values increased to 1,642 mg C m^{-2} d^{-1} (1.5 to 2 fold increase within the patch) and remained high (1,314 mg C m^{-2} d^{-1}) after the 2nd fertilisation but did not increase further.

10.2 Fluorometric chlorophyll *a* measurements

Work at sea

Fluorometric chlorophyll *a* was measured to provide concentrations of plant biomass. Roughly 2,600 chl a samples were run during LOHAFEX. Vertical distribution of chl *a* in upper 200 m was monitored almost at all the station besides routine surface measurements within the patch and also during surveys in and out of the patch. At stations, water samples were taken at 10 discrete depths from each cast and from the surface down to 200 m (occasionally 250 m depth). Samples (1 L) were filtered onto GF/F filters (nominal pore size ~0.7 µm). At major stations, where primary productivity was measured, chlorophyll biomass was fractionated into two major size classes (>20 µm and <20 µm size fraction) using nylon filters and following gravity filtration. Chlorophyll was then extracted following standard procedure. Sample processing was done at low temperature with utmost care.

Preliminary results

Chlorophyll *a* followed primary productivity trend and increased markedly after 13 - 14 days of fertilization during both the stages of fertilisation. Integrated biomass in upper 150 m (in some cases 200 m) was ca. 37 mg m^{-2} at the beginning of the experiment (time zero), lower than that of maximum values recorded during first (93 mg m^{-2}; see Fig. 11.1b) and second (78 mg m^{-2}) fertilization. This suggests that both experiments produced notable increases in biomass. Maximum surface chlorophyll *a* biomass recorded inside the patch during this experiment was 1.6 mg m^{-3}. Size fractionated biomass showed that 60 - 90 % of phytoplankton biomass was in the <20 μm fractions in upper 150 m water column. Hence during the whole duration of LOHAFEX phytoplankton community was dominated largely by pico- and nano-fraction. Stations that covered both day and night sampling showed higher values during the day.

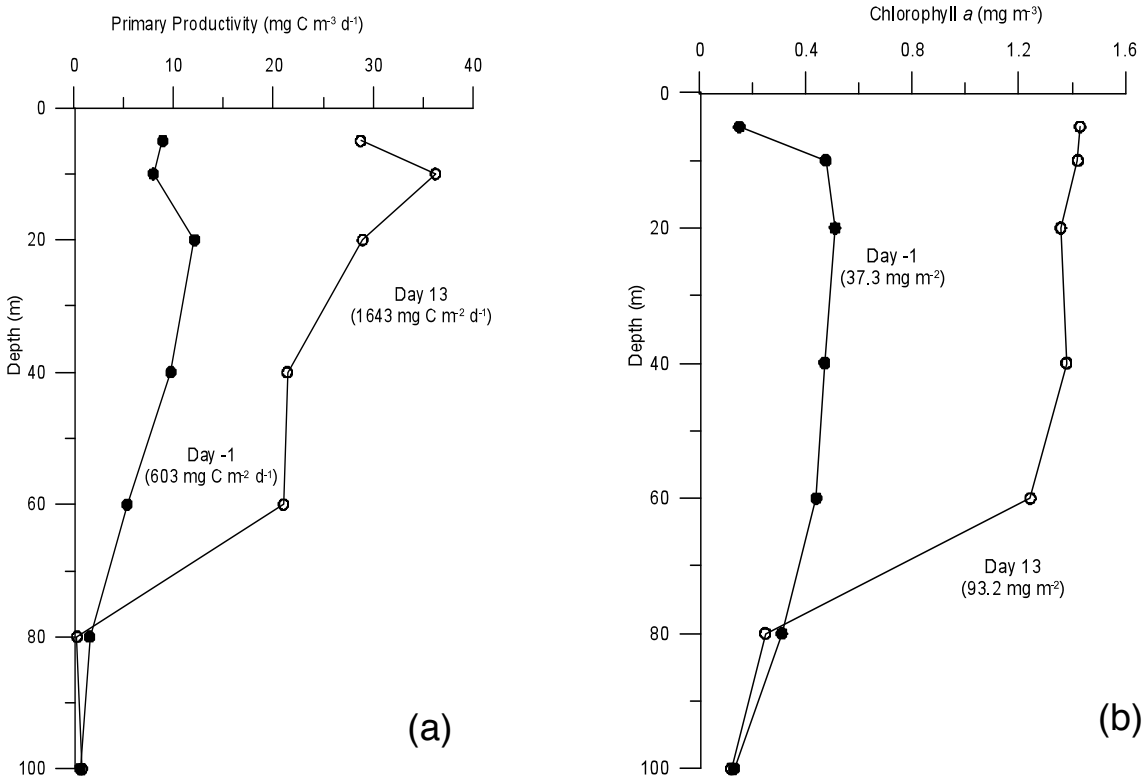

Fig.10.1. Depth profiles of (a) primary productivity (^{14}C- based; mg C m^{-3} d^{-1}) and (b) chlorophyll a (fluorometric; mg m^{-3}) at the beginning and on day 13 after fertilization when both biomass and production rates were at the maximum recorded during LOHAFEX. Day $^{-1}$ indicate one day prior to Fe-fertilization.

10.3 Photochemical efficiency: Fast Repetition Rate Fluorometer (FRRF)

Photosynthetic physiology of phytoplankton in the water column was also investigated at most major stations during the experiment using FRRF (Chelsea Technology Group; UK).

Preliminary results

The photochemical quantum efficiency (Fv/Fm) of photosystem II for the phytoplankton community prior to Fe enrichment was ca. 0.25 that gradually increased by ~ 45 % inside the Fe-enriched patch. Vertical profiles also depicted subsurface maxima (80 - 100 mts), roughly occurring at the base of the photic zone. Fv/Fm values at these sub-surface maxima were ~25 - 50 % larger than that at the surface.

10.4 Stable isotope analysis of zooplankton

Objectives

The stable isotope composition of organic carbon (^{13}C:^{12}C) and nitrogen (^{15}N:^{14}N) can be used to provide detailed description of aquatic food web structure and understand the fish and zooplankton diet. The stable carbon isotope signature (δ^{13}C)

of a consumer reflects its source of dietary carbon, whereas the stable nitrogen value ($\delta^{15}N$) reflects the trophic position of an organism. Therefore, the combined measurements of $\delta^{13}C$ and $\delta^{15}N$ can provide insights into flow of biomass into the food web as it is successively transferred to higher trophic levels.

Work at sea

Samples were collected in vertical net hauls (0 - 200 m) with the help of a specially designed combination of three different superimposed nets with cod-end buckets attached to the same frame. The mesh size of the nets were 200 μm (first internal net), 100 μm (middle net) and 60 μm (outer net). Samples retained by each net were split into two parts. One part was immediately filtered onto a precombusted Whatmann GF/F filter and dried overnight (60°C) for isotopic analyses in the shore laboratory. The second fraction was fixed with 5 % formalin (buffered with hexamine) for microscopic examination back home.

10.5 Phytoplankton pigments (HPLC based)

Objectives

To overcome some of the inadequacies of microscopy, high performance liquid chromatography (HPLC) pigment method has been used in recent years to obtain accurate chlorophyll *a* data as well as detailed information about the composition of phytoplankton communities. This method is based on the premise that different algal classes have specific signature, or marker pigments. For example, fucoxanthin, zeaxanthin, and chlorophyll *b* have been selected as taxonomical pigments for Bacillariophyta (diatoms), Cyanobacteria (blue-green algae), and Chlorophyta (green algae), respectively.

For HPLC analysis 1 - 1.5 l of samples were filtered through GF/F (25 mm) filter paper and stored at -80°C. An HPLC system was carried onboard but due to increase in baseline noise presumably due to ship's vibration it was decided to analyses the samples back at lab in NIO, Goa. However, a measurement was carried out onboard for station PS/73-148. At this station the following marker pigments were present: peridinin, fucoxanthin, neoxanthin, prasinoxanthin, 19' hexanoyloxyfucoxanthin, 19 butanoyloxyfucoxanthin and chlorophyll *b* belonging to groups like (Diatoms, dinoflagellates, prymnesiophytes and chlorophytes). Our result from this station indicated that much of the biomass during LOHAFEX was contributed by the smaller fractions of the phytoplankton community with groups like chlorophytes and haptophytes being the dominant phytoplankton within the water column however minor contribution could also be seen from diatoms and dinoflagellates. Interestingly, two prasinoxanthin-like pigments were also identified during this cruise. These pigments showed similar spectra as prasinoxanthin but eluted at different retention times.

References

UNESCO (1994). Protocols for the Joint Global Ocean Flux Study (JGOFS). Manual and Guides, 29, 170pp.

11. PHYTOPLANKTON PIGMENTS, DILUTION EXPERIMENTS

S. Patil[1], B. Fuchs[2], J. Wulf[2], G. Mahadik[1], C. Klaas[3]

[1)] NIO
[2)] MPI
[3)] AWI

Objectives

The smaller heterotrophs (nano- and microzooplankton) have been shown to be the main grazers of phytoplankton in surface waters of the world's oceans (Landry and Calbet, 2004). Plankton communities in HNLC waters of the Southern Ocean tend to be dominated by nanophyto- and nanozooplankton as well as microprotozoan grazers (Klaas, 1997; Smetacek et al., 2004) while transient blooms tend to be dominated by the large diatoms. Some nanophytoplankton (Phaeocystis species and coccolithophore species), however, can make large blooms in areas were nutrients are available but diatom growth is limited by silicic acid availability. LOHAFEX presented a unique opportunity to study the development of the plankton community under such conditions. In this study, we followed the development of the nanoplankton community and micro- and nanozooplankton grazing in order to understand factors affecting community dynamics in iron replete and low silicic acid conditions in the Antarctic Circumpolar Current.

Work at sea

Nanoplankton assemblage biomass and distribution

Water samples for nanoplankton counts were collected at 9 discrete depths (from 10 to 200 m depth) with Niskin bottles mounted on a CTD rosette. 125 mL subsamples were fixed with glutaraldehyde (0.3 % final concentration) and stored at 40°C. Forty to 100 mL of water samples were filtered onto 25 mm, 0.8 µm, black polycarbonate filters. Before the end of the filtration, samples were stained for 5 minutes with 4 - 6-diamidino-2-phenyl indole (DAPI, 5 µg mL^{-1} final concentration) and for one minute with proflavin (5 µg mL^{-1} final concentration). After this staining procedure and upon filtration of the remaining sample filters were immediately transferred onto glass slides, mounted in low fluorescing immersion oil and stored at -80°C until further analysis.

Micro- and nanozooplankton grazing

The dilution method of Landry and Hassett [1982] was used in order to estimate Micro- and nanozooplankton grazing rates. Nine in-patch and three out-patch grazing experiments were carried out during the expedition.

Before starting the experiments all the bottles were thoroughly cleaned with 1N HCl and rinsed with Milli Q water. 50 liters of seawater collected from the 20 m depth was

prescreened with 1 mm mesh to exclude larger copepods. 25 liters seawater was filtered through 0.2 μm capsule filters and used to prepare different dilutions of prescreened seawater. Typical concentrations used in dilution series were 100 %, 75 %, 50 %, 25 % and 10 % of the ambient concentration. Each dilution series was incubated in duplicates, in 2L acid cleaned polycarbonate bottles. In some experiments, dark bottles with undiluted and 50 % diluted pre-screened seawater were also incubated. In addition, screened seawater (200 μm mesh size) was incubated in order to compare with experiments carried out using larger zooplankton (Mazzochi et al., this volume) as well as determine potential trophic-cascade effects within the community. T0 and T24 samples were collected for measurements of chlorophyll *a* concentrations (Chl*a*) as well as for microscopy determination of microplankton and nanoplankton biomass and assemblage composition. In addition samples for flow cytometry analysis were collected from day 23 after fertilization onwards. Chl*a* and flow cytometry analyses for pico- and nano-eukaryotes and bacterioplankton abundance were carried out on board.

Microscopy counts of microplankton and nanoplankton will be carried out in the laboratory ashore.

Preliminary results

*Grazing based on Chl*a *measurements*

Apparent growth rates based on Chl*a* measurements ranged between -0.16 to 0.35 d^{-1} for the highest dilution (10 % unfiltered seawater) and -0.27 to 0.19 d^{-1} for undiluted incubations, with highest values at the end of the experiment. These results indicate that grazers consumed at least 50 % of phytoplankton production. However, regression curves between T24 and T0 differences in apparent growth rates and dilution factor were not significant as overall variability of Chl*a* values exceeded differences between T0 and T24. These results are due partly to due to the low net phytoplankton growth rates during the experiment combined with the variability of measurements (±4 % average analytical errors and similar values for the variability from replicate incubation bottles). In addition, Phaeopigments concentrations (Phaeop) in surface waters during LOHAFEX where high reaching maximum values of over 40 % of Chl*a* + Phaeop. This is more than twice the phaeopigments contribution found in a previous iron fertilization experiment (EIFEX) resulting in a bloom dominated by diatoms (Klaas et al., unpublished data). The high phaeopigments concentrations might have further contributed to the variability in Chl*a* measurements and are an additional indication of high grazing rates by zooplankton during LOHAFEX.

Grazing based on flow cytometry counts

Flow cytometry analyses of dilution experiments carried out at the end of the iron fertilization experiment are shown in Figs. 11.1 and 11.2. Apparent growth and grazing-mediated mortality rates of picoheterotrophs (mainly bacteria) showed no difference inside and outside the fertilized patch (Fig. 11.1). In both areas, grazing and growth rates where similar (0.3 to 0.5 d^{-1}).

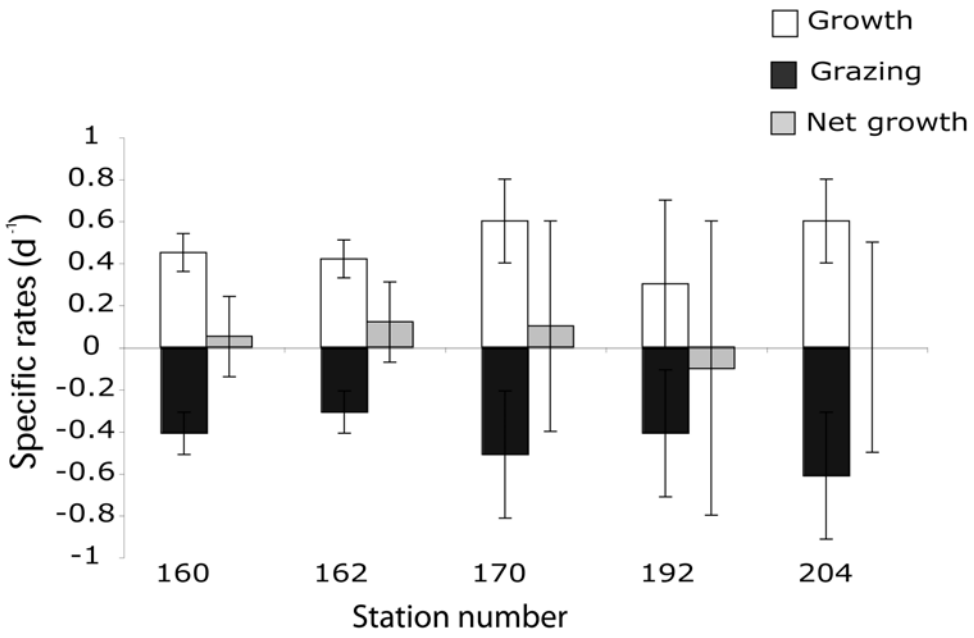

Fig. 11.1: Apparent growth rates (μ) and grazing-mediated mortality rates (g) for the picoheterotrophs. The resulting net growth rates (μ-g) are also given in the figure. Station 160 was carried-out outside the fertilized patch, all others stations where in-patch stations. Stations 160, 162, 170, 192 and 204 took place on day 23, 24, 27, 33 and 36 after fertilization, respectively. Error bars correspond to one standard deviation.

Growth and grazing-mediated mortality rates of pico- and nanophytoplankton showed strong variability both inside and outside the fertilized patch (Fig. 11.2). Apparent growth rates reached higher values inside the fertilized patch (maximum of 1 d^{-1}). Overall grazing rates were similar to growth rates both inside and outside the fertilized patch.

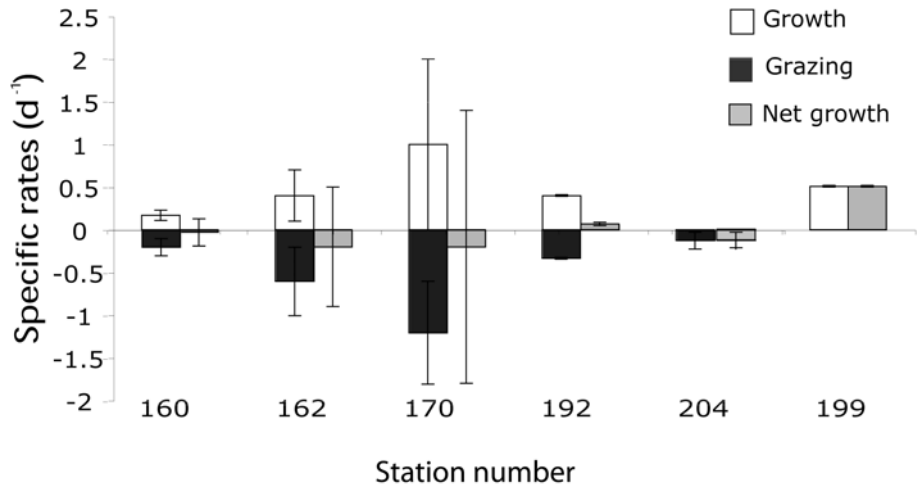

Fig. 11.2: Apparent growth rates (μ) and grazing-mediated mortality rates (g) for the pico- and nanophytoplankton. The resulting net growth rates (μ-g) are also given in the figure. Station 160 and 199 were carried-out outside the fertilized patch, all others stations where in-patch stations. Stations 160, 162, 170, 192, 199 and 204 took place on day 23, 24, 27, 33, 35 and 36 after fertilization, respectively. Error bars correspond to one standard deviation.

Our results indicate that nano- and microzooplankton grazers consumed most of the production of pico- and nanoplankton both inside and outside the fertilized patch during LOHAFEX.

References

Klaas C (1997) Microzooplankton distribution and their potential grazing impact in the Antarctic Circumpolar Current. Deep-Sea Research II, 44, 375-393.

Landry MR, Hassett RP (1982) Estimating the grazing impact of marine micro-zooplankton. Marine Biology, 67, 283-288.

Landry MR, Calbet A. (2004) Microzooplankton production in the oceans, Journal of Marine Sciences, 61, 501-507.

Smetacek V, Assmy P, Henjes I (2004) The role of grazing in structuring Southern Ocean pelagic ecosystems and biogeochemical cycles. Antarctic Science, 16, 541-558.

12. DOC, DTN, POC, PON, ^{13}C, ^{15}N

M. Gauns, M. Muthirenthy, R. Kanta, S. Karapurkar, S. Kurian, A.K. Pratihary, A. Sarkar, S.W.A. Naqvi — NIO

12.1 Dissolved organic carbon (DOC) and dissolved total nitrogen (DTN)

Muthirenthy M.

Objective

To investigate the variability of DOC and DTN in surface waters caused by the iron-induced phytoplankton bloom for quantifying the conversion of new biomass produced to dissolved organic fractions.

Work at sea

Seawater samples at the in-patch and out-patch stations were collected for DOC and DTN in pre-combusted EPA glass vials having silicone septa. Samples were filtered avoiding any contamination using a glass syringe through GF/F 0.45 µM acrodisc syringe filters and immediately frozen at -4°C. These samples were carried to National Institute of Oceanography, Goa, for analysis. DOC and DTN were measured simultaneously using the TOC-V-CSH analyzer by high temperature catalytic oxidation method and DTN was analyzed using the chemiluminscence detector. Prior to analysis the column was conditioned with multiple injections of Mili-Q water and calibration was performed every analytical day using potassium hydrogen phthalate and potassium nitrate standards for DOC and DTN, respectively. The instrument performance was checked each time after calibration by running three consensus reference samples (CRM) which had deep sea DOC of 44 - 46 µM and DTN of 32.8 µM. These CRMs were kindly provided by Prof. D.A. Hansell, University of Miami. Standard deviations of triplicate measurements were found to be about 0.2 %.

Preliminary results

The DOC and DTN changes in the surface water (10 m depth) are shown in Figs. 12.1 and 12.2, respectively, for in-patch stations, and in Figs. 12.3 and 12.4, respectively, for out-patch stations. The initial concentration of DOC in surface water was 71±5µM. As the bloom progressed from day 0 to day 13, DOC in the surface layer gradually increased by 13 µM and remained roughly constant up to day 23. Subsequent re-fertilization did not have any significant

effect on DOC levels showing a net gain of only 4 µM from day 23 to day 37 (note that values of both DOC and DTN on Day 28 were anomalously low). Surface DTN however showed a patchy distribution within the patch and an overall decrease of 5 µM was observed from day 0 to day 37. Average surface DOC concentration at the OUTPATCH stations was 68 µM, while DTN showed an average of 22.3 µM.

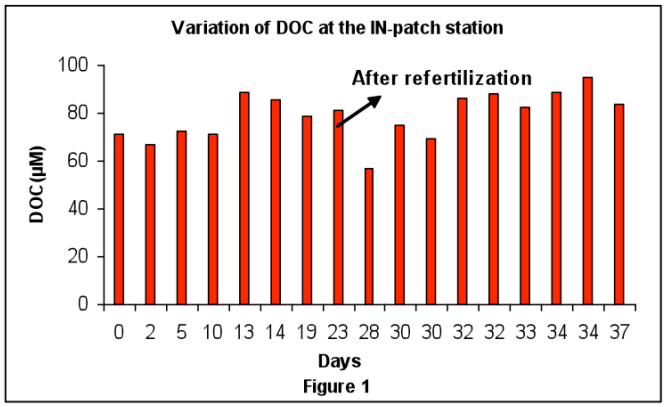

Fig. 12.1.1: Variation of DOC at the in-patch stations during LOHAFEX

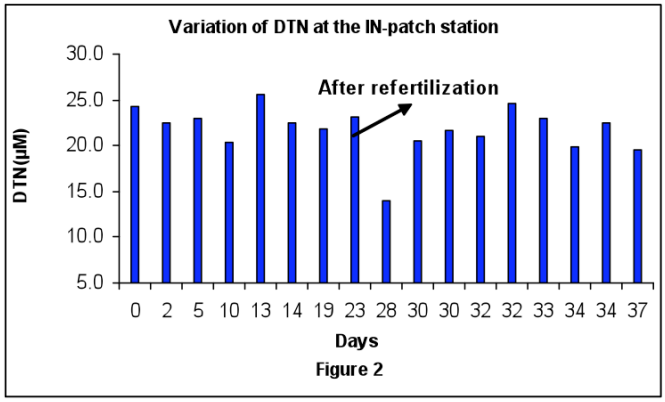

Fig. 12.1.2: Variation of DTN at the in-patch stations during LOHAFEX

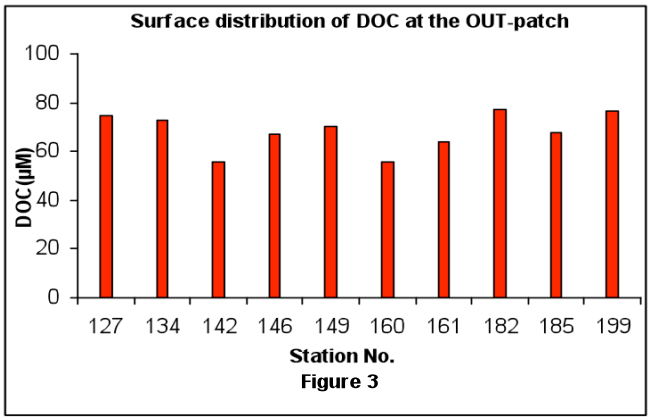

Fig. 12.1.3: Variation of DOC at the out-patch stations during LOHAFEX

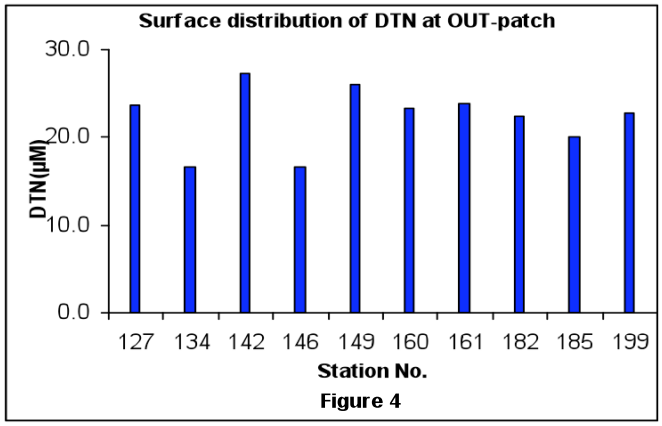

Fig. 12.1.4: Variation of DTN at the out-patch stations during LOHAFEX

12.2 Natural isotope abundance in dissolved nitrate

A. Sarkar, M. Muthirenthy, S.W.A. Naqvi and S. Karapurkar — NIO

Objectives

To investigates nitrogen uptake and regeneration through analysis of isotopic composition of nitrate following iron enrichment.

Work at sea

Sea water samples were collected during the expedition at 27 stations. One of these stations was sampled before fertilization and four stations were located outside the Fe-fertilized patch. The remaining stations sampled the fertilized patch. Samples were collected from 9 standard depths down to 200 m. Samples were immediately filtered through GF/F filters and the filtrates were poured into acid-washed 500-ml Tarson bottles and acidified with 2 ml of 50 % hydrochloric acid. The acidified samples were stored at room temperature for analysis in the shore laboratory.

12.3 POC, PON, δ13C, and δ15N of particulate matter

A. Sarkar, M. Muthurenthy, S. Kurian, S.W.A.Naqvi — NIO

Objectives

To estimate various organic fractions of carbon and nitrogen and their isotopic composition for constraining the budgets of these elements and to investigate changes caused by iron fertilization.

Materials and Method

Sea water samples were collected at 27 stations. One of these stations was sampled before fertilization and four stations were located outside the Fe-fertilized patch. The

remaining stations sampled the fertilized patch. Samples were collected from 9 standard depths down to 200 m. 2 L of the sample was filtered immediately through pre-combusted GF/F filters (25 mm diameter, 0.7 μm pore size) under vacuum (~100 mm Hg). The filters were preserved frozen (-20°C) for analysis in NIO using an elemental analyzer coupled to an isotope ratio mass spectrometer.

12. 4 ^{13}C- and ^{15}N-based primary, new and regenerated production

A. Sarkar, M. Gauns, A. K. Pratihary, S.W.A. Naqvi, S. Kurian, S. Karapurkar — NIO

Objectives

To estimate primary production including its 'new' and 'regenerated' components using ^{13}C- and ^{15}N-labelled tracers to quantify carbon fixation and its export flux. This would also lead to better understanding of relevant biogeochemical processes that control the distributions and fluxes of carbon and nutrients in the surface ocean.

Work at sea

Carbon, nitrate, ammonia and urea uptake rates were measured during LOHAFEX. Sea water was sampled using Niskin bottles at thirteen stations including one before fertilization and three out-patch sites from five depths down to 100 m. Samples were collected late at night or early dawn. The background nutrient concentrations, except for urea, were measured immediately using an auto analyser. Aliquots of the samples were poured in pre-cleaned transparent polycarbonate bottles. Each aliquot was spiked with 0.2 μM, 0.05 μM and 0.05 μM of ^{15}N labelled nitrate, ammonia and urea, respectively, along with 20 μM of ^{13}C-labelled HCO_3^-. After the addition of tracers the bottles were covered by appropriate neutral density light filters in order to simulate the natural light conditions. The bottles were incubated in deck incubators and the incubation temperature was maintained by continuous sea water flow. The incubation time was 12 - 14 hours, from dawn to dusk. After the incubation the samples were filtered through pre-combusted GF/F filter papers under vacuum (<100 mm Hg). The filters were preserved frozen (-20°C) for mass spectrometric analysis at NIO.

13. PHYTOPLANKTON PHOTOPHYSIOLOGY AND BIO-OPTICS

M. Ribera d'Alcalá[1], C. Klaas[2]

[1)] SZN
[2)] AWI

Objectives

It is well established from the first pioneering fertilization experiment that phytoplankton relieved from iron limitation displays a measurable increase in the Fv/Fm ratio which can be easily tracked by a FRRF or similar sensors. Because of such evident response different equipments capable to measure variable fluorescence and the related parameters, e.g., the functional cross section of PSII (PSII, have always been used to track the location of the fertilized patch to be distinguished from the areas or the water parcels not affected by iron addition. Also during LOHAFEX and despite the relatively low amplitude of the Fv/Fm ratio in many circumstances the FRRF measurements confirmed to be the most reliable sign of being inside or outside the patch.

Work at sea

A recently calibrated Chelsea Fastracka was immersed in a plastic tank with moon pool water continuously pumped through the dark cell of the instrument. To prevent air bubbles flowing through the cell a T bypass was mounted before the cell entrance with the pump sucking on the exit side of the cell to avoid sample contamination. The immersion of the Fastracka in the tank full of water allowed also thermal stability of the measurements with the temperature continuously monitored by the instrument sensor.

The setup profited of the acquisition procedure set up by Rüdiger Röttgers and his group in the previous EIFEX experiment. Briefly, the procedure was the following:

- the instrument was running all the time, except when downloading data, preferably during stations;
- to warrant both internal storage of data and their visualization in real time for ship operation, Fastracka was set in verbose mode with the interface transmitting to a modem the readings pertaining to each excitation curve;
- a dedicated script in Matlab, using the proper constants stored in a file, was continuously converting readings in photosynthetic parameters which could be plotted in real time on the PC screen;
- to display the data to the other participants a VNC server was activated on the PC for a display mirror of the PC interfaced with the instrument;
- a remote connection was also activated to have a remote control of the software when needed.
- The original protocol developed by Röttgers group included also an empirical compensation for non-photochemical quenching during the day. It was active

also during LOHAFEX but, likely because the different amplitude of variable fluorescence response as compared to EIFEX and the poor results of various attempts to recalibrate the empirical relation, the corrections produced by the routine were never robust. Therefore only the relative signals were considered.

- Also the real time synchronization with the ship position was not active because of the change in the software for ship location and the difficulty to interface the PC with the source of location information. However this lack of information was easily handled with an effective link with the bridge. In some cases, profiting of the remote VNC link, a PC was set to run on the bridge for real time decisions.
- Every 24 - 36 hours, when not in a crucial phase and generally at stations, the instrument was stopped to download the binary data, while carefully cleaning the cuvette;
- binary data were afterwards processed by a routine written by Sam Laney (WHOI, MA, USA) to convert the data in the proper format to be processed by the FRS code by Chelsea Instruments;
- thus two parallel data sets where generated which correspond to two different fitting routines for the excitation curves;
- finally the data where merged, using time as the common unit, with atmospheric and hydrographic data plus, obviously, ship location.

The overall procedure, besides providing real time information of the phytoplankton physiology as a proxy of iron stimulation, allowed a daily representation of the spatial distribution of the response, with the intrinsic limitation of measurements taken in daylight.

A typical map produced with an ad hoc MATLAB script is reported in Fig. 13.1.

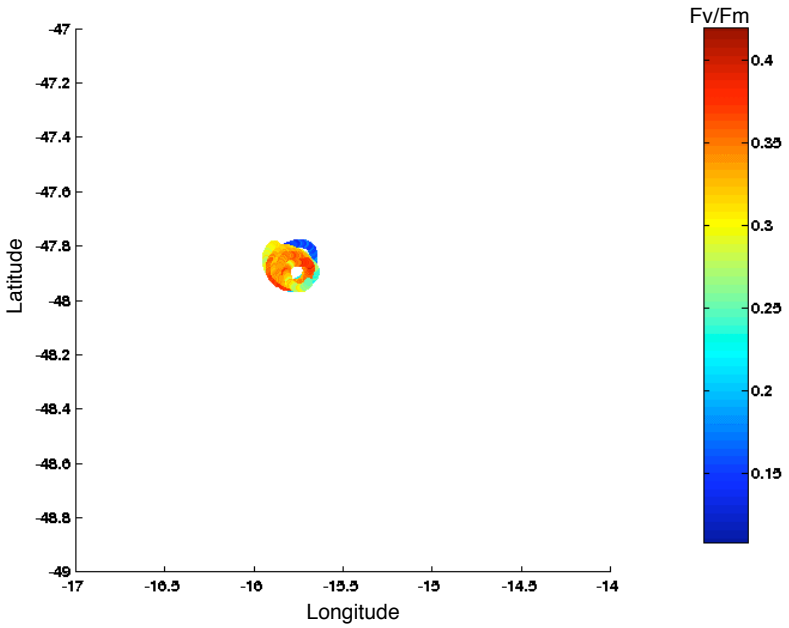

Fig. 13.1: Map of Fv/Fm during the first fertilization

A comparison with chlorophyll *a* concentration and other data showed that measurements carried out during daylight were very seldom indicative of being in the patch. The values of Fv/Fm in daylight were generally very low (0.1 - 0.2 Fv/Fm relative units), even when inside the patch, as testified by night measurements and complementary data. Part of the problem may arise because of the low chlorophyll concentrations with correspondent low values of both F0 and Fm, with a very noisy ratio. Another part might be due to a weaker, than in previous experiments, photo-physiological response of phytoplankton. Both hypotheses have to be analyzed in more detail during post-cruise phase. During all the experiment the value of 0.5 was very seldom reached, with most of the values inside the patch being in the range of 0.3 - 0.4. In some occasions other fluorescence based parameters, namely connectivity p, were positively correlated with a community exposed to iron enrichment.

Another interesting feature was the recurrent increase of Fv/Fm at the time of sunrise, which suggests either an internal rhythm of the algae or an acute response to the dawn light.

Maps of the FRRF were overlapped with independent dynamical measurements, e.g., drifters, and the few satellite images available for the whole duration of the cruise. Those corroborated the real time evaluation of being inside or outside the patch. Two examples are reported in Figs. 13.2 and 13.3.

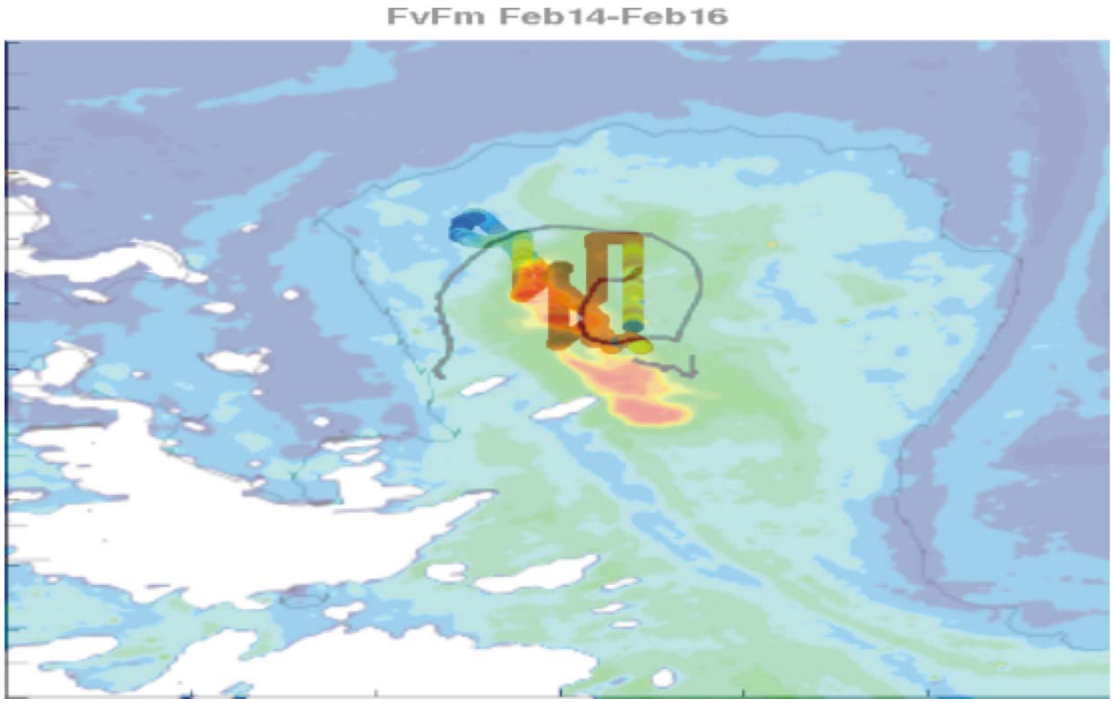

Fig. 13.2: The Fv/Fm track is overlapped on the February 14 MODIS image of the patch. Correspondence between high chlorophyll values due to iron addition and stronger photo-physiological activity (red shifted dots) by phytoplankton is clearly visible.

During the whole cruise variable data were used mostly as a diagnostic tool to follow the patch. Especially after the second fertilization, because of the very weak response to the second iron addition, the spread of the values of Fv/Fm, also due to changes in the illumination over the day-night cycle, made more difficult to use the parameter as a robust indicator of the patch in real time. In the last phase, before leaving the area, Fv/Fm values tended to be always lower than during the starting and the mid-phase of the experiment. Integrated data analysis, e.g., a merge of variable fluorescence, chlorophyll *a* and dynamical reconstruction could be carried out only using graphic representations, since no numerical circulation model was running on the ship.

Despite this, the whole data series of Fv/Fm maps, merged with the few satellite images and the altimeters derived flow fields, showed that all the operations aimed at sampling the patch, have been conducted within the patch.

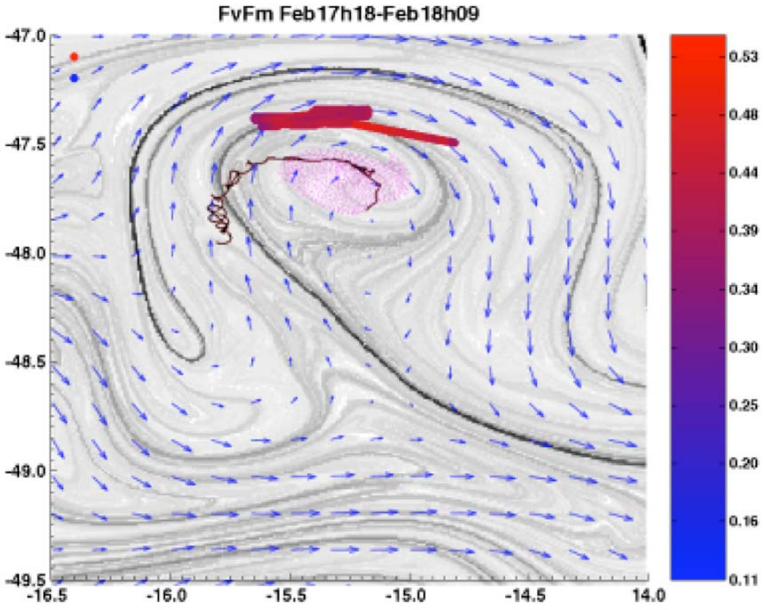

Fig. 13.3: Fv/Fm map is overlapped on the Finite Size Lyapunov Exponent distribution and the reconstructed flow field, based on the altimeter data.

Far from the daily urgency of sampling, post-cruise processing will better clarify the dynamics of the patch and allow for a better assessment of which part of the patch have been sampled at each moment of the experiment.

14. MICROBIOLOGY

B. Fuchs[1], J. Wulf[1], N. Ramaiah[2], S. K. Singh[2], V.R. Sundareswaran[3], G.S.N. Reddy[3]

[1)] MPI Bremen
[2)] NIO
[3)] CCMB

14.1 Bacterioplankton composition

B. Fuchs[1], J. Wulf[1]

[1)] MPI Bremen

Objectives

Iron-fertilization experiments are well suited to follow induced shifts in community composition under controlled conditions and to reveal the links between the different trophic levels. Recently it has been shown, that within a naturally fertilized area at the Kerguelen upwelling plateau the bacterioplankton community was qualitatively and quantitatively different from the community outside (West et al. 2008). We hypothesized that in an artificially fertilized patch similar a community shift in bacterioplankton will be observed.

Work at sea

On board, we closely followed the picoplankton community by flow cytometric counting. Both, heterotrophic Bacterioplankton and autotrophic Picoplankton populations were recorded from most of the stations and depths sampled.

To determine the bacterioplankton community composition, samples for fluorescence *in-situ* hybridisation (FISH) were taken. For some representative stations and depths the samples were analysed already on board by epifluorescence microscopy. Fluorescently labelled oligonucleotide probes specific for chosen key groups of the bacterioplankton community have been used to follow the community composition during the experiment.

At every major station during the experiment large volumes of water (60 - 90 l) was sampled for the later analysis of the metagenomes. The water was pre-screened through filters of 5.0 μm and 3.0 μm pore size, respectively, in order to separate the majority of the eukaryotic plankton from the smaller bacterioplankton, which was filtered onto filters of 0.2 μm pore-size. These biomasses will serve as the basis for a metagenomic approach to reveal the metabolic potential of the pico- and bacterioplankton community present at a certain time point during the experiment. The large pore size filters will be processed later on at the AWI Bremerhaven in collaboration with Klaus Valentin and Claudia Metfies.

The metabolic activity of specific groups of bacterioplankton was assessed by pilot experiments with isotopically labelled substrates. As substrates ^{15}N labelled nitrate

and ^{13}C labelled bicarbonate were used. The amount of uptake of substrates and the simultaneous identification by FISH will be determined back home at the institute by a technique called Nano-SIMS – a next generation mass spectrometer with submicron spatial resolution.

Preliminary results

The bacterioplankton abundance fluctuated during the experiment between 360.000 cells ml^{-1} and 670.000 cells ml^{-1} inside the fertilised patch at 20 m depth (Fig. 14.1.1). Cell numbers increased slightly after fertilisation to 550.000 cells ml^{-1}, but decreased dramatically to almost half of the initial numbers on day 12 after fertilisation. Afterwards, they increased again to the highest level measured (670.000 cells ml^{-1}) at days 30 - 32 after fertilisation. At the end of the experiment, the bacterioplankton cell numbers was around 450.000 cells ml^{-1}.

Surprisingly, the bacterioplankton cell numbers were in the same range outside and inside the patch in the mixed surface layer (Fig. 14.1.1.). Only in the beginning of the experiment at one station on day 8 the cell numbers were significantly lower outside (250.000 cells ml^{-1}) than inside the patch (450.000 cells ml^{-1}).

The bacterioplankton cell counts inside the patch varied up to 20 % as measured on three transects through the patch. However at each station, the cell counts within the surface mixed layer was more constant and varied often less than 5 %, pointing to spatial patchiness of the bacterioplankton abundance rather than an experimental variation.

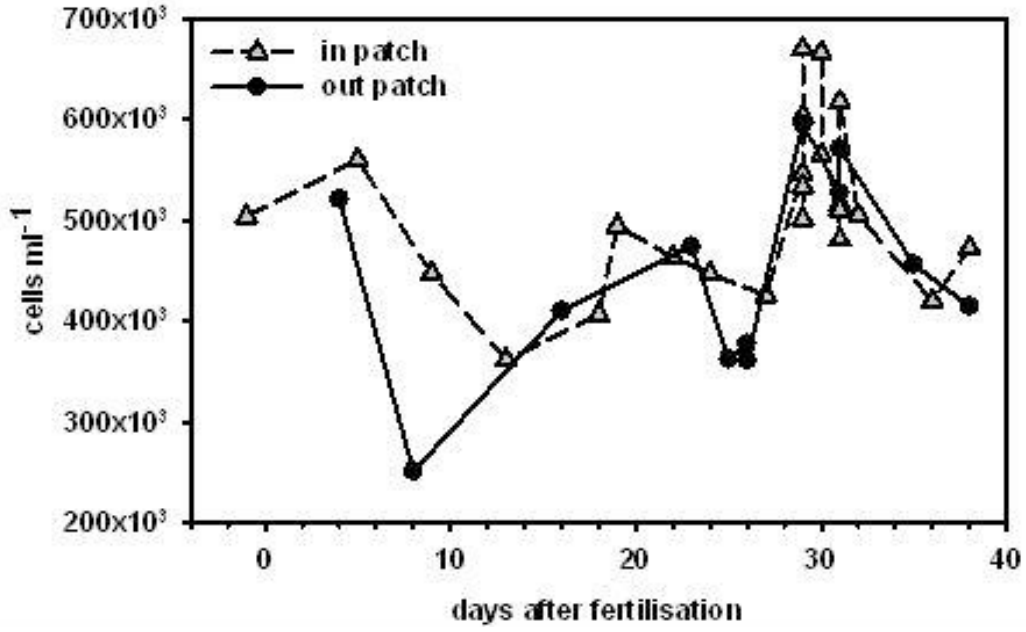

Fig. 14.1.1: Bacterioplankton abundance during the course of the experiment at 20 m water depth. Note: On days 29 to 32 several transects with multiple stations were recorded.

In contrast to the bacterioplankton community, the autotrophic pico- and nanoplankton responded to the fertilisation and doubled in numbers until day 22 of the experiment (Fig. 14.1.2). With one exception on day 8 and 9, there were regularly higher cell counts inside the patch compared to stations outside the patch. The picture blurred after day 24, when there were similar autotrophic pico- and nanoplankton counts measured inside and outside the fertilised patch and the variance inside the patch was high. Also there is no clear effect of the second fertilisation on the autotrophic pico- and nanoplankton discernable.

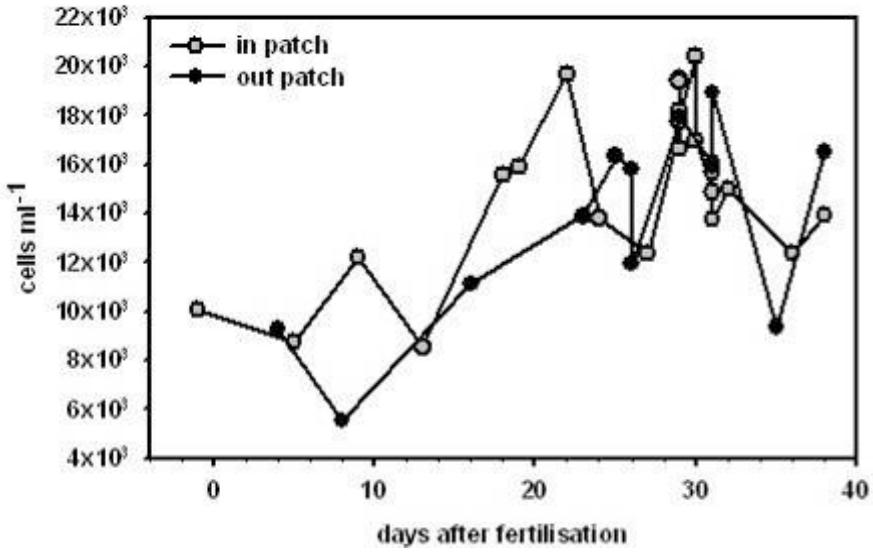

Fig. 14.1.2: Autotrophic pico- and nanoplankton abundance during the course of the experiment at 20 m water depth.

The bacterioplankton composition as determined by fluorescence *in-situ* hybridisation pointed to a rather stable community dominated by the alpha subgroup of Proteobacteria, whereas the gamma Proteobacteria and Bacteroidetes made up only a minor fraction of the community. However the data gained on board needs to be verified by additional experiments back home in the lab.

References

West NJ, Obernosterer I, Zemb O, Lebaron P (2008) Major differences of bacterial diversity and activity inside and outside of a natural iron-fertilized phytoplankton bloom in the Southern Ocean. *Environmental Microbiology* 10, 738-756.

14.2 Bacterial productivity and other measurements

N. Ramaiah N., S. K. Singh NIO

Objectives

In most pelagic ecosystems, bacterioplankton biomass is a substantial fraction of the total biomass and, bacterial carbon can often exceed that of phytoplankton carbon especially in the regions of low chlorophyll concentrations. It is realized that primary production and, consequent availability of easy-to-assimilate dissolved organic matter (DOM) facilitate heterotrophic bacterial growth and abundance. Since much of the primary production is grazed upon by larger, herbivorous zooplankton communities, proliferation of bacteria is essential for nourishing a plentitude of microzoans: ciliates (eg., tintinnids) and heterotrophic flagellates particularly in regions - and seasons - of low chlorophyll production and, concentrations. Thus, proliferation of bacteria by their unique ability of assimilating DOM, helps nourishing particulate-ingesting phagotrophic micro-, meso-zooplankton and/or other fauna. Further, their role is important in the biogeochemical cycling of biologically essential elements in any ecosystem. Measurements of bacterioplankton abundance, community composition and productivity processes are useful indicators of biological response to iron-fertilization. Thus, we aimed at following fertilization induced shifts in bacterial production.

Work at sea

As a part of the LOHAFEX the following measurements were carried out.

1. Total counts of DAPI stained bacteria were made to follow as to how bacteria respond to iron fertilization.
2. Direct viable counts were made to estimate the metabolically active fraction of heterotrophic bacteria.
3. Bacterial growth rate measurements were made to assess the change in their growth rates in response to fertilization.

In addition as planned, water samples from in and out patches were collected from discrete depths and, microbes therein have been strained on Sterivex filters for DGGE profiling and other molecular analyses of in- & out- patch bacterial community later in the Institute (Goa).

Sampling

Water sampling was carried out from 5 out patch (St No: PS73-112, 114, 146, 160 and 199) and 10 in-patch (PS 73-114 [d-1]; 132 [day 4]; 135[d 9];137 [d 12]; 139 [d 13]; 148 [d 18]; 162 [d 24]; 170 [d 28]; 192 [d 33] and 204 [d 36]) stations. From all these stations water samples were collected from 5, 10, 20/chl max, 50, 100, 200, 300, 500 and 1,000 m.

Total counts

For estimating bacterioplankton abundance standard epifluorescence microscopic method was followed. From these stations, water samples from all depths were fixed with 0.22 μm prefiltered buffered formaldehyde (2 % final concentration) and stored at 4ºC in the dark until slide preparation, usually within 3 - 5 hrs of sample collection. Subsample volumes of 5 ml were stained with DAPI (final concentration 0.01 %) for 5 mins, filtered (0.22 μm black Nucleopore filters) and slides prepared, epifluorescence microscopic counts from 10 - 15 fields made and total bacterial abundance estimated. Similarly, for estimating direct viable counts, 10 ml samples from each sampling depths were amended with 150 μl 2 % (wt/vol) yeast extract and 10 μl nalidixic acid (0.1 μgml^{-1}) and, incubated for 8 - 10 hrs in dark at 4ºC. Following incubation, the contents were stained with DAPI (final concentration 0.01 %) for 5 mins, filtered (0.22 μm black Nucleopore filters) and slides prepared as described above. Enlarged cells discernible as bacteria were counted from atleast 15 fields for obtaining the direct viable counts and their percent fraction in each sample was calculated.

Bacterial production rate (BPR): The BPR was estimated from the measurements of methyl-^{3}H-thymidine and leucine incorporation rates by following the standard procedures. The zero-time blanks were run for all the samples in order to obtain correction for abiotic/filter adsorption.

Preliminary results

In the in-patch stations, the total counts in the top 50 - 100 m showed increases by day 5. Ranging narrowly between ~450,000 and 650,000 cell counts in the top 50 m, the profile to profile variations in these counts was imminent and, fertilization did not enhance the bacterial abundance drastically. In comparison with out-patch stations or with the day -1, the highest increase in surface to 100 m column integrated bacterial counts was ~160 % in the in-patch. Fig. 14.2.1 depicts the vertical profiles of total and direct viable counts of bacteria from a few locations in-patch.

The fractions of direct viable counts ranged between 10 and 15 % in the top 50 m and were lower between 2 and 5 % in the deeper depths. As an example, Fig. 14.2.2 denotes the percentage of DVC in the total counts at different depths at two in-patch locations. A cursory look at the DVC data from all the stations suggests that the percent fractions of DVC remained more or less similar both in patch and out patch indicating that the general proportion of metabolically active fractions is around 10 % in the top 100 m and ~ 3 % between 200 and 500 m.

Between thymidine (Fig. 14.2.3) and leucine (Fig. 14.2.4), the latter appears to be preferentially taken up by bacteria in the LOHAFEX region. In comparison with the EISENEX results, it is apparent that the rates of incorporation of both thymidine and leucine are twice as fast as were observed during the EISENEX. Detailed analyses of the bacterial growth rates from different regions in the Southern Ocean will be made to elucidate the mechanisms leading to such increased uptake potential. Further data

on bacterivores, phytoplankton composition and zooplankton details will be made use of to present a detailed analyses/interpretation of these data.

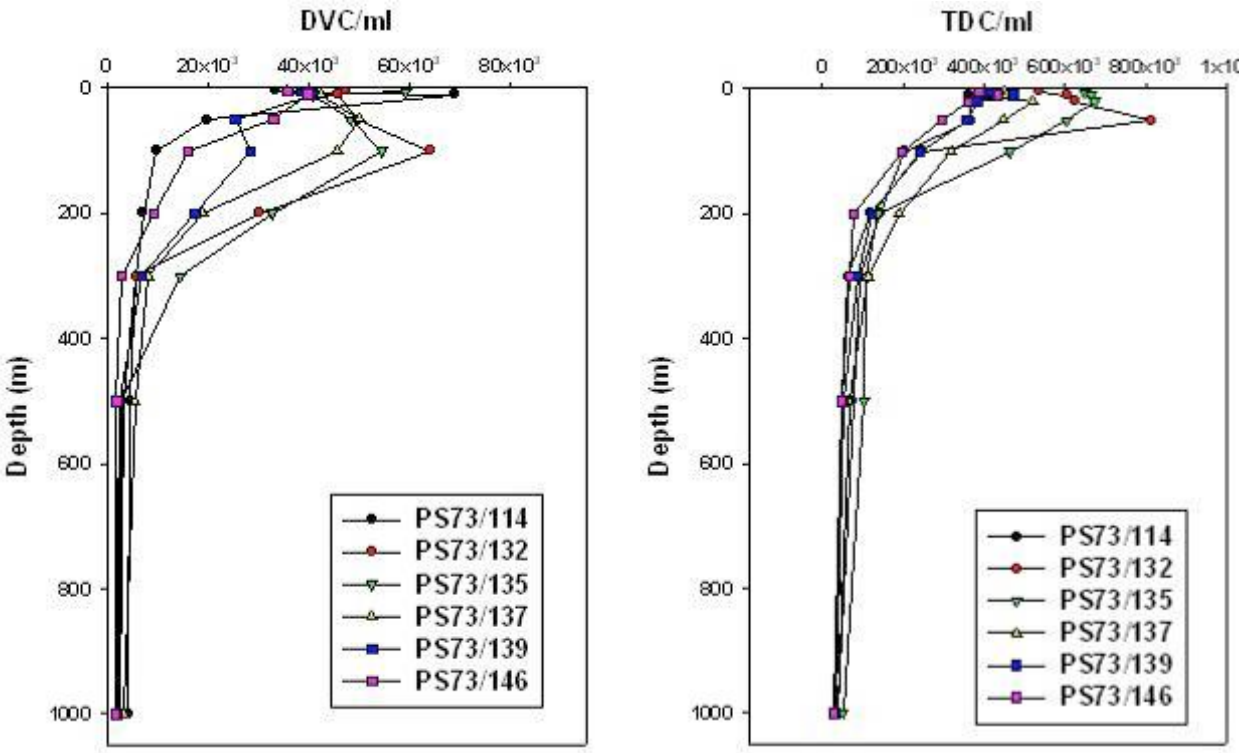

Fig. 14.2.1: Total counts and direct viable counts of bacteria in the in-patch stations during LOHAFEX

.

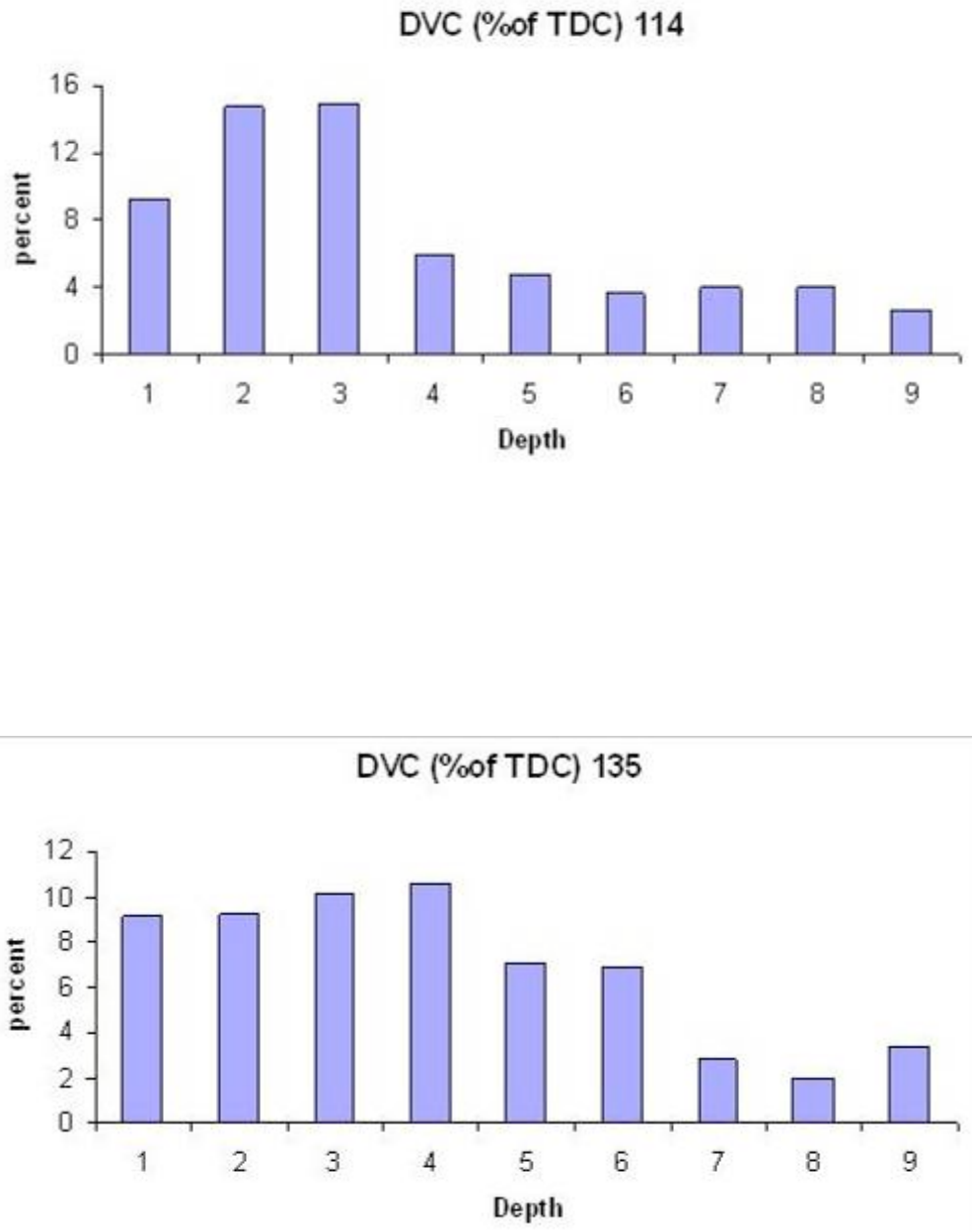

Fig. 14.2.2: Percent fractions of direct viable counts at two in-patch stations, PS73-114 [d-1] and PS73-135 [d 13] during LOHAFEX. Sampling depth denoted in both panels are, 1for 5 m; 2 - 10 m; 3 - 20 m; 4 - 50 m; 5 - 100 m; 6 - 200 m;7 - 300 m; 8 - 500 m and 9 for 1,000 m.

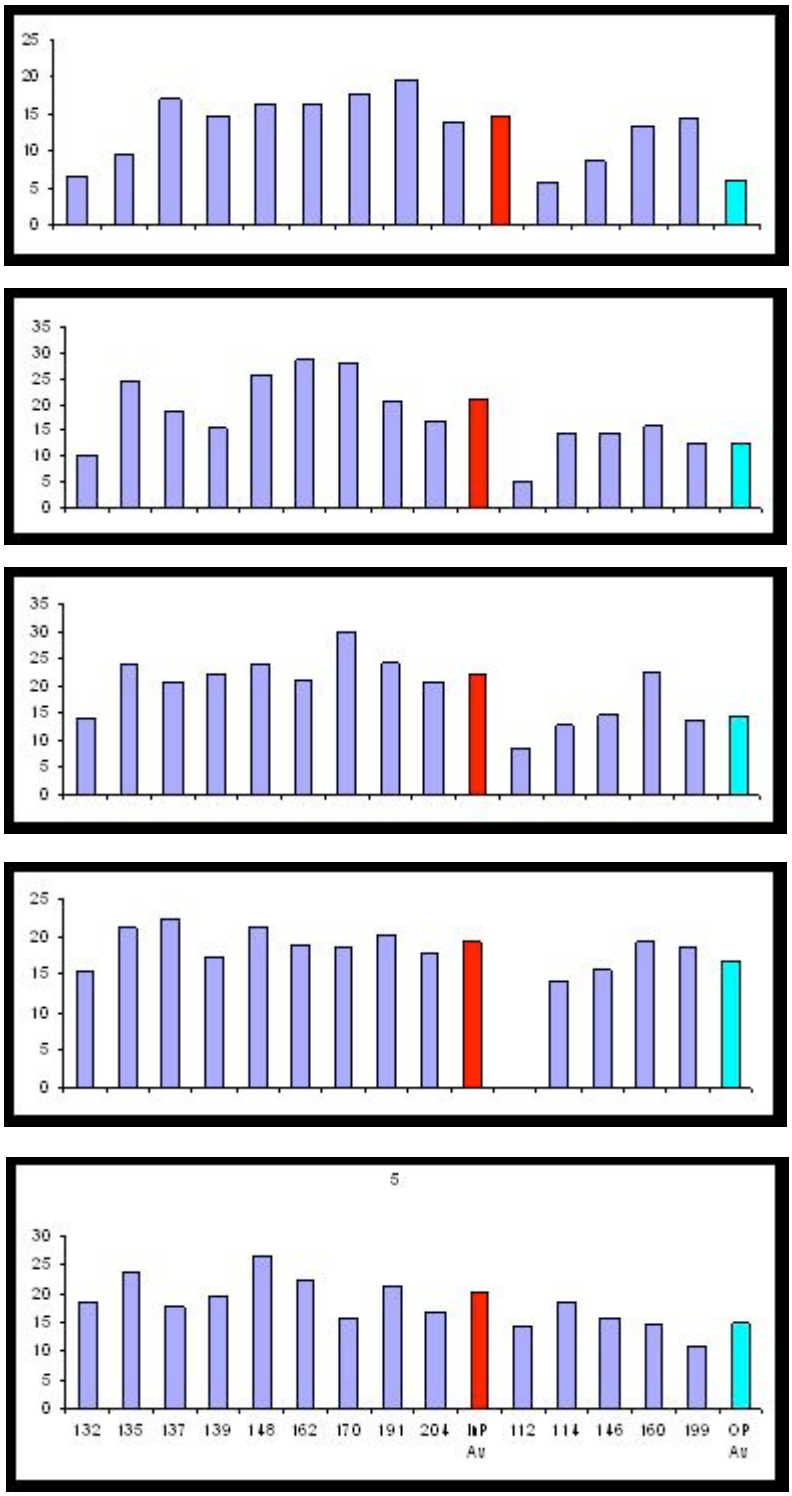

Fig. 14.2.3: Thymidine Incorporation Rates ($pML^{-1}h^{-1}$) measured from 5 different depths (from top to bottom: 100 m, 50 m, 20 m/chl max, 10 m and 5 m) during LOHAFEX. Average values for in-patch and out-patch stations are represented by red and light blue bars, respectively.

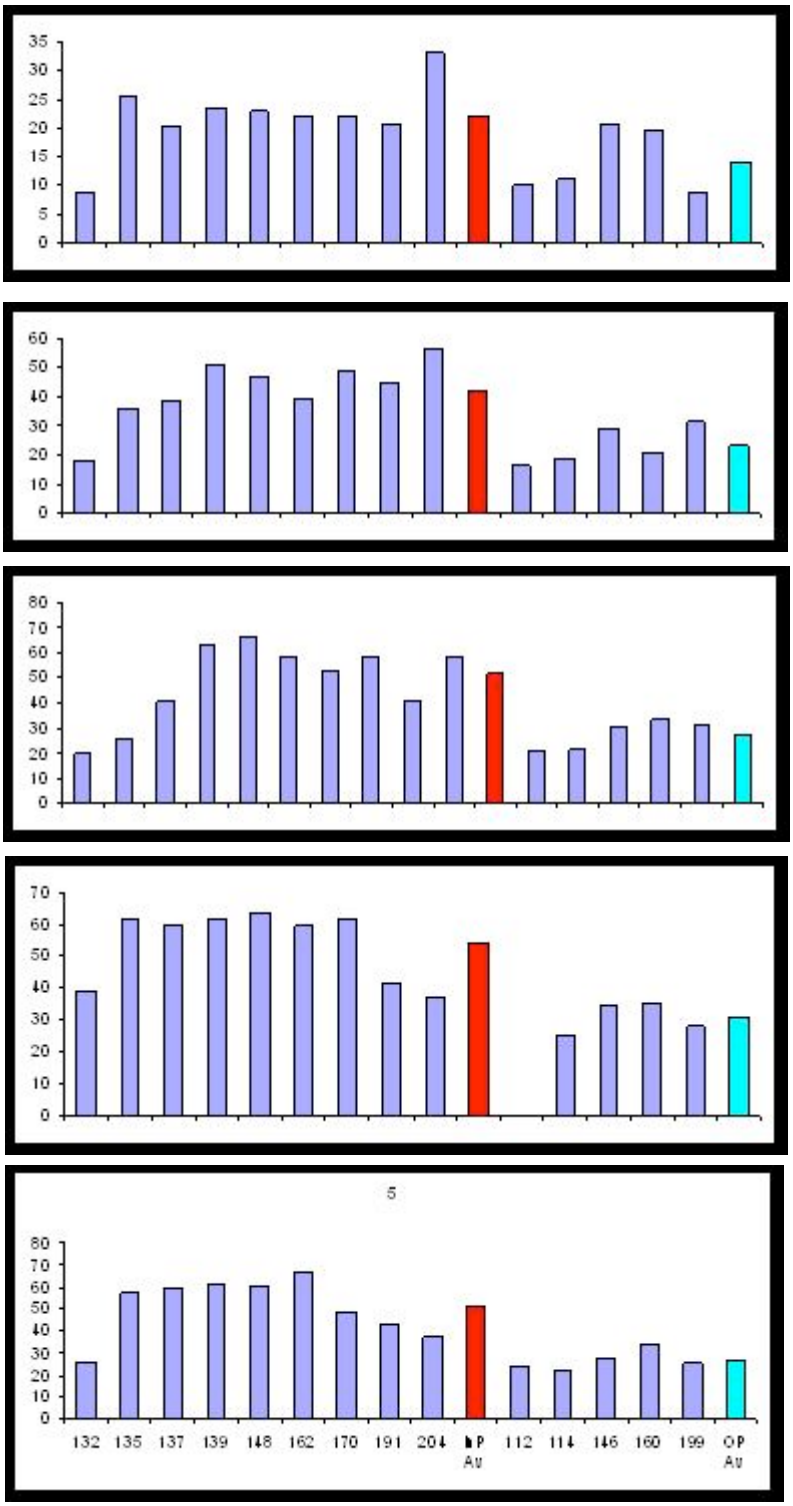

Fig. 14.2.4: Leucine Incorporation Rates ($pML^{-1}h^{-1}$) measured from 5 different depths (from top to bottom:100 m, 50 m, 20 m/chl max, 10 m and 5 m) during LOHAFEX. Average values for in-patch and out-patch stations are represented by red and light blue bars, respectively.

14.3 Bacterial biodiversity

V.R. Sundareswaran, G.S.N. Reddy
CCMB

Objectives

The objective of the present cruise was to study (i) the variation in prokaryotic community before and after fertilization and (ii) to determine the plate count and isolate novel prokaryotes. In order to fulfill the above objectives, approximately 5 lit of water was collected, before and after iron fertilization, from fourteen stations (Tab. 14.3.1) from 12 different depths (surface to 1,000 meters) and filtered through 0.22 μm millipore filters, in duplicates. DNA would be isolated from these filters and prokaryotic community fingerprinting would be done, on the on-shore laboratory, using various molecular tools such as DGGE, tRFLP and cloning of 16S rRNA gene. These studies would result in understanding the prokaryotic community composition and also their ecological relevance.

Tab. 14.3.1: Samples collected from various stations from LOHAFEX cruise

S. No.	Date	Stations	Latitude	Longitude	Remarks
1	22-1-09	PS73/112	48° 39.95' S	34° 44.83' W	Out patch
2	26-1-09	PS73/114*	47° 59.63’ S	15° 50.54’ W	In patch
3	31-1-09	PS73/132	47° 37.40’ S	15° 42.98’ W	In patch
4	5-2-09	PS73/135	47° 43.61' S	15° 07.56' W	In patch
5	8-2-09	PS73/137	47° 52.33' S	15° 16.04' W	Out patch
6	9-2-09	PS73/139	47° 54.52' S	15° 07.98' W	In patch
7	12-2-09	PS73/146	47° 30.31' S	15° 26.51' W	In patch
8	14-2-09	PS73/148	47° 54.69' S	15° 18.83' W	In patch
9	19-2-09	PS73/160	47° 18.25' S	15° 38.97' W	Out patch
10	20-2-09	PS73/162	47° 23.49' S	14° 36.90' W	In patch
11	24-2-09	PS73/170	48° 06.07' S	14° 27.73' W	In patch
12	27-2-09	PS73/191	48° 47.71' S	15° 14.94' W	In patch
13	3-3-09	PS73/199	48° 02.27' S	15° 14.43' W	Out patch
14	5-3-09	PS73/204	48° 58.10' S	15° 11.12' W	In patch

*Station before fertilization

To fulfill the second objective, 4 representative samples, one before fertilization (PS73/114) and three after fertilization (PS73/139, PS73/162 and PS73/191), were plated on Zobell marine agar and incubated at 4°C for 15 days. Different colonies were observed to have appeared after 10 to 12 days of incubation from samples spread from stations PS73/114 an PS73/139, but no growth was observed on plates from stations PS73/162 and PS73/191. The colony count for samples from station PS73/114 ranged from 0.72 X 10^3 to 2.0 X 10^4 ml^{-1} for different depths, where as for samples from station PS73/139, the colony count ranged from 0.1 X 10^2 to 0.26 X 10^3 ml^{-1} (Tab. 14.3.2). Though the colony counts were drastically lower for the station no.139 (day 14 after fertilization) as compared to station no. 114 (before fertilisation),

nothing definite could be deduced from these results, as there was no growth seen at all in either of the remaining sampling stations. The fact that the samples were plated only on zobell medium, which may not be conducive to growth of all the bacteria, also has to be borne in mind. Close to seventy morphotypes were picked up from the bacteria grown at different depths from both stations (st.114 and 139) and were clonally purified. All these bacteria would be subjected to polyphasic characterisation and identified upto the species level. Further, bio-prospecting of these bacteria would also be evaluated out in the on-shore laboratory.

Tab. 14.3.2: Bacterial colony counts from representative stations

S. No.	Depths	Stations			
		PS73/114	PS73/139	PS73/162	PS73/191
		Colony counts (ml^{-1})			
1	5		0.1×10^2	No growth	No growth
2	10	5.0×10^3	1.9×10^2		
3	25	7.2×10^3	0.4×10^2		
4	50	2.8×10^3	NC		
5	100	2.5×10^3	0.4×10^2		
6	200	4.6×10^3	0.9×10^2		
7	300	9.3×10^3	0.1×10^2		
8	400	NC	2.2×10^2		
9	500	NC	0.3×10^2		
10	600	2.1×10^3	2.6×10^2		
11	800	0.72×10^3	0.2×10^2		
12	1000	20×10^3	1.1×10^2		

NC, samples not collected

15. PHYTO- AND PROTOZOOPLANKTON

P. Assmy[1], F. Ebersbach[1], N. Fuchs[1], C. Klaas[1], M. Montresor[2], V. Smetacek[1]

[1)] AWI
[2)] SZN

Objectives

The main objective of the phytoplankton group during LOHAFEX was to study the composition of the phyto- and microzooplankton assemblage and its quantitative and qualitative response to iron addition. Both the quality and quantity of the organic matter produced by iron addition as well as its fade along the water column will ultimately be determined by the properties of the species dominating the iron-induced bloom. Species-specific studies are therefore highly warranted because they not only provide a deeper understanding of pelagic ecosystem functioning but also link plankton ecology with biogeochemical fluxes. In previous experiments, the addition of iron induced a rapid growth response of different diatom species and during EIFEX – the longest fertilization experiment carried out up to now – it has been possible to follow the sinking of selected diatom species along the deep water column to the seafloor. The EIFEX plankton community was characterised by typical oceanic diatom species that have a strong impact on the silica flux but relatively little on the carbon flux. During LOHAFEX we aimed at fertilizing a coastal plankton assemblage to study whether it had a different bearing on the fate of the organic matter produced and the effect on higher trophic levels. Besides following the plankton composition over time we used fluorescent dyes to study the mechanisms associated with the wax and wane of individual diatom species populations.

.

Work at sea

Water samples for estimating phyto- and microzooplankton abundance and biomass were collected at all IN- and OUT-patch stations (sampling depths: 10, 20, 40, 50, 60, 80,100,150, 200 m). Duplicate samples were collected and fixed with hexamine-buffered formaldehyde and Lugol, respectively. Lugol fixation allows a better preservation of ciliates and small phytoflagellates, while neutralized formaldehyde is better for the identification of diatoms and coccolithophores. At the same stations, large volumes of water were gently concentrated over 20 µm mesh-sized gauze for estimating the concentration of larger phyto- (e.g. large diatoms of the genera *Rhizosolenia, Proboscia* and *Corethron*; autotrophic dinoflagellates such as *Ceratium*) and protozooplankton (heterotrophic dinoflagellates of the genus *Protoperidinium,* tintinnid ciliates, Foraminifera, Acantharia and Radiolaria) as well as copepod nauplii and mesozooplankton faecal pellets. Twelve litres of seawater were concentrated at 10, 20, 40, 60, 80, 100 and 150 m, while 24 litres of seawater were concentrated at 200, 250, 300, 350, 400, 450 and 500 m depth. At all IN- and OUT-patch stations water samples were also collected for estimating the concentration of Transparent Exopolimeric Particles (TEP).

Additional seawater and concentrated samples were collected over a reduced number of depths at 16 'biological stations' sampled along two transects through the patch (from 24 to 27 February).

Phytoplankton hand net samples were collected from the surface layer of all stations (0 - 10 m); an aliquot of these samples was examined on board to gain insights of the species characterizing the plankton community and/or to isolate phytoplankton species to bring in culture; the remaining material was preserved for further taxonomic investigations. In total about 200 unialgal cultures of different diatom species as well as the haptophyte alga *Phaeocystis antarctica* were successfully grown and maintained on board.

On two occasions – prior to fertilization and towards the end of the experiment (day 28), 24 - 36 litres of sea water were collected along the deeper portion of the water column (depths 200 – 3,000 m) and filtered over a 10 µm mesh size net. Next to the deep water column surface sediments collected at five stations with the multicorer were sampled for phytodetritus (see contribution by Fuchs et al.). Sub-samples for the estimation of the contribution of phyto- and microzooplankton as well as TEP to the vertical particle flux were gained from the sediment traps deployed both in and outside the fertilized patch (see contribution by Martin and Saw). Additionally polyacrylamide gel cups were deployed on the sediment traps on various occasions along the experiment to collect undisturbed particles as they gently sink into the gel matrix.

In order to obtain a preliminary estimate of the composition of the phyto- and microzooplankton assemblage over the course of the experiment, 5 L seawater samples were collected from the online seawater supply system (water intake at 11 m) at all IN- and OUT-patch stations and concentrated over 10 µm mesh size gauze. Plankton organisms were enumerated on 3 ml aliquots of the sample at the inverted microscope (Axiovert 135 and 200, Zeiss, Oberkochen), if possible at the species level. In order to estimate the cell abundance of flagellates and coccoid cells < 2 μm 10 or 25 ml of Lugol-fixed samples were settled in an Utermöhl chamber and enumerated at the inverted light microscope (Axiovert 200, Zeiss, Oberkochen). A rough preliminary estimate of the carbon content of the different components of the phyto- and protozooplankton assemblage was derived using carbon concentrations $cell^{-1}$ obtained during previous cruises or from the literature.

At selected stations along the experiment, phytoplankton samples were stained with SYTOX Green - in order to test cell viability - and incubated under natural light and temperature conditions after staining with the fluorochrome PDMPO that binds to the newly deposited silica to infer *in-situ* division rates of selected diatom species.

At regular depth intervals within the upper 200 m 1 - 2 liter of seawater were collected for the quantification of biogenic silica (BSi). Samples were gently filtered onto 0.8 μm-pore-size polycarbonate filters, dried at 60°C and stored at room temperature until further analysis in the home laboratory. Filters will be analysed following the wet alkaline digestion method by Müller and Schneider (1993).

Preliminary results

The plankton community of the eddy chosen as the experimental container was characteristic of the late stage of the seasonal cycle. This was evidenced by the very low silicic acid concentrations (< 2 μM) down to 100 m depth used up by the spring-summer diatom blooms prior to our arrival in the area.

LOHAFEX was characterised by a flagellate dominated phytoplankton community
Small flagellates accounted for about 70 - 80 % of the phytoplankton biomass all over the experiment at both the IN- and OUT-patch stations (Fig. 15.1 & Fig. 15.3 b, c, d). The flagellate assemblage included solitary cells of the prymnesiophyceans *Phaeocystis antarctica*, other haptophytes (distinguishable by the presence of the haptonema and two prominent chloroplasts), prasinophytes (as indicated by the relatively high concentration of chlorophyll *b*), coccoid cells, choanoflagellates and cryptophytes. Unfortunately, the identification of these flagellates at the genus or even class level is impossible in fixed water samples. An integrated approach – in collaboration with other groups and including metagenomics – will be applied in order to obtain an estimate of the diversity, abundance and trophic status (autotrophic *versus* heterotrophic) of this important component of the phytoplankton assemblage. Coccolithophores, almost exclusively represented by *Emiliania huxleyi,* were present in the eddy at our arrival. The cells of coccolithophores are covered with calcareous platelets (coccoliths) and form massive blooms both in the open ocean and in coastal areas and therefore have a great bearing for the global carbon cycle. However, cell numbers of *E. huxleyi* started declining after iron addition indicating that factors other than iron are controlling its population.

Rapid diatom growth despite low silicic acid concentrations but high grazing mortality
Diatoms usually dominate phytoplankton biomass throughout the Southern Ocean, but they only contributed to a minor percentage the total autotrophic phytoplankton biomass (Fig. 15.2). Nevertheless we could observe a slight increase in cell numbers of some species following fertilization. Species diversity of the diatom community was comparably low; *Fragilariopsis kerguelensis* and *Corethron pennatum* – species characterizing the Antarctic phytoplankton assemblage – were relatively abundant and responded to the iron fertilization inside the patch (Fig. 15.3 e). They were accompanied by *Thalassionema nitzschioides*, and species of the genera *Thalassiosira* and *Pseudo-nitzschia.* However, diatom abundances rapidly declined within 2 - 3 weeks after fertilization. The decline could have been due to the depletion of silicic acid to limiting concentrations and/or heavy copepod grazing pressure. High *in-situ* division rates derived from the silica staining method indicate that the dominant diatom species were growing at near maximum rates despite the low silicic acid concentrations and the fact that these high division rates were not reflected in the accumulation of cells in the field samples emphasises the strong grazing pressure exerted by the zooplankton community. Natural cell death and protozooplankton grazing could not have been responsible for the lack in biomass build-up since the number of empty cells as well as full but dead cells (stained by SYTOX Green) only had a minor contribution to the total cell numbers of the diatom species investigated. Thus it can be concluded that crustacean grazers, in particular

copepods, were the major grazers on diatoms. This is further supported by the abundant occurrence of both broken as well as intact diatom cells and chains in copepod fecal pellets. Interestingly a large percentage of diatoms were still viable within the fecal pellets and could even be brought in culture after incubation of fecal pellets (Fig. 15.3 a).

Phaeocystis antarctica solitary cells represented a considerable fraction of the phytoflagellate biomass. This prymnesiophycean – responsible for extensive blooms in the Ross Sea - has a heteromorphic life cycle including solitary flagellate cells, coccoid stages as well as large colonies surrounded by a though and elastic skin. In the second week after fertilization, we observed many small compact colonies attached to diatoms spines (*Corethron pennatum*) and chitin threads (*Thalassiosira*) inside the fertilized patch. This was the first stage in the transformation of solitary flagellates to large colonies; small free floating colonies were in fact recorded in water samples at the end of the second week, but they suddenly disappeared, most probably because they represent a highly valuable food source for the copepod population.

Ceratium: slow growing but persistent
Dinoflagellates were the second most abundant group and included a considerable fraction of heterotrophic species (*Protoperidinium* and unarmoured species) spanning in size from 5 to 50 - 60 µm (Fig. 15.2). *Ceratium pentagonum* dominated the biomass of phototrophic species both at the IN- and OUT-patch stations as well as in many of the net samples collected over the first weeks of our cruise, when we cruised further south in the iceberg fields. This conspicuous species has rarely been reported in the Southern Ocean at the abundances we recorded and likely accumulated as compared to other larger phytoplankton species because it is less preferred by the prominent copepod grazers. Nevertheless we observed whole cells of *C. pentagonum* in copepod fecal pellets indicating that the preferred food of copepods was not in sufficient supply so they referred to less preferred food items like *C. pentagonum*.

Microzooplankton: a possible link from flagellates to larger zooplankton
The microzooplankton biomass was equally divided between heterotrophic dinoflagellates and ciliates, dominated by tintinnids (Fig. 15.3 f). The presence of many empty and crushed tintinnid loricae in the water samples and in copepod fecal pellets indicated a high grazing pressure exerted on these organisms which, in turn, graze upon the small sized flagellates. This link in the pelagic food web most likely channelled a considerable fraction of the flagellate biomass not readily accessible by the larger mesozooplankton to higher trophic levels.

Work on cultures
About 200 monoclonal strains of various phytoplankton species (mainly belonging to the diatom genera *Fragilariopsis, Pseudo-nitzschia, Chaetoceros* and the haptophyte *Phaeocystis*) were brought in culture. These cultures will be used for phylogenetic and life cycle investigations in the home laboratories. A number of serial dilution

cultures were also established with the aim of obtaining strains of phytoflagellate species.

Conclusions

The initially anticipated phytoplankton bloom dominated by coastal diatom species could not develop due to the low silica concentrations and instead a flagellate dominated plankton community responded to the iron addition. The first preliminary conclusions that can be derived from the above findings indicate a rapid turn-over of a flagellate dominated phytoplankton community via protistan grazers to copepods and ultimately amphipods (see report by Mazzocchi et al.). From our preliminary results no significant differences in both abundance and biomass of the phyto- and microzooplankton community could be observed between IN- and OUT-patch stations. However, both chlorophyll and primary productivity data show a substantial increase inside the patch as compared to outside indicating that more in depth analysis of the phytoplankton community will likely result in a refined picture of the processes within the autotrophic community. Nevertheless the rapid turn-over of organic matter within the system is consistent with findings from other groups and iron addition likely boosted the turn-over as compared to the outside situation. Thus most of the organic matter produced was passed to higher trophic levels and the bulk of fecal material produced by the zooplankton was recycled within the mixed surface layer. These findings have interesting implications for the understanding of the pelagic ecosystem of the northern, silicic acid limited ACC, its role for the carbon flux and cast doubt on the suitability of this vast oceanic area for iron-induced carbon sequestration.

References

Mueller PJ, Schneider R. (1993). An automated leaching method for the determination of opal in sediments and particulate matter Deep-Sea Res. I 40(3): 425-444

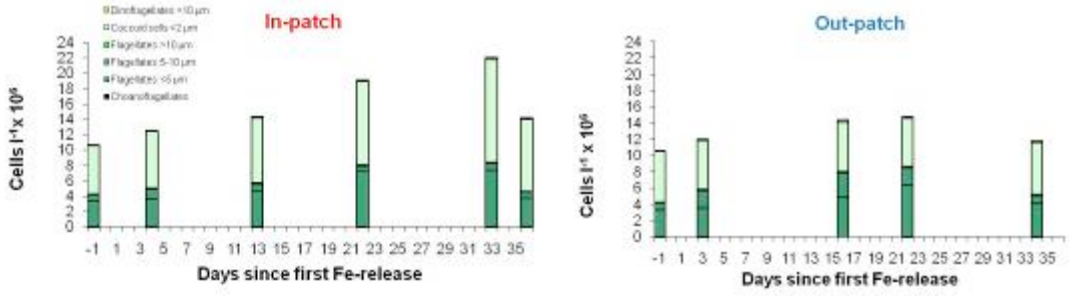

*Fig. 15.1: Flagellate abundance (in cells*10^6 l^{-1}) inside and outside the fertilized patch. Cell numbers were derived from samples collected from 20 m depth with the CTD.*

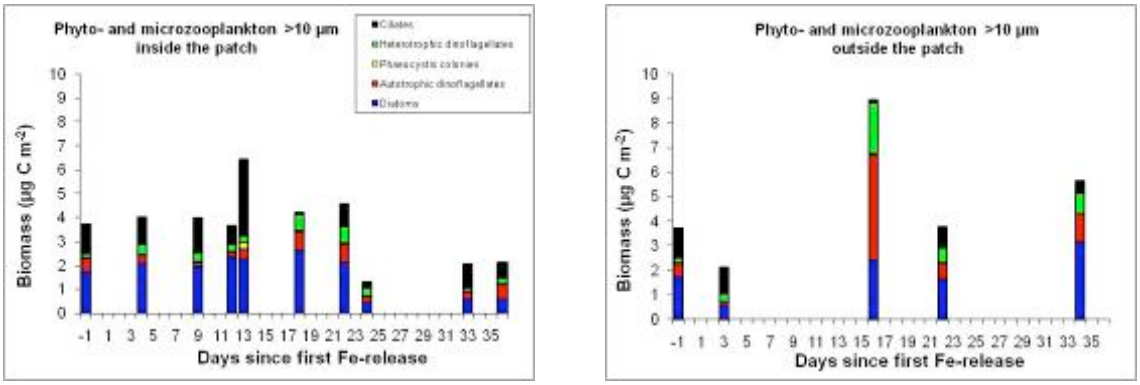

Fig. 15.2: Biomass (in µg C l^{-1}) of phyto- and microzooplankton >10 µm inside and outside the fertilized patch. Samples were collected from the seawater underway system at 11 m depth and concentrated over 10 µm gauze.

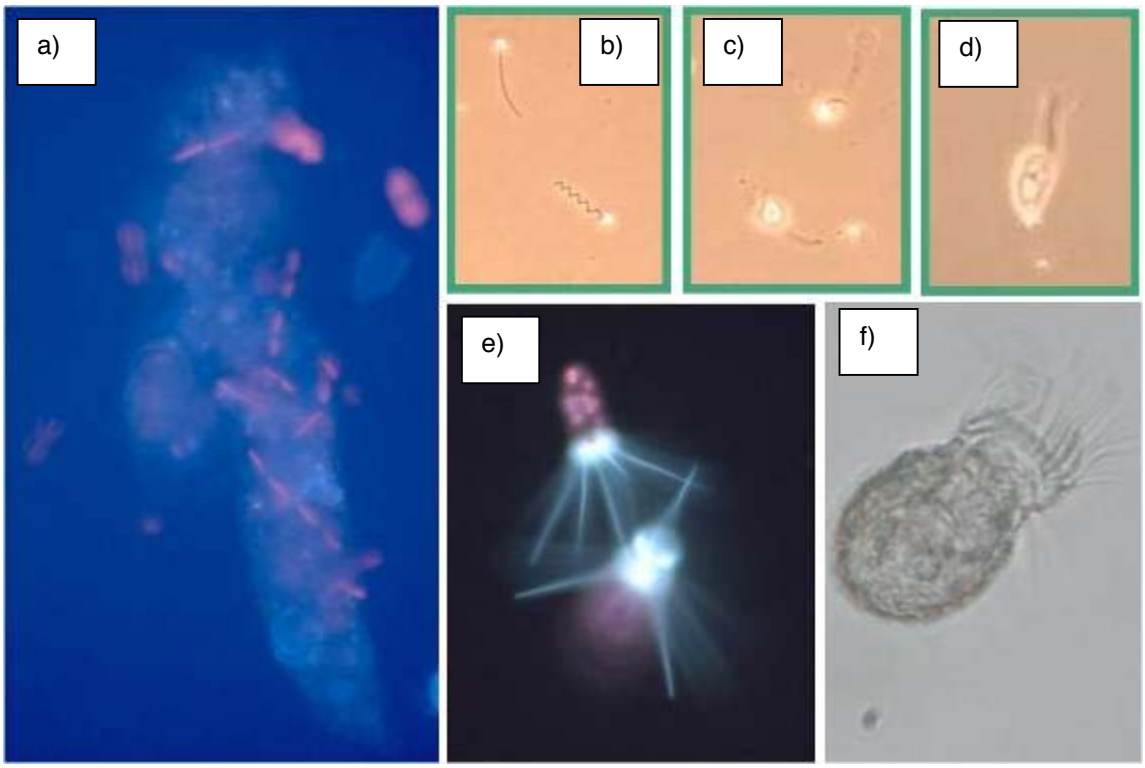

Fig. 15.3: Lightmicrographs taken on board during LOHAFEX. a) copepod fecal pellet under epifluorescence showing viable chains of the diatom Pseudo-nitzschia, b) flagellates < 5 µm, c) flagellates > 5 µm, d) cryptophyte flagellate, e) recently divided cells of Corethron pennatum stained with the silica stain PDMPO and f) tintinnid ciliate of the genus Codonellopsis.

16. MESO- AND MACRO-ZOOPLANKTON

M.G.Mazzocchi[1], H.E. González [2], I. Borrione[3], P. Vandromme[4], M. Ribera d'Alcalà[1]

[1)] SZN
[2)] UACH-COPAS
[3)] AWI
[4)] UPMC-CNRS

Objective

The general objectives of the zooplankton studies during LOHAFEX were 1) to evaluate the structural and functional responses of primary and secondary consumers to food availability (both quantity and quality), and 2) to estimate the impact of zooplankton activities on the carbon flux during the evolution of the phytoplankton dynamics induced by the iron fertilization.

Work at sea

Sampling activities

Meso-zooplankton samples for species composition and abundance were collected at 18 stations, in 5 discrete depth layers (500 - 300 m, 300 - 200 m, 200 - 100 m, 100 - 50 m, 50 - 0 m), twice a day during both day and night. Vertical tows were performed by using, in succession, two MultiNets (MN) equipped with 200 μm and 55 μm mesh nets, respectively. Integrated samples in the 0 - 200 m water column were collected with the 200 μm MN at further 19 stations along SN and WE transects. The samples were fixed and preserved in a sea water-buffered formaldehyde solution (4 % final concentration).

Samples for acquiring functional parameters (lab experiments) were collected by gentle vertical tows with a WP2 200 μm mesh net equipped with a non-filtering 10 L bucket as codend.

Macro-zooplankton samples for species and/or major groups composition and abundance were collected at 18 stations. Oblique tows were performed by using a Rectangular Midwater Trawl (RMT net), towed at 2.5 knots within the upper 100 m water column.

Structural parameters

Species identification and abundance (ind. m^{-3}) were preliminarily assessed onboard in 62 selected samples of the 149 collected with the MN 200 μm. Aliquots of the original samples were counted under a dissecting microscope by using an Utermöhl chamber. Macro-zooplankton species were identified and counted in 18 samples collected with RMT and their abundance was expressed as ind. 100 m^{-3}.

For later measurements of *biomass* as dry mass and C/N content at CHN, specimens of the most abundant meso- and macro-zooplankton species were dried in the oven (24 hours at 60°C).

For later analyses of *lipid* content, individuals of *Calanus simillimus* and *Oithona frigida* were sorted and preserved at -80°C.

For later *DNA extraction,* individuals of target copepod species were sorted and preserved in ethanol 96 % at 4°C and will be analysed in association with Census of Marine Zooplankton.

Functional parameters
Copepod grazing rates were estimated (mostly for *C. simillimus*) in six incubation experiments conducted with the food removal method. From the control and experimental bottles, chlorophyll concentrations were measured onboard (by M. Gauns group) while phyto- and microzoo-plankton will be counted later in samples preserved in formaldehyde and in Lugol solution (2 %).

Faecal pellet production rates were estimated for *C. simillimus*. Four individuals (C4-C5) were incubated immediately after collection in 2 L polycarbonate bottles for periods between 1 and 2 hours. The bottles were placed on a plankton wheel at *in-situ* water temperature (5 - 7 ºC).

Copepod egg production rates were estimated (mainly in *Oithona similis* due to the rare occurrence of *C. simillimus* females) by incubating individual adult females in 70 ml flask filled with water containing natural particle assemblages collected from the moon pool (~ 11 m depth).

Ingestion rates were also estimated in the amphipod *Themisto gaudichaudi*. One control (4 *T. gaudichaudi*) and three treatments (4 *T. gaudichaudi* and 40 *C. simillimus*) were incubated for 24 hrs in 20 L polycarbonate bottles, at *in-situ* temperature. The numbers of copepods were counted at the beginning and at the end of the experiment.

The *vertical flux* of faecal pellets (i. e. copepod, amphipod, krill and salp faecal material) will be later estimated through the analysis of sediment trap samples collected in neutrally-buoyant, free floating sediment traps (Mod. Pelagra). The traps were deployed inside and outside the iron fertilized patch in 7 and 3 occasions, respectively, for periods between 3 and 6 days (see Report by P. Martin). This information will be used to estimate the impact of the zooplankton on both the carbon flux and the possible fate of the photoautotrophic generated POM both inside and outside the patch.

Underwater Vision Profiler v5 (UVP5)
The quantitative and qualitative distribution of particles in the water column from the surface to 3000 m depth was recorded with the UVP5, an underwater camera system mounted on the Rosette. The camera takes pictures at a full rate of 5 per second,

one image being referred to 1 L water volume. The pixel size of the camera is 170 μm, but because of the reflectance of light, object as small as 60 μm are recorded, while the maximum size appears to be around 2 - 3 cm Equivalent Spherical Diameter (ESD). Each object of more than 30 pixel (equivalent to 600 μm ESD) is stocked as a single thumbnail. All thumbnails are then visually classified in few groups. The UVP5 is both a tool for studying the inert particles (with their size spectra we can have an approximation of the flux of matter) and the major groups of the zooplankton community (depth and size distribution with a high definition). During the LOHAFEX cruise a total of 57 UVP casts were made. The maximum depth of these cast vary from 200 to 3,000 m depth with a mean of 1,050 m, representing > 70,000 thumbnails.

Preliminary results

Meso-zooplankton

The communities in the upper 200 m water column were characterized by low diversity and the dominance of three copepod species: *Calanus simillimus* CIV-CV (as biomass), *Oithona similis* adults and juveniles (as numbers), and *Ctenocalanus citer* adults and juveniles. In the integrated 0 - 100 m water column, the highest abundances estimated, from preliminary counts conducted onboard, ranged from 199 ind. m^{-2} x 10^3 for *Oithona* spp. to 90 ind. m^{-2} x 10^3 for *C. simillimus*, and 31 ind. m^{-2} x 10^3 for *C. citer*, all recorded at in- stations within the 20 day after fertilization. However, the three species showed different distributions inside and outside the-patch, indicating species-specific responses to the environmental conditions induced by the iron fertilization experiment. On average, *C. simillimus* was more abundant at the out-stations, while *O. similis* and *C. citer* were more abundant at the in-stations. However, high spatial variability was observed in the distribution of the most abundant copepods and only *C. citer* showed consistent patterns with marked preference for the in-stations and a gradual decrease from the beginning to the end of the experiment. A general feature of mesozooplankton at all stations was the remarkable difference in the vertical distribution during day and night hours, due to nocturnal upward migration of various species (mainly *C. simillimus, Pleuromamma, Euchaeta*).

The faecal pellet production rate in *C. simillimus* (given as volume of faecal pellets) was ca. two times higher inside than outside the fertilized patch (37 and 59 x 10^6 µm^3 $ind.^{-1}$ d^{-1}, respectively).

Macro-zooplankton

The integrated average abundance of *T. gaudichaudi* in the upper 100 m water column was two-fold higher inside (24 ind. 100 m^{-3}) than outside the patch (12 ind 100 m^{-3}). The relative abundance of amphipods to total number of animals collected in the RMT fluctuated from 6 to 98 %, denoting its highly patchy distribution, vertical migration and swarm-forming behaviour, i. e. at St. 170, a total of 150 ind. m^{-2} were collected, being the largest catch during the cruise (Fig. 16.1).

UVP

All UVP casts have been processed day by day during the cruise (Fig. 16.2) and a visually validated classification of the thumbnails in 21 groups (9 for the different kinds of detritus and 11 for the zooplankton) (Fig. 16.3) was also made during the experiment. This first classification will be checked, corrected and detailed afterward on land.

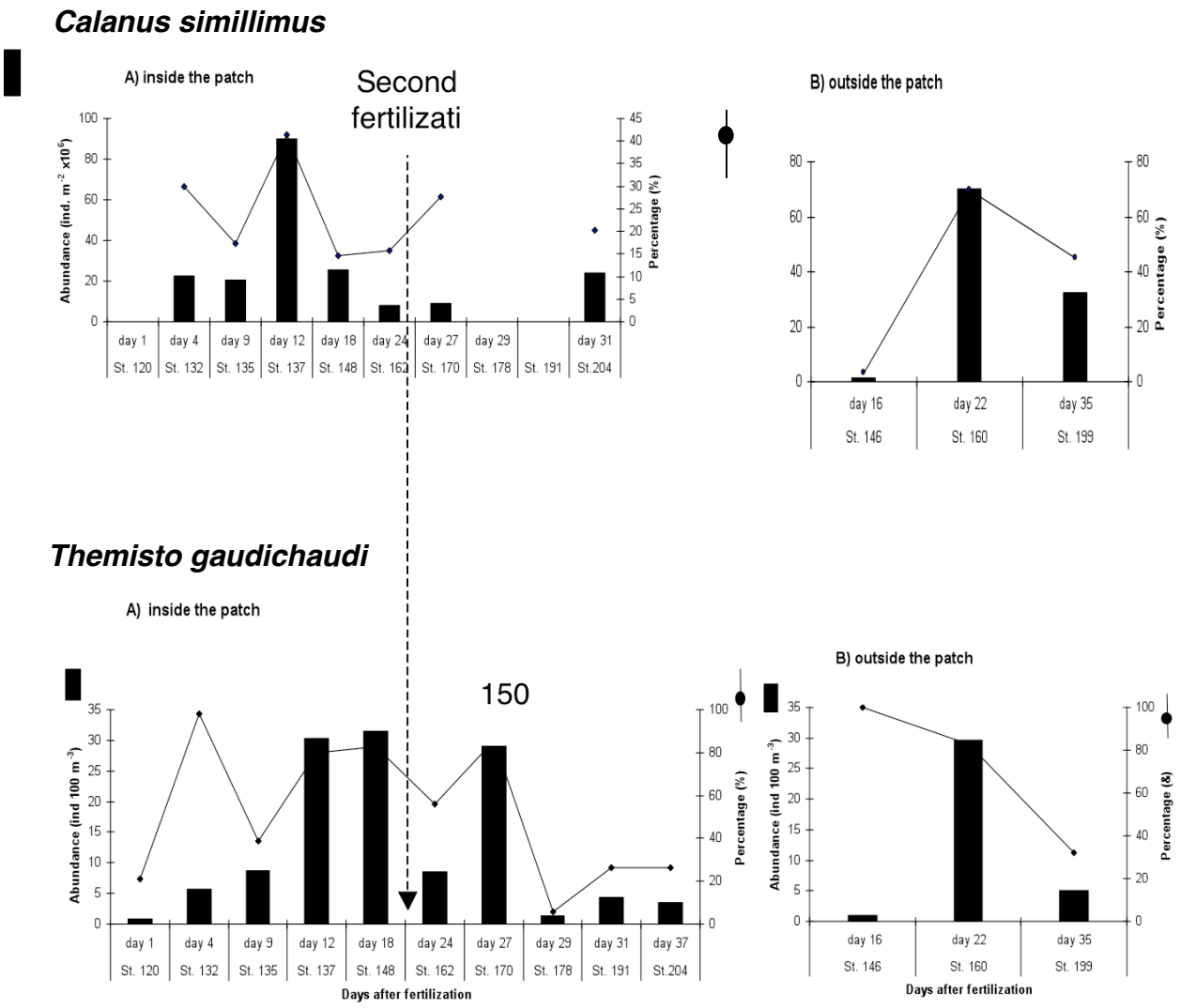

Fig. 16.1: Absolute (ind. m^{-2} upper 100 m water column) and relative abundance (percentage in number of total animals) of:
Upper panel: C. simillimus in MN samples collected inside (A) and outside (B) during LOHAFEX
Lower panel: T. gaudichaudi in RMT-net samples collected inside (A) and outside (B) during LOHAFEX.

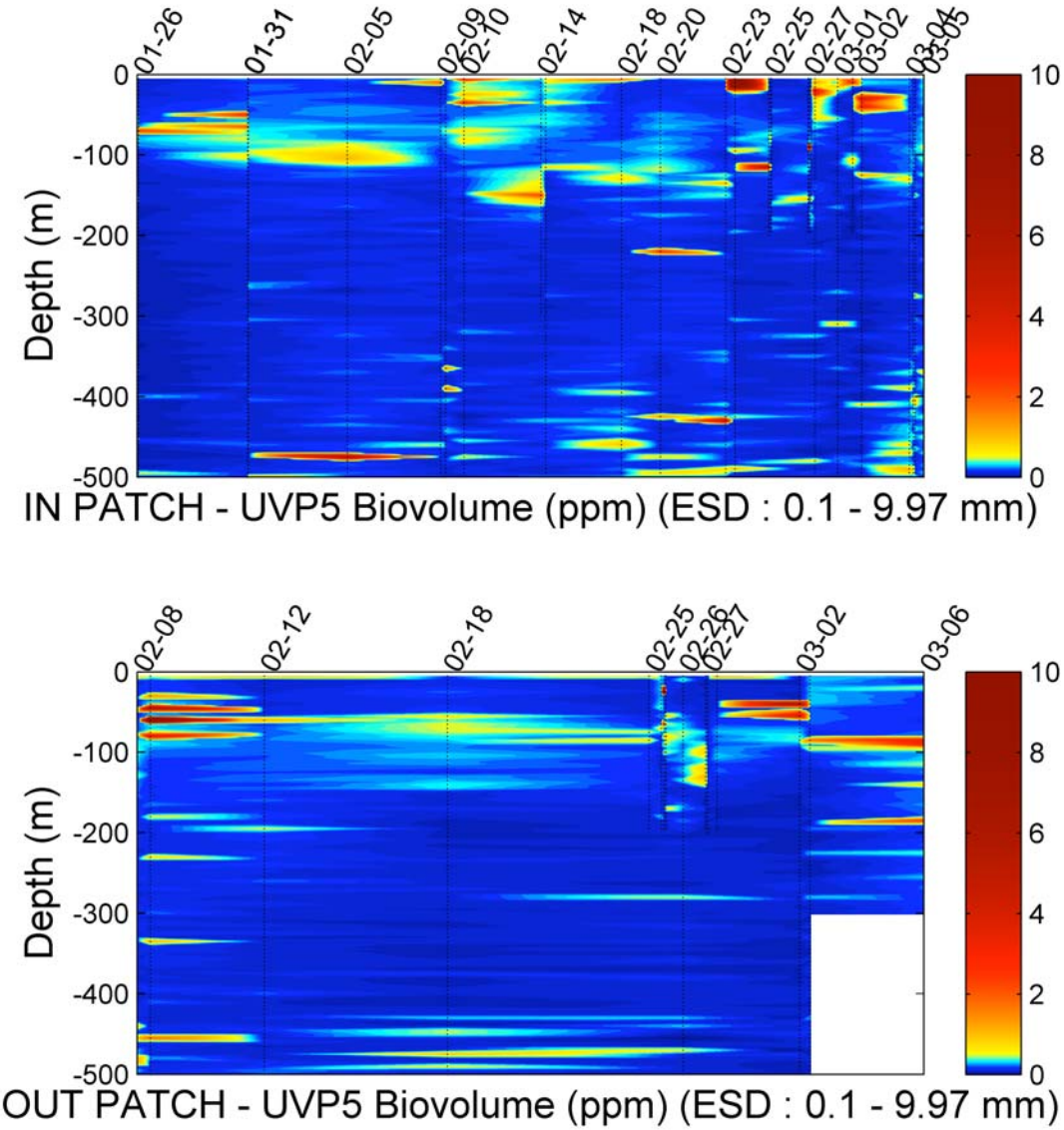

Fig. 16.2: Profiles limited to 500 m depth of biovolume (in ppm) measure for particles from 0.07 to 9.97 mm ESD both IN (top) and OUT (down) patch

1.)

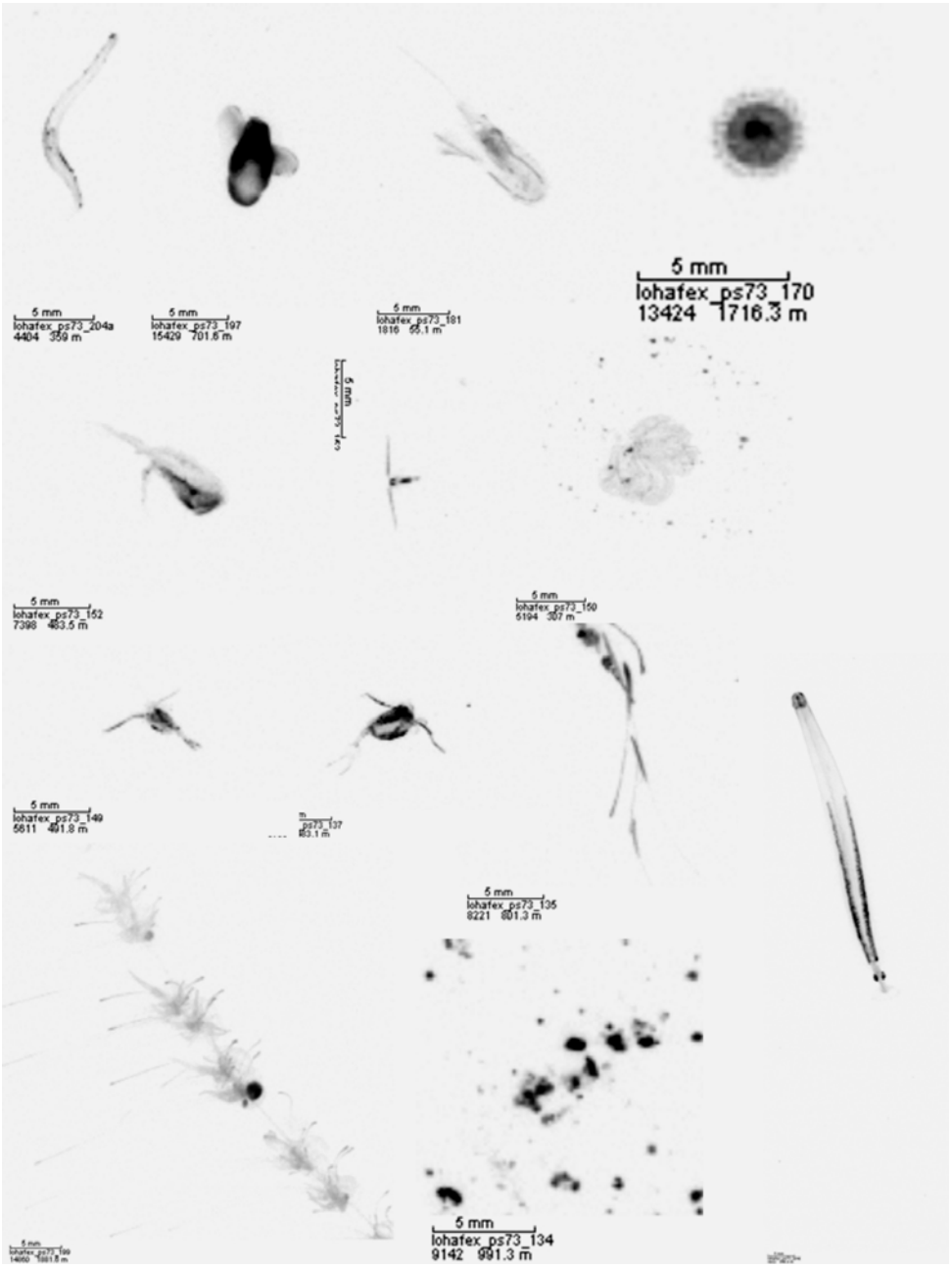

Fig. 16.3: Example of thumbnails obtained with the UVP5

17. SEDIMENTS

B. Fuchs[1], J. Wulf[1], M. van der Loeff[2], P. Assmy[2]

[1)] MPI
[2)] AWI

Objectives

In previous the iron fertilisation experiment EIFEX (European Iron Fertilization EXperiment) signs of export of organic material originating from the iron-induced phytoplankton bloom were detected in the underlying sediment (Sachs et al., ms; Sauter et al. in Smetacek et al., 2005). We hypothesised that during the LOHAFEX experiment bloom-produced organic material fluff should accumulate as fluff on the surface of the underlying sediment. Within the framework of ongoing analyses the sediment core material will yield valuable insights into the distribution of sedimentation in the Southern Ocean.

Work at sea

The sediment was sampled with a multicorer (MUC) at different locations within the studied eddy (Tab. 17.1). The seafloor was characterised by sometimes steep slopes rendering the site selection (using hydrosweep bottom topography) of a suitable sampling location within the experimental area difficult. The first MUC (st. 120 - 7) was taken on a hill top and yielded a carbonaceous sediment that was clearly affected by winnowing. As we hoped to find a corresponding area of sediment focusing, we selected the second location in a deep valley. The first cast (127 - 2) yielded only a few Mn-covered stones from the side of the valley. Therefore a second cast (127 - 7) was taken that recovered intact cores, however still with embedded stones. We decided to try to sample a wider deep valley on the third MUC deployment, but the sediment was unsuitable for studying the sediment surface, because during processing the sediment was perturbed and mixed, again as a result of abundant stones. The last two MUC stations were aimed at plateaus, from which we could retrieve compact cores with variable amount of organic material on top of the sediment.

Tab. 17.1: List of MUC-stations taken during LOHAFEX with date, location, relation to the fertilized patch (in or out), days of experiment, water depth and brief description of the sediment characteristics

Station-cast	Date (2009)	Time (UTC)	Latitude (°S)	Longitude (°W)	in / out	Depth (lot)	Appearence
120-7	29.01.	05:00	47 51.89	15 48.70	in +1	3340	whitish, oxic, some stones, rich in carbonate and course
127-7	31.01.	04:51	47 59.54	16 0.24	out +4	4113	whitish, stones on top, some of them brittle, maybe metaloxide nodules ?, biofilm with fluff on the surface; less carbonate, rich in diatoms.
140-1	10.02.	13:13	47 54.47	15 23.98	out +14	4183	only 3 intact cores retrieved, whitish, very coarse, sandy, stones within the sediment, stones and metaloxides, could not be sliced due to leaking, no fluff layer,
171-1	24.02.	12:56	47 54.10	14 30.05	+ 28	3444	8 intact cores retrieved, grey, compact, with thick fluff layer
195-1	02.03.	04:18	48 39.61	15 5.65	in +34	3758	5 intact cores retrieved, grey compact, thin fluff layer; rich in carbonate.

Apparently undisturbed sediment cores were sampled for phytoplankton composition, pigment analysis, particulate organic carbon (POC) and nitrogen (PON) and biogenic silica (BSi). Only the overlaying water and the fluff layer, if present, were sampled for the above parameters. For phytoplankton composition the fluff was carefully pipetted off the sediment surface and preserved in hexamine-buffered formaldehyde solution at a final concentration of 2 % and stored dark at 4°C. An additional sample of the fluff was shock frozen and stored at –80°C. Overlaying water and fluff was carefully siphoned off of the sediment surface for pigments, POC, PON, ^{234}Th and BSi analysis and pooled in a rinsed PE-bottle. Subsequently the sample was distributed into four even splits by a sample splitter. Pigment and POC/PON samples were filtered on pre-combusted GF/F filters and immediately frozen at –80°C in case of the former and dried at 60°C in case of the latter. Samples for BSi were filtered on cellulose-acetate filters and dried at 60°C. Furthermore samples of the bulk sediment were taken from the upper 1 - 2 cm of the core. One sample was stored at –80°C whereas the other one was dried at 60°C.

Preliminary microscopic analysis showed a strong contribution of both siliceous (mainly diatoms) and calcareous (mainly foraminifera but also single coccoliths) particles to the uppermost layer of the cores. Diatoms were mainly composed of heavily silicified species characteristic for sediments in this area (e.g. *Fragilariopsis kerguelensis*, *Thalassiosira lentiginosa*, *Eucampia antarctica*). Foraminifera comprised both pelagic and benthic species whereas coccoliths were mainly of

Emiliania huxleyi. However, the relative contribution of siliceous to calcareous components varied considerably between sampling locations.

For molecular biological analyses of the microbial community, samples from the overlaying water layer, the fluff interface and the top 1 cm of the sediment cores were sampled, respectively. Sediment samples were preserved in 1 % formaldehyde for 12 h at 4°C, transferred into PBS/ethanol (1:1 v/v) after settling of the sample and frozen at -20°C. Water samples were fixed in 1 % formaldehyde for 12 h at 4°C, filtered onto polycarbonate filter (0.2 μm pore size) and frozen at -80°C. Untreated samples for DNA extraction were frozen directly at -80°C.

Samples of surface sediment were collected for microfossil and geochemical analysis.

Expected Results

We will analyse the ^{230}Th content of the surface sediment in order to derive local sediment rain rates. Comparison of rain rates obtained for the plateau and valley cores will be used to judge the validity of ^{230}Th as tracer to correct for winnowing and focusing.

References

Smetacek V, Bathmann U, Helmke E (2005) The expeditions Antarktis XXI/3-4-5 of the Research Vessel "Polarstern" in 2004. Reports on Polar and Marine Research 500, 302.

APPENDIX

A.1 PARTICIPATING INSTITUTIONS

A.2 CRUISE PARTICIPANTS

A.3 SHIP'S CREW

A.4 STATION LIST

A.1 TEILNEHMENDE INSTITUTE / PARTICIPATING INSTITUTIONS

	Adresse /Address
AWI	Alfred-Wegener-Institut für Polar- und Meeresforschung in der Helmholtz-Gemeinschaft Postfach 12 01 61 27515 Bremerhaven Germany
CCMB	Centre for Cellular and Molecular Biology Uppal Road, Hyderabad 500007 India
CSIC-IMEDEA	Mediterranean Institute for Advanced Studies (IMEDEA) C/ Miquel Marquès, 21 07190 Esporles, Mallorca Illes Balears Spain
DWD	Deutscher Wetterdienst Hamburg Abteilung Seeschifffahrt Bernhard-Nocht Str. 76 20359 Hamburg Germany
GLOMAR	Bremen International Graduate School for Marine Science "Global Change in the Marine Realm" MARUM - University of Bremen Leobener Strasse 28359 Bremen Germany
LAEISZ	Reederei F. Laeisz GmbH Brückenstr. 25 27568 Bremerhaven Germany
MPI Bremen	Max Planck Institute for Marine Microbiology Celsiusstrasse 1 D-28359 Bremen Germany
NEERI	National Engineering Research Institute Nehru Marg, Nagpur 440020 India

Adresse /Address	
NIO	National Institute of Oceanography Dona Paula - 403 004, Goa India
NOCS	National Oceanography Centre, Southampton (NOCS) University of Southampton Waterfront Campus, European Way, Southampton SO14 3ZH UK
PRL	Physical Research Laboratory Navrangpura 380 009, Ahmedabad India
SZN	Stazione Zoologica Anton Dohrn Villa Comunale 80121 - Napoli Italy
UACh-COPAS	Universidad Austral de Chile Independencia 641 Valdivia Chile
UPMC-CNRS	Laboratoire d'Oceanologie de Villefranche Université Pierre et Marie Curie, Paris Station Zoologique, Chemin du Lazaret, 06234 Villefranche sur mer France

A.2 FAHRTTEILNEHMER / CRUISE PARTICIPANTS

Name	Vorname/ First Name	Institut/ Institute	Beruf/ Profession
Almeida	Anselm	NIO	Physics technician
Assmy	Philipp	AWI/GLOMAR	Biologist
Bansiwal	Amit	NEERI	Chemical engineer
Baraniya	Divyashree	NIO	Student, biochemistry
Borrione	Ines	AWI	Student, oceanography
Bresinsky	Thomas	Caligari Film	Camera man
Buldt	Klaus	DWD	Technician
Dalvi	Hanamant	NIO	Chemist
Desai	Vineet	NIO	Chemist
Ebersbach	Friederike	AWI/GLOMAR	Student, biology f
Fuchs	Bernhard	MPI, Bremen	Microbiologist
Fuchs	Nicole	AWI	Student, biology
Gauns	Mangesh	NIO	Biologist
González	Humberto	UACh –COPAS	Biologist
Gundlapally Sathya	Reddy	CCMB	Microbiologist
Hartig	Rüdiger	DWD	Meteorologist
Kalarikkal	Sujith	NIO	Chemist
Kankonkar	Ashok	NIO	Electronics engineer
Kanth	Reshma	NIO	Student, chemistry f
Klaas	Christine	AWI	Biologist
Laglera Baquer	Luis	CSIC-IMEDEA	Chemist
Mahadik	Gauri	NIO	Student, biology
Martin	Patrick	NOCS	Student, biogeochemistry
Martinez Castillo	Regino	CSIC-IMEDEA	Chemist
Mazzocchi	Maria Grazia	SZN	Biologist
Methar	Anand	NIO	Electronics technician
Mochemadkar	Sunita	NIO	Student, biology
Montresor	Marina	SZN	Biologist
Muthirenthy	Maya	NIO	Chemist
Nagappa	Ramaiah	NIO	Microbiologist
Naik	Hema	NIO	Chemist
Naqvi	Syed Wajih A.	NIO	Chemist, co-Chief scientist
Narvekar	Pradip	NIO	Chemist
Narvenkar	Gayatree	NIO	Chemist
Simoes	Leao		Indian cook
Patil	Shrikant	NIO	Student, biology
Pratihary	Anil	NIO	Chemist
Rengarajan	Ramab.	PRL	Geochemist
Ribera d'Alcalà	Maurizio	SZN	Biologist
Roy	Rajdeep	NIO	Student, biogeochemistry
Rutgers van der Loeff	Michiel	AWI	Geochemist
Sarkar	Amit	NIO	Student, chemistry
Saw	Kevin	NOCS	Engineer
Singh	Sanjay	NIO	Microbiology Student,

Name	Vorname/ First Name	Institut/ Institute	Beruf/ Profession
Smetacek	Victor	AWI	Biologist, Chief scientist
Soares	Melena	NIO	Chemist
Thorat	Babasaheb	NIO	Student, chemistry
Vadlamani	Murty	NIO	Physicist
Vetaikorumagan	Sundareswaran	CCMB	Microbiologist
Vandromme	Pieter	Villefranche	Student, biology
Wolf-Gladrow	Dieter	AWI	Physicist
Wulf	Joerg	MPI, Bremen	Microbiologist

A.3 SCHIFFSBESATZUNG / SHIP'S CREW

No.	Name	Rank
1.	Schwarze, Stefan	Master
2.	Grundmann, Uwe	1.Offc.
3.	Krohn, Günter	Ch. Eng.
4.	Peine Lutz	2. Offc.
5.	Fallei, Holger	2. Offc.
6.	Ettlin, Margrith	2.Offc.
7.	Rudde-Teufel, Claus	Doctor
8.	Hecht, Andreas	R.Offc.
9.	Minzlaff, Hans-Ulrich	2.Eng.
10.	Sümnicht, Stefan	2.Eng.
11.	Schaefer, Marc	3.Eng.
12.	Scholz, Manfred	Elec.Tech.
13.	Fröb, Martin	Electron.
14.	Himmel,Frank	Electron.
15.	Muhle, Helmut	Electron.
16.	Nasis, Ilias	Electron
17.	Loidl, Reiner	Boatsw.
18.	Reise, Lutz	Carpenter
19.	Bäcker, Andreas	A.B.
20.	Guse, Hartmut	A.B.
21.	Hagemann, Manfred	A.B.
22.	Kreis, Reinhard	A.B.
23.	Rhau, Lars-Peter	A.B.
24.	Scheel, Sebastian	A.B.
25.	Schmidt, Uwe	A.B.
26.	Wende, Uwe	A.B.
27.	Winkler, Michael	A.B.
28.	Preußner, Jörg	Storek.
29.	Elsner, Klaus	Mot-man
30.	Pinske, Lutz	Mot-man
31.	Teichert, Uwe	Mot-man
32.	Voy, Bernd	Mot-man
33.	Müller-Homburg, Ralf-Dieter	Cook
34.	Silinski, Frank	Cooksmate
35.	Martens, Michael	Cooksmate
36.	Jürgens, Monika	1.Stwdess
37.	Wöckener, Martina	Stwdss/KS
38.	Czyborra, Bärbel	2.Stwdess
39.	Silinski, Carmen	2.Stwdess
40.	Gaude, Hans-Jürgen	2.Steward
41.	Möller, Wolfgang	2.Steward
42.	Huang, Wu-Mei	2.Steward
43.	Yu, Kwok Yuen	Laundrym.
44.	Simoes, Leao	Asst. Cook

A.4 STATIONSLISTE / STATION LIST PS73 - ANT-XXV/3-LOHAFEX

Station PS73	Date	Time (start)	Time (end)	Position (Lat.)	Position (Lon.)	Depth (m)	Gear	srno
098-01	16/1/09	5:29	6:30	48° 00.35' S	15° 59.44' W	3662.5	CTD/rosette	1
098-02	16/1/09	6:44	6:48	48° 00.36' S	15° 59.21' W	3673.2	Hand net	2
098-03	16/1/09	6:50	7:48	48° 00.42' S	15° 59.09' W	3661.2	Multiple net	3
098-06	16/1/09	9:49	9:54	47° 59.89' S	15° 57.61' W	4179.7	CTD/rosette	4
099-01	16/1/09	12:12	12:26	48° 19.95' S	15° 59.68' W	3970	CTD/rosette	5
099-01	16/1/09	13:15	13:38	48° 19.56' S	15° 59.99' W	3948	CTD/rosette	6
100-01	16/1/09	16:14	17:15	48° 39.89' S	16° 00.23' W	3758	CTD/rosette	7
101-01	16/1/09	22:41	23:32	47° 59.94' S	16° 16.17' W	3871	CTD/rosette	8
101-02	17/1/09	0:49	1:21	47° 59.97' S	16° 15.99' W	3866	CTD/rosette	9
102-01	18/1/09	20:08	20:45	49° 32.76' S	25° 16.51' W	4541	CTD/rosette	10
102-02	18/1/09	21:20	21:24	49° 33.19' S	25° 15.44' W	4583.7	Hand net	11
102-04	18/1/09	22:00	23:24	49° 33.09' S	25° 14.33' W	4589.2	Clean Rosette	12
103-02	19/1/09	0:55	1:22	49° 32.85' S	25° 09.50' W	4563.2	CTD/rosette	13
104-01	19/1/09	2:09	2:33	49° 30.43' S	25° 12.68' W	4520.7	CTD/rosette	14
105-01	19/1/09	3:23	3:46	49° 29.61' S	25° 17.04' W	4448.7	CTD/rosette	15
106-01	19/1/09	4:43	5:08	49° 32.13' S	25° 20.63' W	4451.5	CTD/rosette	16
107-01	19/1/09	6:07	6:29	49° 35.50' S	25° 20.74' W	4594.7	CTD/rosette	17
108-01	19/1/09	7:24	7:55	49° 35.99' S	25° 15.78' W	4636.2	CTD/rosette	18
109-01	19/1/09	8:43	9:13	49° 35.18' S	25° 10.95' W	4623.5	CTD/rosette	19
110-01	19/1/09	9:58	10:29	49° 33.14' S	25° 09.90' W	4574.7	CTD/rosette	20
111-01	19/1/09	12:32	13:05	49° 36.39' S	25° 24.80' W	4477.7	CTD/rosette	21
111-02	19/1/09	13:24	14:18	49° 35.99' S	25° 24.72' W	4481.5	Multiple net	22
111-03	19/1/09	14:19	14:24	49° 35.99' S	25° 24.72' W	4481.5	Hand net	23
111-04	19/1/09	14:32	15:24	49° 35.63' S	25° 24.55' W	4493.7	Multiple net	24
111-05	19/1/09	15:38	15:59	49° 35.26' S	25° 24.44' W	4501.7	FRRF	25
112-01	22/1/09	3:15	4:05	48° 39.96' S	34° 44.97' W	5201.5	CTD/rosette	26
112-02	22/1/09	4:08	4:22	48° 39.96' S	34° 44.85' W	5211.5	Hand net	27
112-03	22/1/09	4:31	4:58	48° 39.83' S	34° 44.25' W	5215	Clean Rosette	28
112-04	22/1/09	5:49	5:49	48° 39.68' S	34° 43.01' W	5206.5	FRRF	29
112-05	22/1/09	6:01	6:27	48° 39.58' S	34° 42.37' W	5267	Clean Rosette	30
112-06	22/1/09	6:41	7:31	48° 39.20' S	34° 41.74' W	5235.2	Multiple net	31
112-07	22/1/09	7:41	8:30	48° 38.55' S	34° 40.73' W	5263.7	Multiple net	32

Station PS73	Date	Time (start)	Time (end)	Position (Lat.)	Position (Lon.)	Depth (m)	Gear	srno
112-08	22/1/09	8:39	9:08	48° 38.21' S	34° 40.00' W	5301.5	Clean Rosette	33
112-09	22/1/09	9:20	9:48	48° 37.91' S	34° 39.17' W	5188.7	CTD/rosette	34
112-10	22/1/09	9:55	10:14	48° 37.84' S	34° 39.03' W	5167	Clean Rosette	35
114-01	26/1/09	5:48	6:07	48° 00.11' S	15° 48.50' W	3698	CTD/rosette	36
114-02	26/1/09	6:15	6:47	48° 00.35' S	15° 48.61' W	3796	Clean Rosette	37
114-03	26/1/09	7:15	7:23	48° 00.00' S	15° 48.31' W	3676	Hand net	38
114-04	26/1/09	7:27	9:17	47° 59.88' S	15° 48.20' W	3706	CTD/rosette	39
114-05	26/1/09	9:53	10:48	47° 59.72' S	15° 47.83' W	3678	Multiple net	40
114-06	26/1/09	12:48	13:21	47° 59.99' S	15° 48.41' W	3669	CTD/rosette	41
114-07	26/1/09	13:30	14:25	47° 59.72' S	15° 49.22' W	3765	Multiple net	42
114-09	26/1/09	15:25	16:02	47° 59.68' S	15° 50.06' W	3641	Clean Rosette	43
114-11	26/1/09	16:45	18:39	47° 59.88' S	15° 50.65' W	3639	CTD/rosette	44
114-14	26/1/09	19:44	20:29	48° 00.58' S	15° 50.18' W	3983	Clean Rosette	45
114-15	26/1/09	20:37	21:11	48° 00.68' S	15° 50.14' W	3989	CTD/rosette	46
114-16	26/1/09	21:39	22:04	48° 01.04' S	15° 49.61' W	3934	FRRF	47
114-18	26/1/09	23:09	23:24	48° 01.98' S	15° 47.13' W	3680	CTD/rosette	48
115-01	27/1/09	1:33	2:33	47° 54.70' S	15° 47.79' W	3661	CTD/rosette	49
116-01	27/1/09	3:48	4:45	47° 59.72' S	15° 55.80' W	3966	CTD/rosette	50
117-01	27/1/09	6:03	7:00	48° 05.10' S	15° 48.47' W	3701	CTD/rosette	51
118-01	27/1/09	8:13	9:11	48° 00.12' S	15° 41.52' W	3642	CTD/rosette	52
120-01	28/1/09	20:56	23:11	47° 52.18' S	15° 48.15' W	3411	CTD/rosette	53
120-02	28/1/09	23:17	23:31	47° 52.12' S	15° 48.23' W	3405	Hand net	54
120-04	29/1/09	0:17	1:04	47° 51.74' S	15° 47.78' W	3387	Clean Rosette	55
120-05	29/1/09	1:15	1:31	47° 51.67' S	15° 47.74' W	3383	CTD/rosette	56
120-07	29/1/09	2:20	4:18	47° 51.29' S	15° 48.06' W	3360	Multi corer	57
120-08	29/1/09	4:33	6:45	47° 51.37' S	15° 49.52' W	3372	In situ pump	58
120-09	29/1/09	7:18	8:41	47° 54.02' S	15° 52.56' W	3585	RMT	59
120-10	29/1/09	10:05	11:29	47° 43.88' S	15° 47.26' W	3372	Scan-Fish	60
121-01	29/1/09	13:26	14:08	47° 50.23' S	15° 47.56' W	3313	GoFlo bottles	61
121-02	29/1/09	14:15	14:24	47° 50.17' S	15° 47.49' W	3308	GoFlo bottles	62
121-03	29/1/09	14:28	14:53	47° 49.95' S	15° 47.29' W	3354	GoFlo bottles	63
121-04	29/1/09	14:58	15:24	47° 49.70' S	15° 47.02' W	3388	GoFlo bottles	64
121-05	29/1/09	15:32	15:46	47° 49.50' S	15° 46.69' W	3306	CTD/rosette	65
122-01	29/1/09	20:12	20:23	47° 49.42' S	15° 34.94' W	3581	CTD/rosette	66

Station PS73	Date	Time (start)	Time (end)	Position (Lat.)	Position (Lon.)	Depth (m)	Gear	srno
123-01	29/1/09	21:05	21:18	47° 49.68' S	15° 40.84' W	3175	CTD/rosette	67
123-02	29/1/09	21:24	21:36	47° 49.79' S	15° 40.90' W	3187	Clean Rosette	68
124-01	29/1/09	22:42	22:54	47° 49.55' S	15° 52.52' W	3536	CTD/rosette	69
125-01	29/1/09	23:31	23:45	47° 49.69' S	15° 58.48' W	2882	CTD/rosette	70
126-01	30/1/09	9:35	9:35	47° 49.16' S	15° 46.91' W	3310	Trap, sediment	71
126-02	30/1/09	10:31	10:31	47° 50.69' S	15° 45.86' W	3354	Trap, sediment	72
126-03	30/1/09	10:57	10:57	47° 50.80' S	15° 46.23' W	3372	Trap, sediment	73
126-04	30/1/09	11:13	11:53	47° 50.55' S	15° 46.30' W	3379	Clean Rosette	74
127-01	30/1/09	16:52	19:52	47° 59.83' S	16° 00.03' W	4112	CTD/rosette	75
127-02	30/1/09	20:00	22:36	48° 00.05' S	16° 00.10' W	3982	Multi corer	76
127-03	30/1/09	22:56	23:01	47° 59.75' S	16° 00.00' W	4165	CTD/rosette	77
127-04	31/1/09	23:34	0:23	47° 58.79' S	15° 59.75' W	3978	Multiple net	78
127-05	31/1/09	0:39	1:30	47° 58.68' S	15° 59.78' W	3962	Multiple net	79
127-06	31/1/09	1:41	2:05	47° 58.53' S	15° 59.83' W	3946	CTD/rosette	80
127-07	31/1/09	2:28	5:08	47° 59.55' S	16° 00.29' W	4096	Multi corer	81
128-01	31/1/09	7:29	7:49	47° 51.50' S	15° 46.98' W	3384	CTD/rosette	82
129-01	31/1/09	8:58	9:15	47° 44.53' S	15° 46.13' W	3406	CTD/rosette	83
129-02	31/1/09	9:24	9:41	47° 44.65' S	15° 46.02' W	3408	Clean Rosette	84
130-01	31/1/09	10:42	11:07	47° 36.73' S	15° 45.91' W	3620	CTD/rosette	85
130-02	31/1/09	11:23	11:39	47° 36.77' S	15° 45.89' W	3617	Clean Rosette	86
131-01	31/1/09	12:22	12:43	47° 32.41' S	15° 44.44' W	3554	CTD/rosette	87
132-01	31/1/09	13:41	14:19	47° 39.39' S	15° 43.91' W	3514	CTD/rosette	88
132-01	31/1/09	14:25	16:29	47° 38.84' S	15° 43.50' W	3357	CTD/rosette	89
132-03	31/1/09	17:09	17:19	47° 38.67' S	15° 43.45' W	3395	Hand net	90
132-04	31/1/09	17:28	17:48	47° 38.59' S	15° 43.36' W	3440	FRRF	91
132-06	31/1/09	18:21	18:42	47° 38.60' S	15° 43.53' W	3496	CTD/rosette	92
132-07	31/1/09	19:53	20:19	47° 38.58' S	15° 43.51' W	3447	CTD/rosette	93
132-08	31/1/09	20:29	20:53	47° 38.68' S	15° 43.76' W	3564	Clean Rosette	94
132-09	31/1/09	21:22	21:40	47° 39.12' S	15° 43.82' W	3533	CTD/rosette	95
132-10	31/1/09	22:26	23:21	47° 36.96' S	15° 44.81' W	3606	Multiple net	96
132-11	1/2/09	23:29	0:01	47° 37.21' S	15° 44.59' W	3606	CTD/rosette	97
132-12	1/2/09	0:13	1:00	47° 37.50' S	15° 44.26' W	3641	Multiple net	98
132-14	1/2/09	1:32	1:54	47° 37.52' S	15° 43.52' W	3535	FRRF	99
132-15	1/2/09	2:00	2:55	47° 37.36' S	15° 42.87' W	3692	CTD/rosette	100

Station PS73	Date	Time (start)	Time (end)	Position (Lat.)	Position (Lon.)	Depth (m)	Gear	srno
132-16	1/2/09	3:26	3:58	47° 36.93' S	15° 43.25' W	3680	RMT	101
132-17	1/2/09	4:13	5:00	47° 36.27' S	15° 44.27' W	3653	RMT	102
132-18	1/2/09	8:26	9:32	47° 35.00' S	15° 39.50' W	3530	Scan-Fish	103
133-02	2/2/09	11:22	11:42	47° 33.18' S	15° 33.84' W	3546.3	Scan-Fish	104
134-02	4/2/09	15:27	16:33	48° 13.74' S	12° 58.78' W	2872.9	Hand net	105
134-01	4/2/09	16:15	16:26	48° 13.74' S	12° 58.78' W	2872.9	CTD/rosette	106
135-01	5/2/09	9:18	11:08	47° 41.65' S	15° 05.87' W	2808.9	CTD/rosette	107
135-02	5/2/09	11:34	11:42	47° 41.79' S	15° 06.08' W	2826	Hand net	108
135-03	5/2/09	11:46	11:50	47° 41.83' S	15° 06.14' W	2840.3	Hand net	109
135-04	5/2/09	11:54	12:12	47° 41.89' S	15° 06.33' W	NaN	FRRF	110
135-06	5/2/09	13:05	13:31	47° 42.01' S	15° 06.89' W	3072.5	CTD/rosette	111
135-07	5/2/09	13:42	14:09	47° 42.09' S	15° 06.99' W	3085.3	Clean Rosette	112
135-08	5/2/09	14:20	14:35	47° 42.14' S	15° 07.09' W	3132.8	CTD/rosette	113
135-09	5/2/09	14:44	15:35	47° 42.33' S	15° 07.04' W	3116.2	Multiple net	114
135-10	5/2/09	15:43	16:34	47° 42.58' S	15° 06.74' W	3208.5	Multiple net	115
135-11	5/2/09	16:45	17:16	47° 42.83' S	15° 06.44' W	3213.9	CTD/rosette	116
135-12	5/2/09	17:18	19:31	47° 43.42' S	15° 07.13' W	3157.2	In situ pump	117
135-13	5/2/09	19:42	20:34	47° 43.67' S	15° 07.60' W	3124	CTD/rosette	118
135-16	5/2/09	21:56	22:21	47° 43.88' S	15° 07.43' W	3108.5	RMT	119
135-17	5/2/09	22:44	23:38	47° 43.94' S	15° 07.35' W	3109.5	Multiple net	120
135-18	6/2/09	23:46	0:24	47° 44.00' S	15° 07.40' W	3114.7	Multiple net	121
135-18	6/2/09	1:05	1:57	47° 44.23' S	15° 07.20' W	3113.1	Multiple net	122
135-19	6/2/09	2:07	2:25	47° 44.23' S	15° 07.25' W	3127.4	FRRF	123
136-01	6/2/09	20:37	20:37	47° 31.20' S	15° 06.95' W	2928	Trap, sediment	124
137-01	8/2/09	9:46	11:42	47° 51.27' S	15° 14.63' W	NaN	CTD/rosette	125
137-02	8/2/09	11:58	12:11	47° 51.27' S	15° 14.82' W	4028.3	Hand net	126
137-03	8/2/09	12:13	12:15	47° 51.27' S	15° 14.82' W	4028.3	Hand net	127
137-04	8/2/09	12:25	12:43	47° 51.26' S	15° 15.00' W	4024.1	FRRF	128
137-06	8/2/09	13:40	14:07	47° 51.41' S	15° 15.26' W	4031.5	CTD/rosette	129
137-07	8/2/09	14:13	14:37	47° 51.51' S	15° 15.37' W	4041.3	Clean Rosette	130
137-08	8/2/09	14:46	15:00	47° 51.62' S	15° 15.51' W	4039.2	CTD/rosette	131
137-09	8/2/09	15:09	16:04	47° 51.85' S	15° 15.66' W	4059.6	Multiple net	132
137-10	8/2/09	16:15	17:04	47° 52.11' S	15° 15.87' W	4082.8	Multiple net	133
137-11	8/2/09	17:15	17:44	47° 52.33' S	15° 16.04' W	4092.8	CTD/rosette	134
137-12	8/2/09	17:52	20:04	47° 53.08' S	15° 16.18' W	4101.4	In situ pump	135

Station PS73	Date	Time (start)	Time (end)	Position (Lat.)	Position (Lon.)	Depth (m)	Gear	srno
137-13	8/2/09	20:11	21:02	47° 53.48' S	15° 16.31' W	4097.7	CTD/rosette	136
137-16	8/2/09	22:32	22:53	47° 53.07' S	15° 15.83' W	4102.7	RMT	137
137-17	9/2/09	23:19	0:09	47° 52.00' S	15° 16.99' W	4046.2	Multiple net	138
137-18	9/2/09	0:18	1:11	47° 52.04' S	15° 17.29' W	NaN	Multiple net	139
137-19	9/2/09	1:19	1:39	47° 52.10' S	15° 17.28' W	NaN	FRRF	140
137-20	9/2/09	1:50	2:14	47° 52.21' S	15° 17.52' W	4058.6	Bongo net	141
138-01	9/2/09	17:08	17:12	47° 53.60' S	15° 07.06' W	3520.3	Hand net	142
138-02	9/2/09	17:49	17:59	47° 54.34' S	15° 07.24' W	3511.9	CTD/rosette	143
139-02	9/2/09	21:15	22:05	47° 54.49' S	15° 07.78' W	3593.6	CTD/rosette	144
139-03	9/2/09	22:11	22:30	47° 54.48' S	15° 07.80' W	3579.2	FRRF	145
139-04	9/2/09	22:49	23:01	47° 54.48' S	15° 07.83' W	3584.9	Hand net	146
139-05	9/2/09	23:07	23:44	47° 54.51' S	15° 07.89' W	3591.7	Clean Rosette	147
139-06	10/2/09	23:54	0:46	47° 54.55' S	15° 08.06' W	3584.9	CTD/rosette	148
139-07	10/2/09	0:55	1:46	47° 54.65' S	15° 08.16' W	3592.2	Multiple net	149
139-08	10/2/09	1:55	2:46	47° 54.98' S	15° 08.52' W	3611.5	Multiple net	150
139-09	10/2/09	2:53	4:44	47° 55.33' S	15° 08.97' W	3625.1	CTD/rosette	151
139-10	10/2/09	4:51	7:14	47° 56.54' S	15° 08.81' W	3622.1	In situ pump	152
139-11	10/2/09	7:26	7:32	47° 56.57' S	15° 08.81' W	3650.2	CTD/rosette	153
139-12	10/2/09	7:59	8:04	47° 56.77' S	15° 08.86' W	3665.5	Hand net	154
139-13	10/2/09	8:08	8:42	47° 57.20' S	15° 08.62' W	3574.4	CTD/rosette	155
140-01	10/2/09	11:49	14:29	47° 54.48' S	15° 23.98' W	4182	Multi corer	156
141-01	11/2/09	23:58	0:40	47° 58.37' S	15° 08.07' W	3602.3	CTD/rosette	157
142-01	11/2/09	13:37	13:47	47° 37.13' S	16° 00.17' W	3810.5	CTD/rosette	158
143-01	11/2/09	16:08	16:21	47° 41.30' S	15° 29.41' W	3166.7	CTD/rosette	159
143-01	11/2/09	21:44	21:44	48° 01.26' S	15° 09.97' W	3586.9	Trap, sediment	160
144-01	11/2/09	23:40	23:40	47° 49.23' S	15° 25.44' W	3396.2	Trap, sediment	161
145-01	12/2/09	0:29	0:29	47° 45.30' S	15° 27.54' W	3276.9	Trap, sediment	162
146-01	12/2/09	2:36	3:43	47° 29.41' S	15° 26.27' W	3250.2	Multiple net	163
146-02	12/2/09	3:51	5:00	47° 29.23' S	15° 25.88' W	3255.9	Multiple net	164
146-03	12/2/09	5:11	5:29	47° 29.19' S	15° 25.51' W	3347	FRRF	165
146-04	12/2/09	5:38	7:27	47° 29.45' S	15° 25.20' W	3402.6	CTD/rosette	166
146-06	12/2/09	8:06	8:27	47° 29.79' S	15° 26.17' W	3244.8	RMT	167
146-07	12/2/09	8:36	8:42	47° 29.81' S	15° 26.40' W	3384.4	Hand net	168
146-08	12/2/09	8:46	9:09	47° 29.90' S	15° 26.26' W	NaN	Hand net	169
146-09	12/2/09	9:28	9:53	47° 29.92' S	15° 25.95' W	3271.6	CTD/rosette	170

Station PS73	Date	Time (start)	Time (end)	Position (Lat.)	Position (Lon.)	Depth (m)	Gear	srno
146-10	12/2/09	10:02	10:24	47° 29.96' S	15° 25.72' W	3290.1	Clean Rosette	171
146-11	12/2/09	10:39	11:17	47° 30.05' S	15° 25.57' W	3306.7	CTD/rosette	172
146-12	12/2/09	11:23	13:22	47° 30.27' S	15° 26.27' W	NaN	In situ pump	173
146-13	12/2/09	13:27	13:43	47° 30.30' S	15° 26.49' W	3259.7	CTD/rosette	174
146-14	12/2/09	13:50	14:46	47° 30.25' S	15° 26.60' W	NaN	Multiple net	175
146-15	12/2/09	14:53	15:48	47° 30.09' S	15° 26.70' W	3252.9	Multiple net	176
146-16	12/2/09	15:56	16:47	47° 30.03' S	15° 26.61' W	3242.1	CTD/rosette	177
147-01	14/2/09	9:32	9:54	48° 02.48' S	15° 14.79' W	3684.9	CTD/rosette	178
147-02	14/2/09	9:58	10:07	48° 02.43' S	15° 14.94' W	NaN	Hand net	179
148-01	14/2/09	12:52	14:54	47° 56.55' S	15° 17.57' W	NaN	CTD/rosette	180
148-02	14/2/09	15:05	15:55	47° 56.39' S	15° 17.29' W	3733.6	Multiple net	181
148-03	14/2/09	16:03	16:52	47° 56.18' S	15° 17.10' W	3730.3	Multiple net	182
148-04	14/2/09	16:59	17:14	47° 56.15' S	15° 16.89' W	3736.5	FRRF	183
148-05	14/2/09	17:26	17:50	47° 56.09' S	15° 16.79' W	3744	CTD/rosette	184
148-07	14/2/09	18:13	18:20	47° 56.04' S	15° 16.79' W	3745.8	Hand net	185
148-08	14/2/09	18:26	18:49	47° 56.03' S	15° 16.50' W	3772	Hand net	186
148-10	14/2/09	19:35	19:47	47° 55.54' S	15° 17.04' W	3870.8	CTD/rosette	187
148-11	14/2/09	19:54	20:17	47° 55.39' S	15° 17.26' W	3817.1	Clean Rosette	188
148-12	14/2/09	20:35	21:12	47° 55.03' S	15° 17.40' W	NaN	CTD/rosette	189
148-13	14/2/09	21:25	21:51	47° 54.40' S	15° 18.44' W	4040.8	RMT	190
148-14	14/2/09	22:21	22:35	47° 54.83' S	15° 18.60' W	4022.7	FRRF	191
148-15	15/2/09	22:44	0:06	47° 54.66' S	15° 18.93' W	4051.2	CTD/rosette	192
148-16	15/2/09	0:13	2:21	47° 54.85' S	15° 19.69' W	NaN	In situ pump	193
148-17	15/2/09	2:31	3:23	47° 54.91' S	15° 20.11' W	4108.5	Multiple net	194
148-18	15/2/09	3:32	4:25	47° 54.82' S	15° 20.40' W	NaN	Multiple net	195
149-01	15/2/09	11:48	12:18	47° 35.86' S	15° 45.08' W	3634.6	CTD/rosette	196
149-02	15/2/09	12:21	12:28	47° 35.77' S	15° 45.06' W	3589.2	Hand net	197
150-01	15/2/09	13:20	13:44	47° 35.30' S	15° 45.96' W	3502.4	CTD/rosette	198
151-01	15/2/09	14:19	14:43	47° 33.23' S	15° 45.62' W	3528.8	CTD/rosette	199
152-01	15/2/09	15:07	15:39	47° 31.98' S	15° 44.00' W	3541.8	CTD/rosette	200
153-01	15/2/09	17:28	17:53	47° 39.09' S	15° 35.83' W	3386.8	CTD/rosette	201
156-01	18/2/09	6:57	6:57	47° 22.54' S	15° 24.87' W	3224	Trap, sediment	202
157-01	18/2/09	9:36	9:36	47° 31.98' S	14° 42.78' W	2893.6	Trap, sediment	203
158-01	18/2/09	11:01	11:01	47° 38.55' S	14° 59.55' W	2675.5	Trap, sediment	204
159-01	18/2/09	14:09	14:41	47° 21.17' S	15° 24.93' W	3369.2	CTD/rosette	205

Station PS73	Date	Time (start)	Time (end)	Position (Lat.)	Position (Lon.)	Depth (m)	Gear	srno
159-02	18/2/09	14:43	14:49	47° 21.13' S	15° 24.97' W	3353.6	Hand net	206
160-01	18/2/09	18:39	20:52	47° 20.58' S	15° 39.77' W	3240.7	CTD/rosette	207
160-03	18/2/09	21:22	21:33	47° 20.24' S	15° 39.14' W	3374.6	Hand net	208
160-04	18/2/09	21:35	21:43	47° 20.07' S	15° 39.10' W	NaN	Hand net	209
160-05	18/2/09	22:07	22:29	47° 19.91' S	15° 39.08' W	3342.5	RMT	210
160-06	18/2/09	22:53	23:19	47° 19.82' S	15° 39.02' W	3358.6	CTD/rosette	211
160-07	18/2/09	23:30	23:43	47° 19.73' S	15° 38.90' W	3474.2	FRRF	212
160-08	19/2/09	23:47	0:11	47° 19.35' S	15° 38.68' W	3494.3	Clean Rosette	213
160-09	19/2/09	0:22	0:35	47° 19.06' S	15° 38.74' W	3488.7	CTD/rosette	214
160-10	19/2/09	0:42	1:33	47° 18.43' S	15° 38.60' W	3241.6	Multiple net	215
160-11	19/2/09	1:45	2:34	47° 18.21' S	15° 38.89' W	NaN	Multiple net	216
160-13	19/2/09	3:13	4:04	47° 18.30' S	15° 38.93' W	3368.5	CTD/rosette	217
160-14	19/2/09	4:12	6:13	47° 18.60' S	15° 38.37' W	3206.2	In situ pump	218
160-15	19/2/09	6:25	6:43	47° 18.72' S	15° 37.76' W	3163.1	FRRF	219
160-16	19/2/09	6:53	7:27	47° 18.84' S	15° 36.99' W	3131.7	CTD/rosette	220
160-17	19/2/09	7:35	8:23	47° 18.82' S	15° 36.07' W	3064.9	Multiple net	221
160-18	19/2/09	8:34	9:22	47° 18.53' S	15° 34.93' W	3047.7	Multiple net	222
160-19	19/2/09	9:34	9:38	47° 18.37' S	15° 34.47' W	3377.7	CTD/rosette	223
161-01	19/2/09	10:03	23:50	47° 16.42' S	14° 53.94' W	3295.8	Trap, sediment	224
162-02	20/2/09	11:15	13:17	47° 21.33' S	14° 42.94' W	3141.6	CTD/rosette	225
162-03	20/2/09	13:27	14:18	47° 21.62' S	14° 41.72' W	2974.1	Multiple net	226
162-04	20/2/09	14:25	15:15	47° 21.83' S	14° 40.74' W	3170.8	Multiple net	227
162-06	20/2/09	15:57	16:25	47° 22.24' S	14° 39.62' W	2812.4	CTD/rosette	228
162-07	20/2/09	16:35	16:52	47° 22.36' S	14° 39.08' W	2836.6	FRRF	229
162-08	20/2/09	16:55	17:09	47° 22.57' S	14° 38.74' W	2952.2	Hand net	230
162-09	20/2/09	17:10	17:33	47° 22.67' S	14° 38.41' W	3003.8	Hand net	231
162-10	20/2/09	17:42	17:55	47° 22.86' S	14° 38.12' W	3168.6	CTD/rosette	232
162-11	20/2/09	18:03	18:26	47° 23.11' S	14° 37.45' W	3324.6	Clean Rosette	233
162-12	20/2/09	18:48	19:19	47° 23.55' S	14° 36.94' W	3297.7	CTD/rosette	234
162-13	20/2/09	19:28	21:34	47° 24.43' S	14° 34.95' W	3019.2	In situ pump	235
162-14	20/2/09	21:53	22:12	47° 24.74' S	14° 34.55' W	2969.9	RMT	236
162-15	20/2/09	22:32	22:47	47° 25.00' S	14° 33.80' W	3036.7	FRRF	237
162-16	20/2/09	22:53	23:48	47° 25.54' S	14° 33.02' W	2977.2	CTD/rosette	238
162-17	21/2/09	23:56	0:43	47° 25.99' S	14° 32.32' W	2855.5	Multiple net	239
162-18	21/2/09	1:00	1:50	47° 26.66' S	14° 31.60' W	2979.1	Multiple net	240

Station PS73	Date	Time (start)	Time (end)	Position (Lat.)	Position (Lon.)	Depth (m)	Gear	srno
163-01	21/2/09	15:08	15:34	48° 00.04' S	14° 00.07' W	3248.6	CTD/rosette	241
163-02	21/2/09	18:43	19:49	48° 03.46' S	14° 03.14' W	3405.2	CTD/rosette	242
164-01	21/2/09	22:51	23:12	47° 59.80' S	13° 29.71' W	3504.8	RMT	243
164-02	22/2/09	23:35	0:00	47° 59.85' S	13° 29.91' W	3382.9	Clean Rosette	244
164-03	22/2/09	0:10	1:02	48° 00.06' S	13° 30.04' W	3333.8	Multiple net	245
164-04	22/2/09	1:14	2:20	48° 00.18' S	13° 30.23' W	3265.8	CTD/rosette	246
165-01	22/2/09	3:27	4:33	48° 00.15' S	13° 20.42' W	3067.2	CTD/rosette	247
166-01	22/2/09	5:36	6:27	48° 00.14' S	13° 12.08' W	3191.8	CTD/rosette	248
167-01	22/2/09	7:28	8:22	48° 00.10' S	13° 03.85' W	3189.7	CTD/rosette	249
168-01	22/2/09	9:34	10:32	48° 00.16' S	12° 52.97' W	3157.1	CTD/rosette	250
169-01	22/2/09	21:18	21:18	47° 35.83' S	14° 32.79' W	2902	Trap, sediment	251
170-01	23/2/09	15:00	16:58	48° 01.00' S	14° 28.09' W	3332.2	CTD/rosette	252
170-02	23/2/09	17:09	17:30	48° 01.42' S	14° 28.35' W	3330.8	FRRF	253
170-03	23/2/09	17:36	18:28	48° 02.26' S	14° 28.55' W	3354.2	Multiple net	254
170-04	23/2/09	18:38	19:29	48° 02.91' S	14° 28.78' W	3365.5	Multiple net	255
170-05	23/2/09	19:42	20:05	48° 03.46' S	14° 28.51' W	NaN	CTD/rosette	256
170-06	23/2/09	20:14	20:36	48° 03.89' S	14° 28.47' W	3430.4	Clean Rosette	257
170-07	23/2/09	20:43	20:49	48° 03.95' S	14° 28.51' W	3435.2	Hand net	258
170-08	23/2/09	21:03	21:14	48° 04.22' S	14° 28.34' W	3460.9	Hand net	259
170-09	23/2/09	21:20	21:37	48° 04.49' S	14° 28.28' W	NaN	CTD/rosette	260
170-12	23/2/09	23:04	23:22	48° 05.01' S	14° 28.67' W	3439	RMT	261
170-13	24/2/09	23:45	0:21	48° 05.58' S	14° 28.26' W	3382.8	CTD/rosette	262
170-15	24/2/09	1:08	1:27	48° 06.06' S	14° 27.64' W	3507.7	FRRF	263
170-16	24/2/09	1:38	2:30	48° 06.06' S	14° 27.95' W	3442.5	CTD/rosette	264
170-17	24/2/09	2:35	4:39	48° 06.41' S	14° 28.81' W	3434	In situ pump	265
170-19	24/2/09	5:15	6:07	48° 07.25' S	14° 29.37' W	3480.3	Multiple net	266
170-20	24/2/09	6:19	7:14	48° 08.21' S	14° 30.52' W	3458.1	Multiple net	267
170-21	24/2/09	7:27	9:10	48° 09.97' S	14° 31.92' W	3440.2	CTD/rosette	268
171-01	24/2/09	11:50	14:02	47° 54.11' S	14° 30.04' W	3427	Multi corer	269
172-01	24/2/09	15:36	15:56	47° 53.94' S	14° 44.68' W	3566	CTD/rosette	270
172-02	25/2/09	16:20	10:58	48° 28.65' S	14° 39.66' W	3788	Scan-Fish	271
173-01	25/2/09	11:51	11:51	48° 29.35' S	14° 44.64' W	3729.4	Trap, sediment	272
174-01	25/2/09	12:37	12:58	48° 26.58' S	14° 44.01' W	3787.8	CTD/rosette	273
174-02	25/2/09	13:06	13:29	48° 26.76' S	14° 44.30' W	3805.9	Multiple net	274
174-03	25/2/09	13:29	13:41	48° 26.84' S	14° 44.41' W	3798.7	Hand net	275

Station PS73	Date	Time (start)	Time (end)	Position (Lat.)	Position (Lon.)	Depth (m)	Gear	srno
175-01	25/2/09	14:25	14:46	48° 24.47' S	14° 44.75' W	3730.8	Multiple net	276
175-02	25/2/09	14:57	15:24	48° 24.81' S	14° 45.10' W	3784.2	Multiple net	277
175-03	25/2/09	15:26	15:49	48° 25.13' S	14° 45.48' W	3754.2	CTD/rosette	278
175-04	25/2/09	15:55	16:06	48° 25.38' S	14° 45.60' W	3752.1	Hand net	279
176-01	25/2/09	16:59	17:16	48° 21.73' S	14° 45.89' W	3669.1	CTD/rosette	280
176-02	25/2/09	17:24	17:47	48° 22.00' S	14° 46.06' W	3619.4	Multiple net	281
176-03	25/2/09	17:51	18:05	48° 22.09' S	14° 46.00' W	3611.3	Hand net	282
177-01	25/2/09	18:48	19:08	48° 18.44' S	14° 46.63' W	3783.1	Multiple net	283
177-02	25/2/09	19:17	19:34	48° 18.54' S	14° 46.71' W	3799.1	CTD/rosette	284
177-03	25/2/09	19:38	19:48	48° 18.68' S	14° 46.84' W	3841.3	Hand net	285
178-01	25/2/09	20:29	20:47	48° 16.12' S	14° 46.62' W	3724	CTD/rosette	286
178-02	25/2/09	20:54	21:17	48° 16.20' S	14° 46.62' W	3725.6	Multiple net	287
178-03	25/2/09	21:20	21:38	48° 16.21' S	14° 46.52' W	3723.7	Hand net	288
178-04	25/2/09	21:42	22:05	48° 16.15' S	14° 46.94' W	3724.6	RMT	289
179-01	25/2/09	22:42	23:00	48° 12.87' S	14° 46.26' W	3627.6	CTD/rosette	290
179-02	25/2/09	23:06	23:28	48° 12.99' S	14° 46.15' W	3626.3	Multiple net	291
179-03	25/2/09	23:33	23:42	48° 13.04' S	14° 46.11' W	3668.9	Hand net	292
180-01	26/2/09	0:21	0:45	48° 09.05' S	14° 45.95' W	3496.4	Multiple net	293
180-02	26/2/09	0:54	1:16	48° 08.95' S	14° 45.93' W	3407.6	CTD/rosette	294
180-03	26/2/09	1:21	1:27	48° 08.88' S	14° 46.01' W	3493.8	Hand net	295
181-01	26/2/09	2:20	2:42	48° 05.31' S	14° 45.72' W	3518.1	CTD/rosette	296
181-02	26/2/09	2:51	3:14	48° 05.22' S	14° 45.88' W	3534	Multiple net	297
181-03	26/2/09	3:15	3:20	48° 05.25' S	14° 45.97' W	3506.7	Hand net	298
182-01	26/2/09	15:52	16:23	47° 47.54' S	15° 00.54' W	3624.5	CTD/rosette	299
182-02	26/2/09	16:28	16:53	47° 47.51' S	15° 00.60' W	3616.5	Multiple net	300
182-03	26/2/09	16:55	17:08	47° 47.49' S	15° 00.59' W	3615.1	Hand net	301
183-01	26/2/09	17:31	21:31	48° 13.44' S	14° 23.23' W	3417.4	Trap, sediment	302
183-02	26/2/09	21:49	22:13	48° 13.59' S	14° 23.46' W	3439.1	Clean Rosette	303
184-01	27/2/09	0:49	0:49	48° 36.00' S	14° 32.13' W	3595.6	Trap, sediment	304
185-01	27/2/09	10:05	10:25	48° 46.00' S	15° 28.03' W	4001.9	CTD/rosette	305
185-02	27/2/09	10:33	10:58	48° 46.28' S	15° 28.22' W	4008.7	Multiple net	306
185-03	27/2/09	11:00	11:06	48° 46.32' S	15° 28.19' W	3999.5	Hand net	307
186-01	27/2/09	11:39	11:58	48° 46.10' S	15° 22.86' W	4130.7	CTD/rosette	308
186-02	27/2/09	12:06	12:27	48° 46.10' S	15° 22.70' W	3957.7	Multiple net	309
186-03	27/2/09	12:31	12:41	48° 46.10' S	15° 22.70' W	3958.1	Hand net	310

Station PS73	Date	Time (start)	Time (end)	Position (Lat.)	Position (Lon.)	Depth (m)	Gear	srno
187-01	27/2/09	13:44	14:06	48° 48.09' S	15° 16.40' W	3850.6	Multiple net	311
187-02	27/2/09	14:15	14:33	48° 48.18' S	15° 16.49' W	3871.9	CTD/rosette	312
187-03	27/2/09	14:37	14:49	48° 48.26' S	15° 16.57' W	3879.3	Hand net	313
188-01	27/2/09	15:34	15:52	48° 48.00' S	15° 14.01' W	3839.7	CTD/rosette	314
188-02	27/2/09	16:00	16:23	48° 48.02' S	15° 14.08' W	3779.7	Multiple net	315
188-03	27/2/09	16:26	16:42	48° 48.09' S	15° 14.08' W	3845.6	Hand net	316
189-01	27/2/09	17:23	17:45	48° 48.92' S	15° 09.49' W	3842.9	Multiple net	317
189-02	27/2/09	17:56	18:14	48° 49.00' S	15° 09.38' W	3844	CTD/rosette	318
189-03	27/2/09	18:22	18:25	48° 49.03' S	15° 09.29' W	3848	Hand net	319
190-01	27/2/09	19:20	19:39	48° 49.08' S	15° 05.10' W	3954.2	CTD/rosette	320
190-02	27/2/09	19:45	20:08	48° 49.19' S	15° 05.04' W	3984	Multiple net	321
190-03	27/2/09	20:16	20:20	48° 49.24' S	15° 05.00' W	3982.7	Hand net	322
191-01	27/2/09	21:24	21:44	48° 48.06' S	15° 14.03' W	3843	RMT	323
191-02	27/2/09	22:15	23:02	48° 48.44' S	15° 14.06' W	3851.8	CTD/rosette	324
192-01	28/2/09	20:09	20:12	48° 48.55' S	15° 14.89' W	NaN	Hand net	325
192-02	28/2/09	22:43	23:18	48° 47.75' S	15° 14.80' W	3822.6	CTD/rosette	326
192-05	1/3/09	0:39	2:35	48° 48.25' S	15° 12.23' W	3843	CTD/rosette	327
192-07	1/3/09	3:41	4:33	48° 49.14' S	15° 13.56' W	3910.1	Multiple net	328
192-08	1/3/09	4:50	5:00	48° 49.01' S	15° 13.66' W	3897.7	CTD/rosette	329
192-09	1/3/09	5:06	5:56	48° 48.90' S	15° 13.86' W	3887.1	Multiple net	330
192-10	1/3/09	6:06	6:21	48° 48.86' S	15° 13.94' W	3884.9	CTD/rosette	331
192-11	1/3/09	6:33	8:30	48° 49.14' S	15° 14.79' W	3909.7	In situ pump	332
192-12	1/3/09	8:43	9:15	48° 49.28' S	15° 15.42' W	3922.9	CTD/rosette	333
193-01	1/3/09	18:11	18:31	48° 38.72' S	15° 08.40' W	3721.6	CTD/rosette	334
193-02	1/3/09	18:38	18:42	48° 38.64' S	15° 08.53' W	3727.3	Hand net	335
194-01	1/3/09	22:57	22:57	48° 56.22' S	15° 12.71' W	3860.7	Trap, sediment	336
195-01	2/3/09	1:49	4:18	48° 39.52' S	15° 05.63' W	3800.9	Multi corer	337
195-02	2/3/09	4:38	5:43	48° 40.03' S	15° 04.40' W	NaN	CTD/rosette	338
196-01	2/3/09	9:22	9:40	48° 24.84' S	14° 56.87' W	3525.2	CTD/rosette	339
196-02	2/3/09	9:48	10:11	48° 24.60' S	14° 56.79' W	3535.2	Multiple net	340
196-03	2/3/09	10:13	10:34	48° 24.43' S	14° 56.75' W	3527.1	Hand net	341
196-04	2/3/09	10:41	11:05	48° 24.07' S	14° 56.66' W	3519.3	Clean Rosette	342
197-01	2/3/09	13:36	15:43	48° 25.36' S	15° 15.65' W	3696.2	CTD/rosette	343
197-02	2/3/09	15:51	16:16	48° 25.69' S	15° 15.74' W	3671.3	Multiple net	344
197-03	2/3/09	16:19	16:27	48° 25.83' S	15° 15.96' W	3656.2	Hand net	345

Station PS73	Date	Time (start)	Time (end)	Position (Lat.)	Position (Lon.)	Depth (m)	Gear	srno
198-01	2/3/09	18:17	19:21	48° 15.02' S	15° 14.59' W	NaN	CTD/rosette	346
199-01	2/3/09	21:22	21:41	48° 03.63' S	15° 15.54' W	3714.6	RMT	347
199-02	3/3/09	22:01	0:04	48° 03.68' S	15° 13.92' W	3695.9	CTD/rosette	348
199-03	3/3/09	0:08	0:17	48° 03.51' S	15° 13.88' W	3698	Hand net	349
199-04	3/3/09	0:28	0:41	48° 03.27' S	15° 13.59' W	3721.1	Hand net	350
199-06	3/3/09	1:34	2:07	48° 02.72' S	15° 14.99' W	3691.4	CTD/rosette	351
199-07	3/3/09	2:14	2:32	48° 02.62' S	15° 14.89' W	3687	FRRF	352
199-08	3/3/09	2:46	2:59	48° 02.32' S	15° 14.44' W	3791.3	CTD/rosette	353
199-09	3/3/09	3:21	4:12	48° 02.77' S	15° 15.01' W	NaN	Multiple net	354
199-10	3/3/09	4:21	5:10	48° 02.54' S	15° 14.99' W	NaN	Multiple net	355
199-11	3/3/09	5:22	6:14	48° 02.11' S	15° 15.33' W	3707.1	CTD/rosette	356
199-12	3/3/09	6:22	6:46	48° 02.06' S	15° 15.75' W	3738.7	Clean Rosette	357
199-13	3/3/09	6:53	7:10	48° 02.16' S	15° 15.94' W	NaN	FRRF	358
199-14	3/3/09	7:22	7:53	48° 02.57' S	15° 16.46' W	3798.9	CTD/rosette	359
200-01	3/3/09	9:36	10:38	47° 52.31' S	15° 15.38' W	4095.8	CTD/rosette	360
201-01	3/3/09	12:43	13:46	47° 41.00' S	15° 14.15' W	3774.7	CTD/rosette	361
202-01	3/3/09	15:42	16:48	47° 29.83' S	15° 14.05' W	NaN	CTD/rosette	362
203-01	3/3/09	22:37	22:37	47° 32.54' S	14° 01.28' W	3297.3	Trap, sediment	363
204-01	4/3/09	11:31	13:30	48° 58.49' S	15° 14.05' W	3871.9	CTD/rosette	364
204-02	4/3/09	13:50	14:45	48° 58.29' S	15° 15.59' W	3778.7	Multiple net	365
204-03	4/3/09	14:58	15:50	48° 58.50' S	15° 17.23' W	3822.3	Multiple net	366
204-04	4/3/09	15:58	16:17	48° 58.91' S	15° 17.92' W	3863.3	FRRF	367
204-05	4/3/09	16:25	16:59	48° 59.41' S	15° 18.56' W	3918.4	CTD/rosette	368
204-06	4/3/09	17:03	17:10	48° 59.53' S	15° 18.60' W	3925.9	Hand net	369
204-07	4/3/09	17:14	17:33	48° 59.73' S	15° 18.64' W	3931.3	Hand net	370
204-08	4/3/09	17:38	17:58	49° 00.05' S	15° 18.63' W	3931.2	Hand net	371
204-10	4/3/09	18:25	18:58	49° 01.07' S	15° 18.96' W	3926	CTD/rosette	372
204-11	4/3/09	19:07	21:06	49° 02.21' S	15° 18.47' W	3863.6	In situ pump	373
204-12	4/3/09	21:14	21:37	49° 02.49' S	15° 18.17' W	3866.7	Clean Rosette	374
204-13	4/3/09	21:52	22:11	49° 02.47' S	15° 17.74' W	3809.6	RMT	375
204-14	5/3/09	23:47	0:07	48° 58.12' S	15° 11.28' W	3846.9	FRRF	376
204-15	5/3/09	0:09	0:25	48° 58.12' S	15° 11.19' W	3850.6	CTD/rosette	377
204-16	5/3/09	0:33	1:22	48° 57.93' S	15° 10.96' W	3831.6	Multiple net	378
204-17	5/3/09	1:31	2:22	48° 57.71' S	15° 11.41' W	3848.5	Multiple net	379
204-19	5/3/09	4:25	6:13	48° 54.48' S	15° 11.35' W	4250.7	CTD/rosette	380

Station PS73	Date	Time (start)	Time (end)	Position (Lat.)	Position (Lon.)	Depth (m)	Gear	srno
204-20	5/3/09	6:37	6:58	48° 54.77' S	15° 11.89' W	4073.5	Multiple net	381
204-20	5/3/09	7:00	10:44	48° 55.70' S	15° 11.84' W	3918	Multiple net	382
205-01	5/3/09	14:55	14:55	49° 05.40' S	15° 15.81' W	3698.7	Trap, sediment	383
206-01	5/3/09	15:55	15:55	49° 08.59' S	15° 13.46' W	3958.2	Trap, sediment	384
207-01	5/3/09	19:49	21:51	49° 00.46' S	15° 30.91' W	3737.2	In situ pump	385
207-02	5/3/09	22:21	22:39	49° 02.06' S	15° 31.56' W	3699.5	RMT	386
208-01	6/3/09	0:05	0:19	49° 02.32' S	15° 24.08' W	3984.7	RMT	387
209-01	6/3/09	1:37	1:55	48° 57.84' S	15° 20.86' W	4037.5	RMT	388
210-01	6/3/09	4:19	4:36	48° 56.34' S	15° 12.90' W	3827.7	RMT	389
211-01	6/3/09	12:23	12:40	48° 57.90' S	15° 22.48' W	4028	CTD/rosette	390
211-02	6/3/09	13:01	13:23	48° 58.12' S	15° 22.62' W	4037	Multiple net	391
211-04	6/3/09	13:46	13:49	48° 58.21' S	15° 22.70' W	3980.5	Hand net	392
211-06	6/3/09	14:16	14:38	48° 58.50' S	15° 22.91' W	3963.2	Clean Rosette	393
212-01	6/3/09	17:20	17:40	49° 02.09' S	15° 30.81' W	3721	CTD/rosette	394
212-02	6/3/09	17:52	18:01	49° 02.24' S	15° 30.67' W	3731.7	Multiple net	395

Die "Berichte zur Polar- und Meeresforschung" (ISSN 1866-3192) werden beginnend mit dem Heft Nr. 569 (2008) ausschließlich elektronisch als Open-Access-Publikation herausgegeben. Ein Verzeichnis aller Hefte einschließlich der Druckausgaben (Heft 377-568) sowie der früheren **"Berichte zur Polarforschung** (Heft 1-376, von 1982 bis 2000) befindet sich im Internet in der Ablage des electronic Information Center des AWI (**ePIC**) unter der URL http://epic.awi.de. Durch Auswahl "Reports on Polar- and Marine Research" auf der rechten Seite des Fensters wird eine Liste der Publikationen in alphabetischer Reihenfolge (nach Autoren) innerhalb der absteigenden chronologischen Reihenfolge der Jahrgänge erzeugt.

To generate a list of all Reports past issues, use the following URL: http://epic.awi.de and select the right frame to browse "Reports on Polar and Marine Research". A chronological list in declining order, author names alphabetical, will be produced, and pdf-icons shown for open access download.

Verzeichnis der zuletzt erschienenen Hefte:

Heft-Nr. 601/2009 — "Analyse von Bathymetrie und akustischer Rückstreuung verschiedener Fächersonar- und Sedimentecholot-Systeme zur Charakterisierung und Klassifizierung des Meeresbodens am Gakkel-Rücken, Arktischer Ozean", by Jörn Hatzky

Heft-Nr. 602/2009 — "Cumacea (Crustacea; Peracarida) of the Antarctic shelf – diversity, biogeography, and phylogeny", by Peter Rehm

Heft-Nr. 603/2010 — "The Expedition of the Research Vessel 'Polarstern' to the Antarctic in 2009 (ANT-XXV/5)", edited by Walter Zenk and Saad El Naggar

Heft-Nr. 604/2010 — "The Expedition of the Research Vessel 'Polarstern' to the Antarctic in 2007/2008 (ANT-XXIV/2)", edited by Ulrich Bathmann

Heft-Nr. 605/2010 — "The Expedition of the Research Vessel 'Polarstern' to the Antarctic in 2003 (ANT-XXI/1)", edited by Otto Schrems

Heft-Nr. 606/2010 — "The Expedition of the Research Vessel 'Polarstern' to the Antarctic in 2008 (ANT-XXIV/3)", edited by Eberhard Fahrbach and Hein de Baar

Heft-Nr. 607/2010 — "The Expedition of the Research Vessel 'Polarstern' to the Arctic in 2009 (ARK-XXIV/2)", edited by Michael Klages

Heft-Nr. 608/2010 — "Airborne lidar observations of tropospheric Arctic clouds", by Astrid Lampert

Heft-Nr. 609/2010 — "Daten statt Sensationen - Der Weg zur internationalen Polarforschung aus einer deutschen Perspektive", by Reinhard A. Krause

Heft-Nr. 610/2010 — "Biology of meso- and bathypelagic chaetognaths in the Southern Ocean", by Svenja Kruse

Heft-Nr. 611/2010 — "Materialparameter zur Beschreibung des zeitabhängigen nichtlinearen Spannungs – Verformungsverhaltens von Firn in Abhängigkeit von seiner Dichte", by Karl-Heinz Bässler

Heft-Nr. 612/2010 — "The Expedition of the Research Vessel 'Polarstern' to the Arctic in 2009 (ARK-XXIV/1)", edited by Gereon Budéus

Heft-Nr. 613/2010 — "The Expedition of the Research Vessel 'Polarstern' to the Antarctic in 2009 (ANT-XXV/3 - LOHAFEX)", edited by Victor Smetacek and Syed Wajih A. Naqvi